

GEORGIA INSTITUTE OF TECHNOLOGY
OFFICE OF CONTRACT ADMINISTRATION
SPONSORED PROJECT INITIATION

Date: 8/21/78

no action
ack
DHL

Project Title: Convection in Narrow Vertical^{al} Fracture Spaces

Project No: G-35-639

Gr Cd

Project Director: Dr. Robert P. Lowell

Sponsor: U.S. Department of the Interior; Geological Survey; Reston, VA 22092

Agreement Period: From 7/1/78 Until 12/31/79 (Grant Expiration)

Type Agreement: Grant No. 14-08-0001-G-540

Amount: \$30,777 U.S. Geological Survey (G-35-639)
7,313 GIT (G-35-330)
\$38,090 TOTAL

Reports Required: Quarterly Management Reports; Semi-Annual Technical Reports;
Final Technical Report

Sponsor Contact Person (s):

Technical Matters

Donald W. Klick
Extramural Geothermal Research Program
Office of Geochemistry & Geophysics
U. S. Geological Survey
906 National Center
Reston, VA 22092

Phone: (703) 860-6581

Contractual Matters

(thru OCA)

Galen D. Brooks, Grants Officer
Procurement & Contract, ER
U. S. Geological Survey
291 National Center
Reston, VA. 22092

Phone: (703) 860-7646

Defense Priority Rating: None

Assigned to: Geophysical Sciences (School/Laboratory)

COPIES TO:

Project Director
Division Chief (EES)
School/Laboratory Director
Dean/Director-EES
Accounting Office
Procurement Office
Security Coordinator (OCA)
Reports Coordinator (OCA)

Library, Technical Reports Section
EES Information Office
EES Reports & Procedures
Project File (OCA)
Project Code (GTRI)
Other

GEORGIA INSTITUTE OF TECHNOLOGY
OFFICE OF CONTRACT ADMINISTRATION
SPONSORED PROJECT TERMINATION

Date: 1/16/81

Project Title: Convection in Narrow Vertical^a Fracture Spaces

Project No: G-35-639

Project Director: Dr. R. P. Lowell

Sponsor: USDI/Geological Survey

Effective Termination Date: 7/31/80

Clearance of Accounting Charges: 8/30/80 (reporting)

Grant/Contract Closeout Actions Remaining:

- ☐ Final Invoice and Closing Documents
- ☒ Final Fiscal Report
- ☐ Final Report of Inventions
- ☒ Govt. Property Inventory & Related Certificate
- ☐ Classified Material Certificate
- ☐ Other _____

Assigned to: Geophysical Sciences (School/~~Laboratory~~)

COPIES TO:

Project Director
Division Chief (EES)
School/Laboratory Director
Dean/Director—EES
Accounting Office
Procurement Office
Security Coordinator (OCA)
Reports Coordinator (OCA)

Library, Technical Reports Section
EES Information Office
Project File (OCA)
Project Code (GTRI)
Other OCA Research Property Coordinator

The Onset of Convection in a Fault Zone: Effect of Anisotropic Permeability

Robert P. Lowell

School of Geophysical Sciences
Georgia Institute of Technology
Atlanta, Georgia 30332

ABSTRACT

The condition for the onset of convective instability in a water-saturated, fault or fracture zone in which the permeability is anisotropic is derived. For the case in which the walls of the fault are assumed to be insulated, impermeable boundaries the results show that if the permeability ratio, $\gamma = K_v/K_h$ is less than unity, the critical Rayleigh number is substantially less than for an isotropic medium; whereas if γ is greater than unity the critical Rayleigh number is greater than for an isotropic medium. The flow takes the form of rolls with axes parallel to the short side of the box, the number of rolls contained in the fault zone depend upon the fault zone geometry (length/depth ratio) as well as upon the permeability ratio γ . The number of rolls increases as γ increases.

The convection model is applied to the linear, fault-controlled array of hot springs in the Double Hot Springs area of northern Nevada. If the spring system is a manifestation of roll-like convection within the fault, the results suggest that $\gamma > 1$.

INTRODUCTION

Natural geothermal systems consist principally of a sub-surface heat source and a groundwater circulation system. In most cases little is known concerning the details of the ultimate heat source; and, fortunately, this lack of information is not critical to the development of the resource. The energetics of natural geothermal systems, i.e., the amount of energy available and the rate at which it can be extracted, is primarily dependent upon the patterns of convective circulation within the reservoir rock and the mechanism of heat transfer between the heated rock and the circulating groundwaters. The convection patterns are, in turn, largely controlled by the nature and distribution of permeability within the reservoir.

The permeability of crustal rocks is often tectonically controlled; that is, it is due to fractures and faults rather than to interconnected pore spaces within the rock volume. In many known geothermal systems, the permeability is of this type. In the Basin and Range, for example, the

known geothermal systems appear to be controlled by long, deep, nearly vertical fault zones (Rose and Taylor, 1974). These zones of high permeability may have a linear extent of tens of kilometers and depths of several kilometers with widths of only tens or hundreds of meters. Moreover, as a result of the regional stress pattern, the permeability of the fault or fracture zone may be anisotropic. That is, the horizontal and vertical permeabilities may be unequal.

It is important, therefore, to understand the condition for the convective processes in fault and/or fracture zones. The purpose of this paper is to derive the condition for the onset of convection in a long, deep, but narrow, vertical fault zone with anisotropic permeability. The results will be applied to the Double Hot Springs region, of northern Nevada.

ANALYSIS

The condition for the onset of convection in a homogeneous, isotropic, horizontal, fluid-saturated porous slab, heated from below derived by Lapwood (1948) has formed the basis for convective instability analyses in permeable, porous media. Lapwood showed in a slab of thickness h , bounded by impermeable horizontal planes, and in which the bottom temperature was kept higher than the surface temperature, such that a thermal gradient, β , was maintained, convection would occur provided $R = \rho_f g \alpha \beta h^3 K / \nu \lambda \geq 4\pi^2$. R is called the Rayleigh parameter and ρ_f, α, ν are the density, specific heat, thermal expansion coefficient, and kinematic viscosity of the fluid, respectively; K, λ are the permeability and thermal conductivity of the rock, respectively; and g is the acceleration due to gravity. Since then, the critical condition for materials with temperature dependent properties (Kassoy and Zebib, 1975; Straus and Schubert, 1977) and analyses of finite amplitude convection systems (e.g. Donaldson, 1962; Wooding, 1963; Straus, 1974) have been carried out. Moreover, there have recently been analyses of the onset of convection in a closed rectangular container of water-saturated permeable materials. Beck (1972) and Holst and Aziz (1972) have assumed insulated walls; Lowell and Shyu (1978), Shyu (1979), and Murphy (1979) have assumed conducting walls. The results indicate that the presence of vertical confining walls significantly affects the critical

condition and the form of the convection cells at the onset of instability. The critical number is particularly high for containers with a fault-like geometry, in which one horizontal dimension is much smaller than the height and the other horizontal dimension, if the long side walls are conducting.

The condition for the onset of convection for a container in which the permeability is anisotropic is carried out below. Both the insulated and conducting wall cases are derived. Wooding (1976) has considered the effect of anisotropic permeability in an infinite horizontal slab.

A. Equations and Boundary Conditions

Consider a model fault zone as a rectangular slab of water-saturated, porous material imbedded in impermeable rock. Let the height of the porous zone be L_z and the horizontal dimensions be L_x and L_y . Let a uniform geothermal gradient, β , be applied to the material such that the temperature at the upper surface is $T = 0$ and at the lower surface $T = T_0$ ($T_0 > 0$).

Assuming a Cartesian coordinate system with the axis defined positively downward, the linearized, steady state perturbation equations are:

$$\lambda \nabla^2 T^* = \rho_f \beta w^* \quad (1)$$

$$-\nabla P^* - \rho_f \alpha T^* g z - \rho_f \nabla K^{-1} \cdot \vec{u}^* = 0 \quad (2)$$

$$\nabla \cdot \vec{u}^* = 0 \quad (3)$$

where the * refers to dimensional perturbation quantities and where all the parameters are defined as previously. w^* is the vertical velocity; P^* the pressure perturbation; \vec{u}^* the velocity vector. Note that K is now treated as a tensor. Non-dimensionalizing the above equations by using L as a length scale, T_0 as a temperature scale, and a reference mean flow $q_0 = gK_0 \alpha T_0 / \nu_0$, where K_0, ν_0 refer to values at the top of the layer; and eliminating P^* from the equations gives

$$Rw = \nabla^2 T \quad (4)$$

$$\partial \sigma (\partial w / \partial z) / \partial z + \{ (1/\gamma_1) \partial^2 / \partial x^2 + \quad (5)$$

$$(1/\gamma_2) \partial^2 / \partial y^2 \} (T + \sigma w) = 0$$

$$\text{where } \sigma = (K_0/K_3) (\nu/\nu_0); \gamma_1 = K_3/K_1; \gamma_2 = K_3/K_2$$

$$\text{and } R = \rho_f \alpha g L^2 K_0 / \nu_0 \lambda$$

Equations (4) and (5) have been derived by Wooding (1976) for the case of an infinite horizontal porous layer. To determine the onset of convection in a box-like region equations (4) and (5) must be solved subject to the boundary conditions:

$$\vec{u} \cdot \hat{n} = 0 \text{ at all walls} \quad (6)$$

$$T = 0 \text{ at } z = 0, L_z \quad (7)$$

The temperature conditions on the vertical walls will be either

$$\partial T / \partial x = 0 \text{ at } x = 0, a \quad a = L_x / L_z \quad (8)$$

$$\partial T / \partial y = 0 \text{ at } y = 0, b \quad b = L_y / L_z$$

for insulated walls or

$$\partial T / \partial x = 0 \text{ at } x = 0; a \quad (9)$$

$$T = 0 \text{ at } y = 0; b$$

corresponding to conducting walls on the boundary parallel to the strike of the fault.

For convenience it will be assumed that $\sigma = 1$. This corresponds to the situation in which a decrease in viscosity with increasing temperature (depth) is matched by a decrease in permeability with depth, which is not an unrealistic assumption. Furthermore, the horizontal permeabilities will be assumed to be the same. Thus $\gamma_1 = \gamma_2 = \gamma$.

B. Insulated Boundaries

Combining equations (4) and (5) into a single equation for T and substituting a solution of the form

$$T = \hat{T}(z) \cos \alpha x \cos \beta y$$

where $\alpha = m\pi/a$; $\beta = n\pi/b$ gives

$$\{ D^4 - D^2(1+1/\gamma)(\alpha^2 + \beta^2) + \frac{1}{\gamma}(\alpha^2 + \beta^2)(\alpha^2 + \beta^2 - R) \} \hat{T} = 0 \quad (10)$$

where D represents d/dz . Letting $\hat{T} = \sin \pi z$ in (10) results in an equation for R .

$$R = \pi^2 \left\{ \gamma^2 + \frac{m^2}{a^2} + \frac{n^2}{b^2} \right\}^2 \quad (11)$$

$$+ (\gamma^2 - 1)^2 \left(\frac{m^2}{a^2} + \frac{n^2}{b^2} \right) \left(\frac{m^2}{a^2} + \frac{n^2}{b^2} \right)^{-1}$$

The problem is now to find the minimum value of R for a given γ , a , b and to determine the cell pattern at the minimum Rayleigh number. It is noted that (11) reduces to the isotropic case of Beck (1972) by letting $\gamma = 1$ and to the infinite slab case of Wooding (1976) if a, b are allowed to approach infinity.

Rather than treat the full range of box geometries, only the special case of a fault-like geometry will be considered. Then, $a \gg 1$ and $b \ll 1$. In this case a cursory examination of (11) reveals that R_c will occur for $n = 0$. That is, the cell will take the form of rolls with their axes parallel to the shorter side of the container. Setting $n = 0$ in (11) gives

$$R = \pi^2 \left\{ \gamma \left(1 + \frac{a^2}{m^2} \right) + \frac{m^2}{a^2} + 1 \right\} \quad (12)$$

Table 1 gives the critical Rayleigh number R_c and the number of rolls contained in the fault zone for several values of anisotropy and for fault lengths up to 4 times the depth. The results in Table 1 show that if the horizontal permeability is greater than the vertical ($\gamma < 1$), the critical Rayleigh number is reduced substantially from the isotropic value of $4\pi^2$; and that if $\gamma > 1$, the critical Rayleigh number is increased substantially. Moreover, the results indicate a

remarkable change in aspect ratio as the anisotropy changes from $\gamma < 1$ to $\gamma > 1$. For example, if $a = 2$, there is only one roll present at $R = R_c$ for $\gamma = 0.1$; whereas there are two rolls for isotropic materials, and four rolls for $\gamma = 10$.

C. Conducting Boundaries

If the long sides of the box are conducting, the conditions (9) lead to non-separable solutions. An approximate solution may be found, however, (Lowell, 1977) by assuming a solution of the form

$$T = \hat{T}(z) \cos \alpha x \sin \beta y$$

The equation for the Rayleigh number (11) is identical to the case for insulated walls; however, the solution $n = 0$ is no longer permitted since that would correspond to $T = 0$. The minimum Rayleigh number is now found with $n = 1$ and an appropriate value of m . The solution $(m, n) = (0, 1)$ corresponds to a flow which rises everywhere so one must choose $m > 0$, $n = 1$. An examination of (11) with $b \ll a$ and $n = 1$ is found to be roughly independent of m . Hence the critical number can be found approximately by letting $m = 0$, $n = 1$. This gives

$$R_c \approx \pi^2 \{ \gamma(b^2 + 1) + b^{-2} + 1 \} \quad (13)$$

and since $b^2 \ll 1$, $R_c \approx \pi^2/b^2$, except for exceptionally large values of γ . Thus, if the walls are conducting, the anisotropy has a negligible effect on the critical Rayleigh number. The approximate solution indicates, however, that conducting walls give rise to a rectangular, 3-dimensional cell

TABLE 1. CRITICAL RAYLEIGH NUMBERS AND MODE
FOR SEVERAL VALUES OF ANISTROPY AND FAULT ZONE LENGTH

$a \downarrow \gamma \rightarrow$	0.01	0.1	1	10
1	$R_c = 2.02\pi^2$ $m = 1$	$R_c = 2.2\pi^2$ $m = 1$	$R_c = 4\pi^2$ $m = 1$	$R_c = 17.5\pi^2$ $m = 2$
2	$R_c = 1.3\pi^2$ $m = 1$	$R_c = 1.75\pi^2$ $m = 1$	$R_c = 4\pi^2$ $m = 2$	$R_c = 17.5\pi^2$ $m = 4$
3	$R_c = 1.21\pi^2$ $m = 1$	$R_c = 1.77\pi^2$ $m = 2$	$R_c = 4\pi^2$ $m = 3$	$R_c = 17.4\pi^2$ $m = 5$
4	$R_c = 1.23\pi^2$ $m = 1$	$R_c = 1.75\pi^2$ $m = 2$	$R_c = 4\pi^2$ $m = 4$	$R_c = 17.3\pi^2$ $m = 7$

pattern instead of 2-dimensional rolls. This is because $m \neq 0$ implies that all three velocity components are non-zero (but see Murphy, 1979).

DISCUSSION

The application of the highly idealized fault zone convection model derived here to a complex natural geothermal system is indeed difficult. In fact, the thermal boundary conditions may even be erroneous; or to be more precise, the boundary conditions may change in time. That is, if the fault zone is very narrow, conduction through the side walls may be quite important; and the condition of conducting walls may be the most appropriate for calculating the onset of stability. As pointed out by Murphy (1979) most faults may be stable to spontaneous convection due to the high critical number required in the presence of conducting walls. However, convection may be forced by tectonic movement on the fault, by tidal breathing, or by hydraulically driven flow in the fault due to hydrostatic pressure differences. If forced convection occurs, heat transfer across the walls lowers the thermal gradient in time as $t^{-1/2}$ (Carslaw and Jaeger, 1959). Hence, in time, the walls take on the appearance of being insulated, and free convection is more likely to occur. A more detailed discussion of delayed free convection is given by Murphy (1979).

Nevertheless, despite these real-world difficulties, it is useful to try to apply the analytical results to observational data. One possible application may be found in the Basin and Range Province where observations indicate that the geothermal systems are often fault-controlled. Hose and Taylor (1974) point out that the Double Hot Springs area west of the Black Rock Range in northern Nevada consists of approximately seven springs (or seeps) which emerge at a rather regular spacing along a linear trend of about 10 km. The springs are spaced at roughly 1.5 km and, based on regional thermal gradient data, geochemical data indicate that the springs have a fairly uniform circulation depth of about 3 km. Thus, if the spring system is a manifestation of roll-like convection within the fault, the somewhat small aspect ratio (cell wavelength vs. depth) suggests that the permeability of the fault zone may be anisotropic: the vertical permeability may be greater than the horizontal.

ACKNOWLEDGMENT

This work was supported by Extramural Geothermal Research Program of the U. S. Geological Survey, Department of the Interior under USGS Grant No. 14-08-0001-G-365 and 14-08-0001-G-540.

REFERENCES

Beck, J. L., 1972, Convection in a box of porous material saturated with fluid: *Phys. Fluids*, v. 15, p. 1377-1383.

Carslaw, H.S. and Jaeger, J.C., 1959, *Conduction of heat in solids*, 2nd ed., Oxford, The Clarendon Press, 510 p.

Donaldson, I.G., 1962, Temperature gradients in the upper layers of the earth's crust due to convective water flows: *J. Geophys. Res.*, v. 67, p. 3449-3460.

Holst, P.H. and Aziz, K., 1972, Transient three-dimensional natural convection in confined porous media: *Int. J. Heat and Mass Trans.*, v. 15, p. 73-90.

Hose, R.K. and Taylor, B.E., 1974, Geothermal systems of northern Nevada: U.S. Geol. Survey, Open-file Rept. 74-271, 27 p.

Kassoy, D.R. and Zebib, A., 1975, Variable viscosity effects on the onset of convection in porous media: *Phys. Fluids*, v. 18, p. 1649-1651.

Lapwood, E.R., 1948, Convection of a fluid in a porous medium: *Proc. Cambridge Phil. Soc.*, v. 44, p. 508-521.

Lowell, R.P., 1977, Convection and thermoelastic effects in narrow, vertical fracture spaces: Semi-annual Technical Letter Rept. No. 1, USGS Grant No. 14-08-0001-G-365, 10 p.

Lowell, R.P. and Shyu, C.-T., 1978, On the onset of convection in a water-saturated porous box: effect of conducting walls: *Lett. Heat and Mass Trans.*, v. 5, p. 371-378.

Murphy, H.D., 1979, Convective instabilities in vertical fractures and faults: *J. Geophys. Res.* (in press).

Shyu, C.-T., 1979, Numerical Analysis of Critical Field Functions for Thermal Convection in Vertical or Quasi-Vertical Darcy Flow Slabs: Ph.D. Dissertation, Oregon State University, Corvallis, 190 p.

Straus, J.M., 1974, Large amplitude convection in porous media: *J. Fluid Mech.*, v. 64, p. 51-63.

Straus, J.M. and Schubert, G. 1977, Thermal convection of water in a porous medium: effects of temperature and pressure dependent thermodynamic and transport properties: *J. Geophys. Res.*, v. 82, p. 325-334.

Wooding, R.A., 1963, Convection in a saturated porous medium at large Rayleigh number or Peclet number: *J. Fluid Mech.* v. 15, p. 527-544.

Wooding, R.A., 1976, Influence of anisotropy and variable viscosity upon convection in a heated saturated porous layer: *Applied Math Division, Tech. Rept. No. 55, DSIR, Wellington, N.Z.*, 23 p.

QUARTERLY MANAGEMENT REPORT NO. 1

Grant No: 14-08-0001-540

Reporting Period Covered: 7/1/78 to 9/30/78

Grantee: Georgia Institute of Technology

Supported by: U. S. Geological Survey
Geothermal Research Program
Reston, Virginia

Grant Amount: \$30,777.00

Start Date: 7/1/78

Expiration Date: 12/31/79

Principal Investigator: Robert P. Lowell

USGS Technical Officer: Donald W. Klick

Date Submitted: October 27, 1978

Title of Research Project: Convection in Narrow, Vertical Fracture Space

Objectives of Project: The purpose of this research is to examine thermal convection effects in long, deep, but very narrow vertical fracture spaces. The initiation and time development of the physical processes are to be studied on the basis of mathematical-physical approximation methods and numerical techniques. The results are to be interpreted with regard to known geothermal systems in the Basin and Range Province and other regions where major faults or fractures are the dominant controlling structures.

Major Accomplishments: The principal accomplishment has been the completion and submission of a manuscript reporting the results of work on the onset of convection in a fault zone. The bulk of research had been carried out under a previous USGS grant (see Publications section below).

Publications and Talks: Lowell, R.P. and C.T. Shyu, The onset of convection in a box of water-saturated permeable material: the effect of conducting vertical boundaries, Letters in Heat and Mass Trans., 5, 371-378 (manuscript sent to USGS previously).

Problems Encountered: A new first year graduate student has been hired as a research assistant on this project. As is usually the case, it takes several months before such a student makes important contributions. During this formative stage, therefore, research output is somewhat low; however, I anticipate an improvement in following quarters.

Page Two

Significant Changes in Plans: None

Actions Required by Government: None

Equipment Acquired: Not applicable

Respectfully submitted,

Robert P. Lowell
Associate Professor

QUARTERLY MANAGEMENT REPORT NO. 2

Grant No: 14-08-0001-540

Reporting Period Covered: 10/1/78 to 12/31/78

Grantee: Georgia Institute of Technology

Supported by: U.S. Geological Survey
Geothermal Research Program
Reston, Virginia

Grant Amount: \$30,777.00

Start Date: 7/1/78

Expiration Date: 12/31/79

Principal Investigator: Robert P. Lowell

USGS Technical Officer: Donald W. Klick

Date Submitted: January 10, 1979

Title of Research Project: Convection in Narrow, Vertical Fracture Spaces

Objectives of Project: The purpose of this research is to examine thermal convection effects in long, deep, but very narrow vertical fracture spaces. The initiation and time development of the physical processes are to be studied on the basis of mathematical-physical approximation methods and numerical techniques. The results are to be interpreted with regard to known geothermal systems in the Basin and Range Province and other regions where major faults or fractures are the dominant controlling structures.

Major Accomplishments: (1) An estimate of the time rate of decay of the fluid flow and temperature in a non-steady convecting fracture. (2) Derivation of the condition for the onset of convection in a porous medium overlain by a thin impermeable cap. (3) Completion of an M.S. thesis which was partially supported under this grant.

Publications and Talks: Talk on "Heat transport processes related to fluids flowing in fractured rock" given at Penrose Conference on "Heat Transport Processes in the Earth" Vail, Co., Nov. 13-17, 1978.

Problems Encountered: The graduate student hired for this project in September, 1978 has chosen to resign his assistantship. The research progress will definitely slow down until an adequate replacement is found.

Significant Changes in Plans: None at the present time, although if a graduate assistant is not found quickly, the scope of the project may be narrowed somewhat and some of the numerical work may have to be abandoned.

Page Two

Actions Required by Government: None at present, although it may become desirable to replace the graduate student with a postdoctoral researcher. Mr. C.T. Shyu who has worked on the earlier grant is presently finishing his Ph.D. and may be available to work on this project. However, there are not sufficient funds at this time for adequate support for him. Supplementary support may be sought from USGS to enable us to satisfactorily complete the project.

Equipment Acquired: None

Respectfully submitted,

Robert P. Lowell
Associate Professor

QUARTERLY MANAGEMENT REPORT NO. 3

Grant No: 14-08-0001-540

Reporting Period Covered: 1/1/79 to 3/31/79

Grantee: Georgia Institute of Technology

Supported by: U. S. Geological Survey
Geothermal Research Program
Reston, Virginia

Grant Amount: \$30,777.00

Expiration Date: 12/31/79

Principal Investigator: Robert P. Lowell

USGS Technical Officer: Donald W. Klick

Date Submitted: April 17, 1979

Title of Research Project: Convection in Narrow, Vertical Fracture Spaces

Objectives of Project: The purpose of this research is to examine thermal convection effects in long, deep, but very narrow vertical fracture spaces. The initiation and time development of the physical processes are to be studied on the basis of mathematical-physical approximation methods and numerical techniques. The results are to be interpreted with regard to known geothermal systems in the Basin and Range Province and other regions where major faults or fractures are the dominant controlling structures.

Major Accomplishments: None, specifically. Work is continuing on the problem of non-steady convective flow in fractures, including thermoelastic effects. I have also initiated a study of the effects of temperature gradients transverse to a fracture.

Publications: The paper: "On the Onset of Convection in a Water-Saturated Poursous Box: Effects of Conducting Walls" has appeared in print. Enclosed are reprints.

Problems Encountered: The main difficulty stems from not having a graduate assistant on the project at present. I have contacted Shyu, and he is apparently not interested in pursuing this work as a post-doctoral student here. I hope to obtain a graduate assistant to help with numerical modeling this summer.

Significant Changes in Plans: Research progress has been slow; however, if a suitable graduate student can be found by summer. I expect to be able to complete the research project as planned. It may be desirable to extend the expiration date, but I will think through that further.

Actions Required by Government: Due to lack of graduate assistance, it may be desirable for me to spend 3 full months on the project this summer instead of 2. This would help make up for the slow progress at present and would not require any additional funds - only a transfer of funds from graduate student to Principal Investigator within the personal services part of the budget. A formal request in this regard will be sent shortly.

Equipment Acquired: None

Respectfully submitted,

Robert P. Lowell
Associate Professor

QUARTERLY MANAGEMENT REPORT NO. 4

Grant No: 14-08-0001-G-540

Report Period Covered: 4/1/79 to 6/30/79

Grantee: Georgia Institute of Technology

Supported by: U. S. Geological Survey
Geothermal Research Program
Reston, Virginia

Grant Amount: \$30,777.00

Expiration Date: 12/31/79

Principal Investigator: Robert P. Lowell

USGS Technical Officer: Donald W. Klick

Date Submitted: July 15, 1979

Title of Research Project: Convection in Narrow, Vertical Fracture Spaces

Objectives of Project: The purpose of this research is to examine thermal convection effects in long, deep, but very narrow vertical fracture spaces. The initiation and time development of the physical processes are to be studied on the basis of mathematical-physical approximation methods and numerical techniques. The results are to be interpreted with regard to known geothermal systems in the Basin and Range Province and other regions where major faults or fractures are the dominant controlling structures.

Major Accomplishments: Work is continuing on the problem of non-steady convective flow in fractures, including thermoelastic effects. I have also expanded the work on anisotropic permeability slightly in order to include the effects of conducting walls. A paper on the anisotropic permeability work has been submitted to the Geothermal Resources Council for publication in the Annual Symposium Transactions.

Publications: The Onset of Convection in a Fault Zone: Effect of Anisotropic Permeability, submitted to Geothermal Resources Council September, 1979, Reno, Nevada. Preprints enclosed.

Problems Encountered: Research progress has been slow mainly due to the lack of graduate student assistance. However, a graduate student with experience and an interest in numerical work has been hired effective June 15, in order to initiate the finite-difference modelling. I am also working full time on the project this summer. I am confident the proposed research will reach a satisfactory completion, although the delay in getting started will most likely necessitate an extension of the expiration date of the grant.

Significant Changes in Plans: None at this time.

Actions Required by the Government: None at this time; although it is anticipated that, because of the afore mentioned delays and difficulties, a no cost time extension of approximately six months will be requested.

Equipment Acquired: None.

Respectfully submitted,

Robert P. Lowell
Associate Professor

G 35-457

QUARTERLY MANAGEMENT REPORT NO. 5

Grant No: 14-08-0001-G-540

Report Period Covered: 7/1/79 to 9/30/79

Grantee: Georgia Institute of Technology

Supported by: U. S. Geological Survey
Geothermal Research Program
Reston, Virginia

Grant Amount: \$30,777.00

Expiration Date: 12/31/79

Principal Investigator: Robert P. Lowell

USGS Technical Officer: Donald W. Klick

Date Submitted: October 15, 1979

Title of Research Project: Convection in Narrow, Vertical Fracture
Spaces

Objectives of Project: The purpose of this research is to examine thermal convection effects in long, deep, but very narrow vertical fracture spaces. The initiation and time development of the physical processes are to be studied on the basis of mathematical-physical approximation methods and numerical techniques. The results are to be interpreted with regard to known geothermal systems in the Basin and Range Province and other regions where major faults or fractures are the dominant controlling structures.

Major Accomplishments: Estimates on the magnitude and temporal evolution of thermoelastic effects in a system closely spaced, flat, parallel fractures have been made. Numerical work on convection in fault zones is now underway. A treatment of heat transfer in narrow open fractures, including the effects of transverse temperature gradients and a parabolic velocity profile has been begun.

Publications: The Onset of Convection in a Fault Zone: Effect of Anisotropic Permeability, Transactions, Geothermal Resources Council Annual Meeting, Reno, Nevada, September 1979, p. 377-380.

Problems Encountered: None at this time.

Significant Changes in Plans: None at this time.

Actions Required by Government: Due to the severe delays in initiating the numerical program a no cost time extension of several months will be required to bring the research program to a satisfactory completion. A formal request for such an extension is being sent to the Contracts and Administration Section.

Equipment Acquired: None

Respectfully submitted,

Robert P. Lowell
Associate professor

RPL/dp

QUARTERLY MANAGEMENT REPORT NO. 6

Grant No: 14-08-0001-G-540

Report Period Covered: 10/1/79 to 12/31/79

Grantee: Georgia Institute of Technology

Supported by: U. S. Geological Survey
Geothermal Research Program
Reston, Virginia

Grant Amount: \$30,777.00

Expiration Date: July 31, 1980

Principal Investigator: Robert P. Lowell

USGS Technical Officer: Donald W. Klick

Date Submitted: January 15, 1980

Title of Research Project: Convection in Narrow, Vertical Fracture
Spaces

Objectives of Project: The purpose of this research is to examine thermal convection effects in long, deep, but very narrow vertical fracture spaces. The initiation and time development of the physical processes are to be studied on the basis of mathematical-physical approximation methods and numerical techniques. The results are to be interpreted with regard to known geothermal systems in the Basin and Range Province and other regions where major faults or fractures are the dominant controlling structures.

Major Accomplishments: Numerical modeling of convection in a fault zone is continuing. The computer program is not yet functional, but I expect results will be available in a month or so. The treatment of heat transfer in narrow, open fractures, including the effects of transverse temperature gradients and a parabolic velocity profile is continuing.

Publications: None

Problems Encountered: None at this time.

Significant Changes in Plans: None at this time.

Actions Required by Government: None at this time.

Equipment Acquired: None

Respectfully submitted,

Robert P. Lowell
Associate Professor

RPL/dp

QUARTERLY MANAGEMENT REPORT NO. 7

Grant No.: 14-08-0001-G-540

Report Period Covered: 1/1/80 - 3/31/80

Grantee: Georgia Institute of Technology

Supported by: U.S. Geological Survey
Geothermal Research Program
Reston, Virginia

Grant Amount: \$30,777.00

Expiration Date: July 31, 1980

Principal Investigator: Robert P. Lowell

USGS Technical Officer: Donald W. Klick

Date Submitted: April 18, 1980

Title of Research Project: Convection in Narrow, Vertical Fracture Spaces

Objectives of Project: The purpose of this research is to examine thermal convection effects in long, deep, but very narrow vertical fracture spaces. The initiation and time development of the physical processes are to be studied on the basis of mathematical-physical approximation methods and numerical techniques. The results are to be interpreted with regard to known geothermal systems in the Basin and Range Province and other regions where major faults or fractures are the dominant controlling structures.

Major Accomplishments: The principal emphasis over the past months has been on the development of a finite-difference model for convection in a fault zone. The program has been written, but the first few runs have not been successful due to problems with convergence. I am confident that this matter will be straightened out shortly and that useful results will be acquired. I am also carrying out some analytical computations on convection with time-dependent heat transfer through the vertical walls.

Publications: None

Problems Encountered: None at this time.

Significant Changes in Plans: None at this time.

Actions Required by Government: None at this time.

Equipment Acquired: None

Respectfully submitted,

Robert P. Lowell
Associate Professor

QUARTERLY MANAGEMENT REPORT NO. 8

Grant No.: 14-08-0001-G-540
Report Period Covered: 4/1/80 - 6/30/80
Grantee: Georgia Institute of Technology
Supported by: U.S. Geological Survey
Geothermal Research Program
Reston, Virginia
Grant Amount: \$30,777.00
Expiration Date: July 31, 1980
Principal Investigator: Robert P. Lowell
USGS Technical Officer: Donald W. Klick
Date Submitted: July 10, 1980
Title of Research Project: Convection in Narrow, Vertical Fracture Spaces

Objectives of Project: The purpose of this research is to examine thermal convection effects in long, deep, but very narrow vertical fracture spaces. The initiation and time development of the physical processes are to be studied on the basis of mathematical-physical approximation methods and numerical techniques. The results are to be interpreted with regard to known geothermal systems in the Basin and Range Province and other regions where major faults or fractures are the dominant controlling structures.

Major Accomplishments: The principal emphasis over the past months has been on the continued development of finite difference models for convection in a fault zone. The numerical work is now essentially complete, the principal results being that finite amplitude convection in a fault-shaped porous zone with perfectly conducting walls tends to be three-dimensional, whereas if the walls are imperfectly conducting, the motion tends to take the form of two-dimensional rolls with axes perpendicular to the strike of the fault. This work is being prepared by Heroel Hernandez-Cortez as an M.S. thesis in Geophysical Sciences and should be completed within a month.

In addition to the numerical work, I have been developing a fracture model analog of the fault-zone model of Kassoy (1980).

Publications: None

Problems Encountered: None at this time

Significant Changes in Plans: None, and it looks, finally, as though nearly all the computer work which we hoped to do will be completed on current schedule.

Actions Required by Government:

None at this time

Equipment Acquired:

None

Respectfully submitted,

Robert P. Lowell
Associate Professor

Semi Annual Technical Letter Report No. 1

Grant No: 14-08-0001-G-540

Reporting Period Covered: 7/1/78 - 12/31/78

Grantee: Georgia Institute of Technology

Supported by: U. S. Geological Survey
Geothermal Research Program
Reston, Virginia

Grant Amount: \$30,777.00

Start Date: 7/1/78

Expiration Date: 12/31/79

Principal Investigator: Robert P. Lowell

U.S.G.S. Technical Officer: Donald W. Klick

Date Submitted: January 31, 1979

Title of Research Project: Convection in Narrow Vertical Fracture Spaces

Objectives of Project: The main purpose of this project is to examine thermal convection in long, deep, but very narrow vertical fracture spaces. The initiation and time development of the physical processes are to be studied on the basis of mathematical-physical approximation methods and numerical techniques. The results are to be interpreted with regard to known geothermal systems in the Basin and Range and other areas where faults or fractures are the dominant controlling structures.

I. Introduction

This document represents the first semi-annual technical report on our research on convection in faults and fracture zones and some related problems. This work represents a continuation of our effort which was initiated under the USGS grant number: 14-08-0001-G-365 as part of the Extramural Geothermal Research Program of the U. S. Geological Survey. The initial phase of the work was done in conjunction with Dr. G. Bodvarsson of Oregon State University; however, his group is not directly involved in the present research effort. The present research is being conducted under grant #: 14-08-0001-G-540.

The principal achievements during the past six months have been to (1) publish two papers containing some of the main results of the initial research, (2) determine the condition for convection stability in a porous slab heated from below and with a radiative upper boundary, (3) develop further some aspects of the temporal evolution of thermal convection in fractures which were initially presented by Bodvarsson (1978), (4) present a talk on heat transport process in fractures at the Penrose Conference on "Heat Transport Processes in the Earth's Interior" in Vail, Colorado, November, 1978 and (5) completion of an M. S. Thesis by Mr. J. K. Fulford, which was partially supported by this grant. One of the published papers was delivered as a talk at the Geothermal Resources Council Annual Meeting in Hilo, Hawaii, July, 1978 and has since appeared in the proceedings of the meeting. Copies of the paper have been submitted to the USGS previously, and a complete reference is given in section VIII of this report. The second paper has recently appeared in Letters in Heat and Mass Transfer. Reprints will be sent when they are available. A preprint is attached as an appendix to this report.

The main body of the report which follows is divided into subsections: II. General framework and objectives; III. Onset of convection in a porous slab with radiative boundary conditions; IV. Convection in faults and fracture zones; V. Temporal evolution of convective flow in fractures; VI. Work plan for coming report period; VII. Students supported and theses; VIII. Papers and publications.

II. General Framework and Research Objectives

The energetics of geothermal systems depends fundamentally upon patterns of heat transport and fluid flow within heated, highly permeable regions of the earth's crust. The ultimate source of heat for many geothermal systems is undoubtedly of magmatic origin, but, in some cases the geothermal fluid is heated at depth as a result of an unusually high geothermal gradient. Most of the systems in the Basin and Range province are probably of the latter type (White and Williams, 1975).

Of even more importance, however, is the nature and distribution of permeability within the geothermal reservoir. The permeability may either be primary, resulting from interconnected pore spaces within the rock volume or secondary, resulting from fractures and/or fault zones. In all geothermal fields currently under production, the geothermal fluids are withdrawn from discrete fractured regions within the reservoir, yet most mathematical modeling of geothermal systems has assumed a Darcian type of flow through a rock with a bulk permeability. That is not to say that it has been necessarily assumed that the permeability is of a primary type, but rather that one normally assumes the fractures to be on such a fine scale that, for mathematical (or numerical) convenience, the Darcy flow model is appropriate on spatial scales of the order of the reservoir dimensions.

The mathematical treatment for the onset of thermal convection under such assumptions follows the method of Lapwood (1948), or some deviant of it; and the treatment of finite amplitude convection uses the same basic perturbation equations with the addition of higher order, non-linear transport terms which are neglected in the linear stability analysis. These models have provided many useful results with regard to the physics of geothermal systems, but often this approach may be quite unrealistic. Geothermal systems in which main permeability is furnished by narrow, discrete, widely separated fault and/or fracture zones imbedded in an otherwise impermeable rock are better handled by somewhat different techniques. Examples of the latter systems are found in Iceland, where dikes provide the main vertical permeability, in the Basin and Range, where long, deep, master faults probably provide the main vertical permeability (Hose and Taylor, 1974), and possibly in the oceanic crust (Lowell, 1975; Sleep and Wolery, 1978).

The principal purpose of this research is to examine thermal convection in long, deep, but very narrow vertical fracture spaces. The initiation and temporal evaluation of the physical processes are to be studied on the basis of mathematical-physical approximation methods and finite element and/or finite difference techniques. The results are to be interpreted with regard to known geothermal systems in the Basin and Range and other regions where major faults and fractures are the structures controlling the permeability.

III. The Onset of Convection in a Porous Slab with a Radiative on the Upper Boundary.

In order to introduce the pertinent equations and to set the stage for the development in section IV on convection in a rectangular box (representing a fault zone), we set up and solve a convective

instability problem for an infinite slab of porous material which may be of interest in the geothermal setting. The basic model for convective instability in a porous slab is due to Lapwood (1948).

Lapwood determined the critical condition for the onset of convection in an infinite slab of homogeneous, isotropic porous material of thickness h , bounded by horizontal planes. Within the slab, a vertical conduction temperature gradient, β , was maintained. The bottom of the layer was held at temperature T_0 and the top at $T = 0$. Using stability analysis, Lapwood showed that $R = \frac{\rho_f s \alpha \beta h^2 K}{\nu \lambda} \geq 4\pi^2$ for convection to occur between impermeable boundaries, where ρ_f , s , α , ν represent the density, specific heat, thermal expansivity and kinematic viscosity of the fluid, respectively; K is the permeability, λ is the thermal conductivity of the rock, and g is the acceleration of gravity. The critical Rayleigh number for some other boundary conditions are given in Nield (1968) and also in Lapwood (1948); and the critical number for case of temperature dependent viscosity (Kassoy and Zebib, 1975), temperature dependent expansivity, viscosity, and density (Straus and Schubert, 1977), and anisotropic permeability (Wooding, 1976) have recently been determined.

In the natural geothermal setting, however, the assumption of an impermeable conducting plane at the top of the convecting layer is somewhat unrealistic. In the natural setting, deposition of silica often clogs the permeable zones in the upper part of the reservoir, and the circulation is confined to the reservoir beneath an impermeable layer of caprock of finite thickness. The finite layer of caprock represents a medium of imperfect heat transfer between the convecting fluid and the surface, and thus the convective instability of the fluid in the reservoir may be affected.

To estimate the effect of a thin but finite layer of impermeable cover on the porous layer, we shall treat the surface layer as simply a skin of material through which conductive heat transfer takes place. That is, the layer is assumed to be so thin that its heat capacity can be neglected. In essence, then, the effect of the caprock is to modify the upper boundary condition on the convecting layer. Instead of the temperature condition being $T = 0$, we have radiative transfer $\lambda \partial T / \partial z + \psi T = 0$ at the top of the layer, where ψ is the heat transfer coefficient. Thus in the steady-state case of conductive equilibrium the temperature distribution in the layer is given by

$$T^0(z) = T_0 - \beta n z \quad (1)$$

where $n = \bar{k} / (\bar{k} + 1)$ ($\bar{k} = \psi h / \lambda$) and $\beta = T_0 / h$, the maintained geothermal gradient in the case of infinite heat transfer coefficient ($n = 1$).

The linearized theory of convective instability is based on the principal of exchange of stabilities. That is, a small perturbation to the conductive state leads to a steady state of convective equilibrium. The standard perturbation procedure is outlined in Lapwood (1948) and will not be reproduced here. Instead, we begin with the linearized perturbation equations with the z axis defined positive upwards:

$$\lambda \nabla^2 T^* = \rho_f \sigma \omega^* \beta n \quad (2)$$

$$-\nabla P^* - \rho_f \alpha T^* g \hat{z} - \rho_f \nu \nabla^2 \vec{u}^* = 0 \quad (3)$$

$$\nabla \cdot \vec{u}^* = 0 \quad (4)$$

Equations (2) (3) and (4) correspond to conservation of energy, momentum and mass respectively. The $*$ refers to dimensional quantities: T^* being the perturbation temperature; P^* the perturbation pressure; \vec{u}^* the velocity

vector; w^* the vertical component of velocity. All the physical parameters have been defined previously, but note that in this more general case, the permeability \underline{K} is treated as a tensor. Non-dimensionalizing these equations by using h as a length scale, T_0 as a temperature scale and $q_r = gK_0\alpha T_0/\nu_0$ as a reference mass flow, where K_0, ν_0 refer to values at the top of the layer; and eliminating P^* from the equations gives:

$$Rw = \nabla^2 T \quad (5)$$

$$(\partial\sigma/\partial z)(\partial w/\partial z) + \{ (1/\gamma_1)\partial^2/\partial x^2 + (1/\gamma_2)\partial^2/\partial z^2 \} (T + \sigma w) = 0 \quad (6)$$

where $\sigma = (K_0/K_3)(\nu/\nu_0)$; $\gamma_1 = K_3/K_1$; $\gamma_2 = K_3/K_2$

and $R = \rho_f s \alpha \beta L_z^2 K_0 / \nu_0 \lambda$

Equations (5) and (6) have been derived by Wooding (1976) for the case of infinite heat transfer coefficient (i.e., $n = 1$). Equations (5) and (6) must then be solved subject to boundary conditions:

$$T = 0 \text{ at } z = 0 \quad (7)$$

$$\partial T / \partial z + kT = 0 \text{ at } z = 1 \quad (8)$$

$$w = 0 \text{ at } z = 0, 1 \quad (9)$$

Since the purpose here is to explore the effect of the radiative condition (8) on the upper surface, equation (6) will be simplified by letting $\sigma = \gamma_1 = \gamma_2 = 1$. Equations (5) and (6) can then be combined into a single fourth order equation for T , and using (5) the velocity boundary conditions (9) can be written in the form of temperature conditions. The resulting equation:

$$\nabla_h^4 T = nR \nabla_h^2 T \quad (10)$$

where ∇_h^2 represents the horizontal components of the Laplacian, together with the boundary conditions represents an eigenvalue problem for R . Assuming T is

periodic with semiwavelength a , there is, for a given value of \bar{k} , a particular value of R for every value of a ; and the minimum of R with respect to a at fixed \bar{k} represents the critical Rayleigh number at which instability sets in.

Substituting $T = \theta(z) \sin mx \sin ny$ gives:

$$(\partial^2/\partial z^2 - a^2)^2 \theta = nRa^2 \theta \quad (11)$$

where $a^2 = m^2 + n^2$. A solution which satisfies the boundary conditions at the bottom of the layer, $z = 0$, is:

$$\theta(z) = C_1 \sin Dz + C_2 \sinh Qz \quad (12)$$

where C_1, C_2 are arbitrary constants and $D = (\{Rn\}^{\frac{1}{2}} a - a^2)^{\frac{1}{2}}$, $Q = (\{Rn\}^{\frac{1}{2}} a + a^2)^{\frac{1}{2}}$.

Substituting (12) into the conditions at $z = 1$ gives:

$$\begin{aligned} C_1 (D \cos D + \bar{k} \sin D) + C_2 (Q \cosh Q + \bar{k} \sinh Q) &= 0 \\ -C_1 (Rn)^{\frac{1}{2}} a \sin D + C_2 (Rn)^{\frac{1}{2}} a \sin Q &= 0 \end{aligned} \quad (13)$$

The requirement for a non-trivial solution to (13) is that the determinant of the coefficients of C_1, C_2 vanish identically, this leads to:

$$-2\bar{k} = D \cot D + Q \coth Q \quad (14)$$

Solutions to (14) are given in Figure 1. as plots of R vs. a for several values of \bar{k} . The results in Figure 1. indicate that as \bar{k} approaches infinity \bar{R} , the critical Rayleigh number, approaches the value $4\pi^2$ determined by Lapwood (1978) for an isothermal upper boundary; whereas, as \bar{k} gets smaller, the critical Rayleigh number increases and corresponding semi-wavelength at $R = \bar{R}$ decreases. Figure 1 does point out however, that the effects are quite moderate. A change in \bar{k} by an order of magnitude from 10 to 100 changes \bar{R} by less than 5% and the corresponding change in a is of the same order. It is not until \bar{k} is of the order of unity that the effects become pronounced.

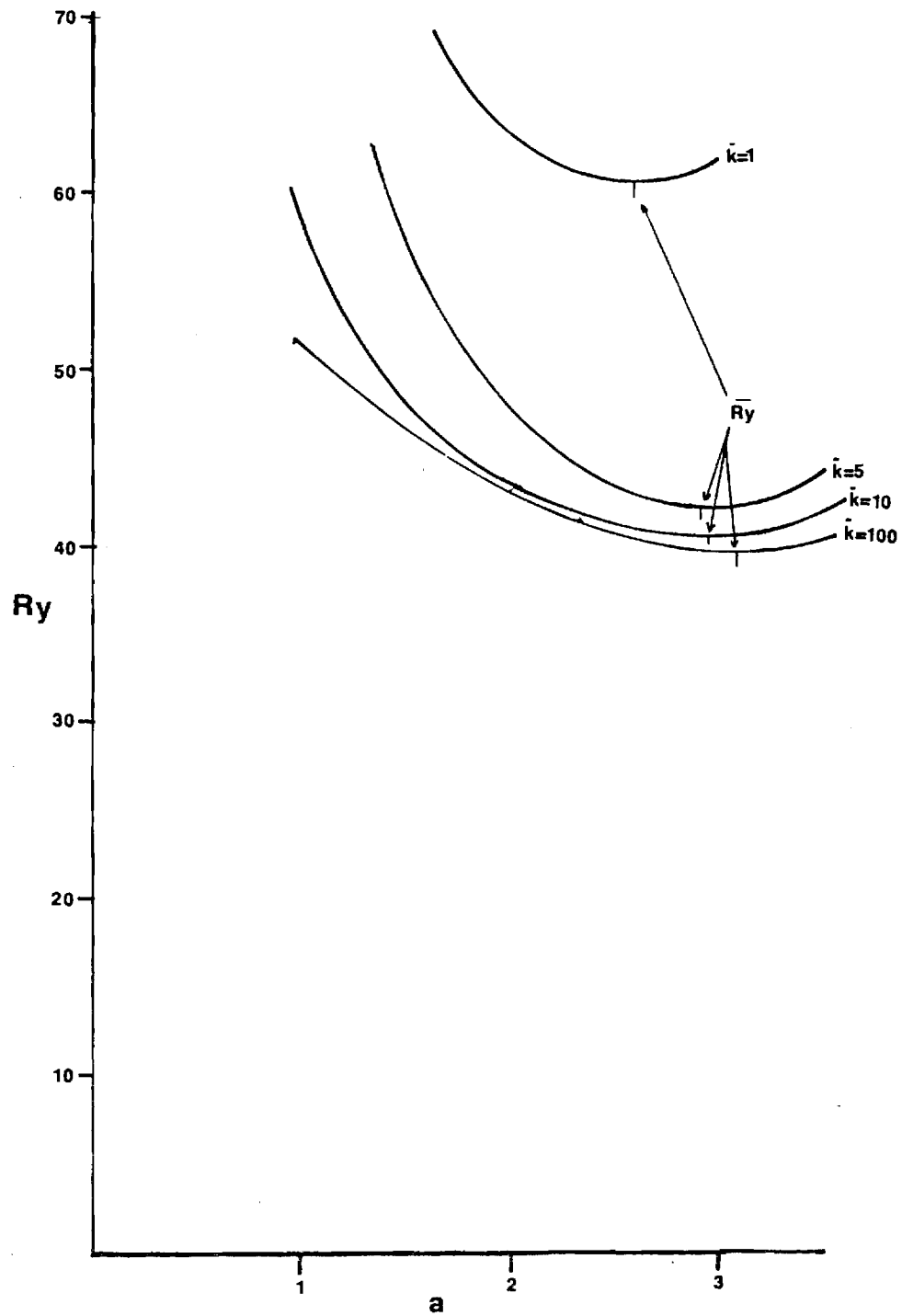


Figure 1. Rayleigh number versus semi-wavelength for isothermal bottom, rigid upper surface.

To interpret this result for a geothermal system, let the heat transfer coefficient $\Psi \approx \lambda' / d$ where λ' is the thermal conductivity of the impermeable cover and d is its thickness. \bar{k} is then given by: $\bar{k} = (\lambda' / \lambda) (h / d)$. Assuming a thickness ratio of 100, corresponding say to a cover of 30 meters overlying a 3 km deep convection system, and a thermal conductivity ratio of 0.25 gives $\bar{k} = 25$. In this range of \bar{k} , the effect of the low conductivity, impermeable caprock has little effect on the critical Rayleigh number or semi-wavelength at marginal instability consequently, it appears that a layer of impermeable caprock will have little effect on natural geothermal convection systems at marginal stability. The effect of imperfect heat transfer through impermeable cover under conditions of finite amplitude convection have not been investigated.

IV. Convection in Faults and Fracture Zones.

As discussed in section II, there are cases in which the permeability is not uniformly distributed throughout a large region of reservoir rock, but rather regions of high permeability may occur in association with certain geologic structures such as faults and fracture zones, the surrounding country rock being essentially impermeable. Figure 2. depicts a simple model of this situation.

A fair amount of work has been accomplished on the problem of the onset of convection in closed containers (e.g. Beck, 1972; Holst and Aziz, 1972; Zebib and Kassoy 1977; Lowell, 1978; Lowell and Shyu, 1978; Shyu, 1979). With the exceptions of Lowell and Shyu (1978) and Shyu (1979), all the work to date has assumed insulated vertical boundaries. The principal difference between the theory for the onset of convection in closed containers and the theory for the porous slab is that for a closed container additional velocity

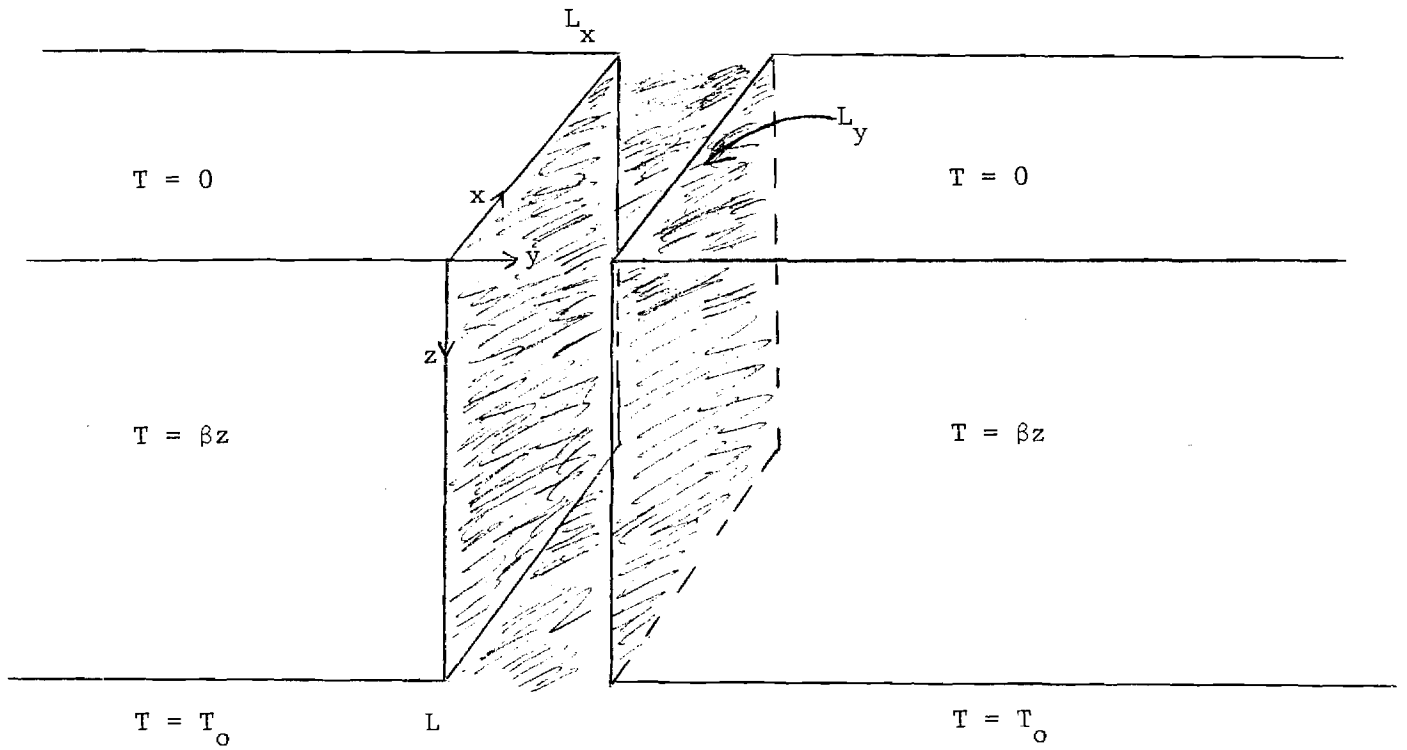


Figure 2. Model of Narrow Vertical Fault Zone

and temperature boundary conditions are required. The velocity conditions ususally take the form:

$$\vec{u} \cdot \hat{n} = 0 \quad \text{all walls} \quad (15)$$

whereas the temperature conditions are of the form:

$$T = 0 \quad (\text{conducting walls}) \quad (16a)$$

$$\partial T / \partial n = 0 \quad (\text{insulated walls}) \quad (16b)$$

$$\partial T / \partial n + \bar{k}T = 0 \quad (\text{imperfectly conducting walls}) \quad (16c)$$

Lowell and Shyu (1978) represents work done under this grant in which the walls transverse to the fault were assumed to be conducting and the walls at the end of the fault were assumed to be insulated. A preprint of this paper is attached as an Appendix to this report.

Shyu is in the process of carrying out further calculations on convection in fault zones, including some time dependent aspects of the circulation. The most complete way in which to include evolutionary processes is to solve the time dependent heat conduction equation in the impermeable rock surrounding the fault zone and add a time-dependent term to the energy and momentum equations discribing the processes within the fault zone. One might also wish to include non-linear convective heat transport terms. Such a complete solution represents a rather formidable task, and it is possible that a lumped parameter approach may provide useful approximate results. I believe that Shyu is carrying out such a calculation in conjunction with Galerkin finite-element techniques.

One of the purposes of this research is also to examine evolutionary aspects of convection in fault and fracture zones. Physical approximation methods, in conjunction with Laplace transforms, will be used, and possibly some explicit finite difference calculations as well. The exact approach used will depend somewhat on Shyu's results, which will be communicated to me within a month or so.

In the next section a very simple approximate calculation of the temporal evolution of convection in a fault is carried out.

V. Temporal Evolution of Convection in a Fault Zone.

Lowell (1975) has treated time dependent convection in a thin, open fracture filled with fluid using finite-difference methods. The results are reproduced in Figures 3 and 4. The Figures show that for a given fracture width d , both the water temperature and flow rate q fall off with time. h and h' represent the fracture depth and horizontal distances between the two vertical fractures, respectively (the vertical fractures are assumed to be connected by a thin horizontal fracture).

The basic equations of such a convecting fracture system are discussed in detail by Lowell (1975). They are:

$$\partial T_r / \partial t = a_r \partial^2 T_r / \partial y^2 \quad (17)$$

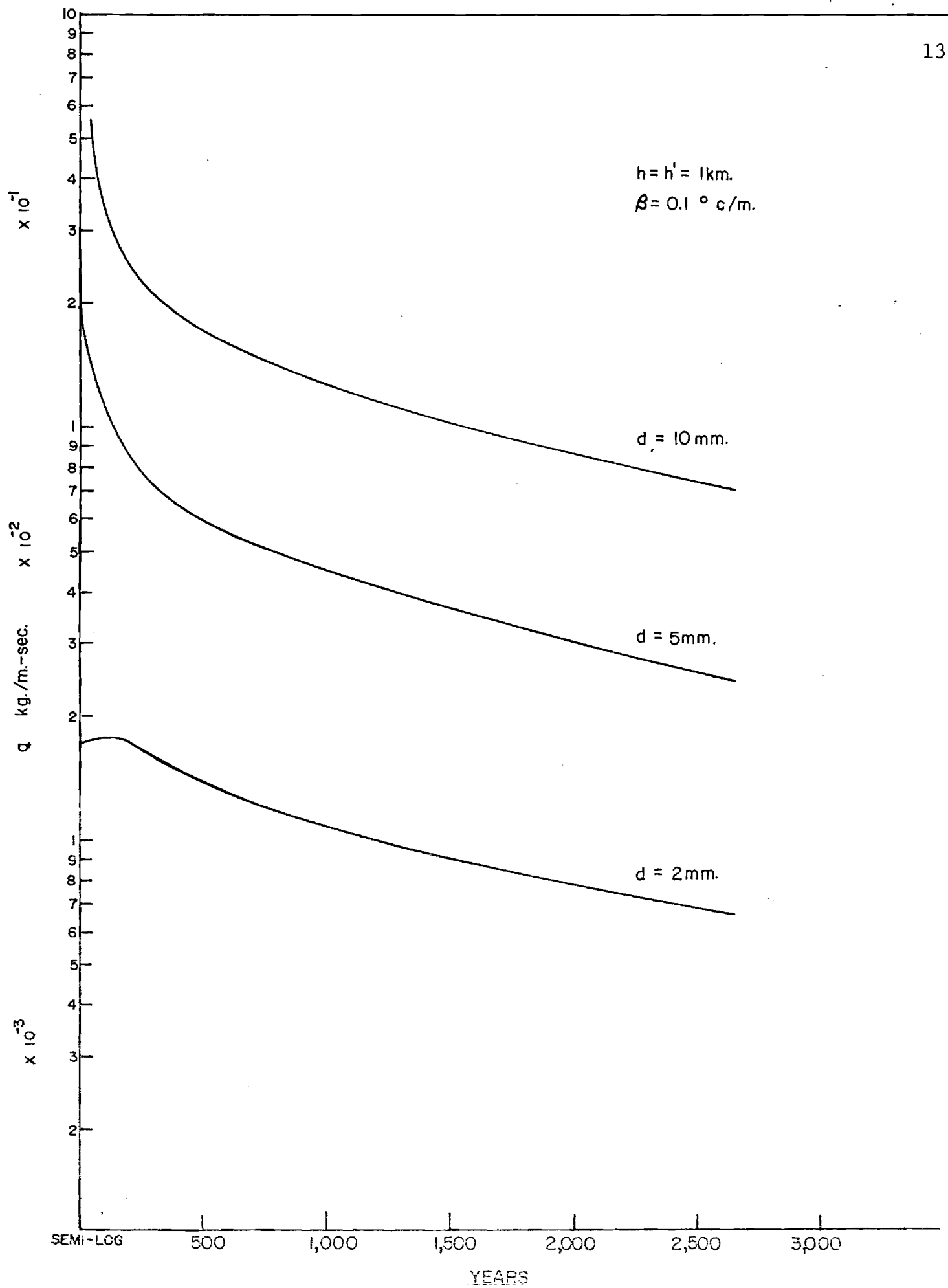
$$sq \partial T_w / \partial x = 2\lambda \partial T_r / \partial y \Big|_{y=0} \quad (18)$$

$$T_w = T_r \quad \text{at } y = 0 \quad (19)$$

$$T_w = 0 \quad \text{at } x = 0 \quad (20)$$

$$T_r = T_o \quad \text{at } t = 0 \quad (21)$$

$$q = \frac{Kd\alpha\rho_f}{\nu h} \int_0^h T_w(x,t) dx \quad (22)$$



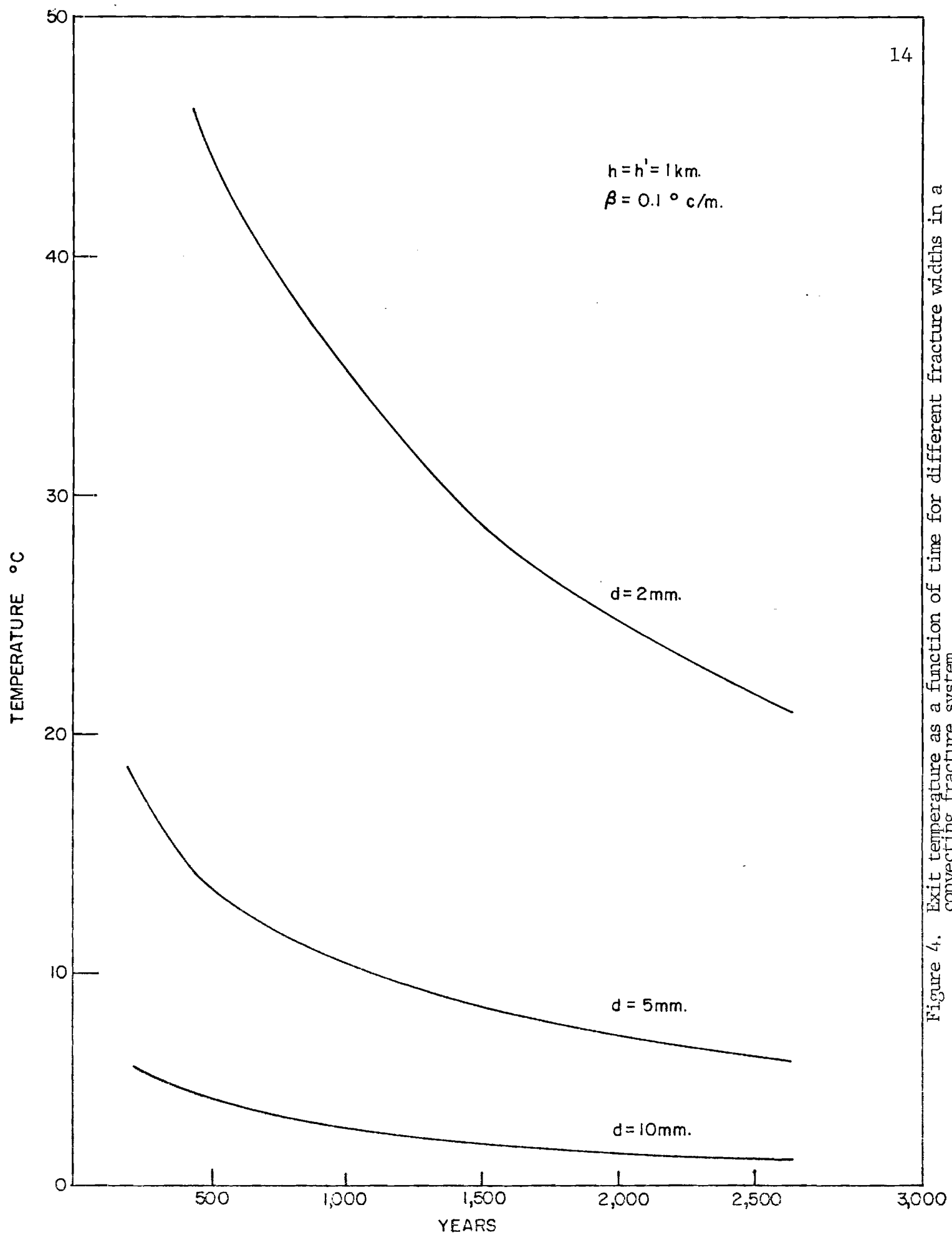


Figure 4. Exit temperature as a function of time for different fracture widths in a convecting fracture system.

where T_r is the rock temperature, T_w the water temperature, and a_r the rock thermal diffusivity. All the other parameters have been defined previously. Equation (17) is the equation for time-dependent heat conduction in the country rock. It has been assumed that conduction along the direction of fluid flow is negligible compared to conduction transverse to the fracture. Equation (18) states that the rate at which the moving fluid transports heat by convection is the same as the rate of conductive heat flow across the fracture walls. It is assumed that the fracture is so thin that the temperature is uniform across the fracture aperture. Equation (19) states the assumption of perfect thermal contact, i.e., the rock and fluid have the same temperature at the fracture boundary. Equation (20) and (21) give the boundary condition at the inlet to the fracture and the initial temperature condition in the rock. These conditions are chosen to be of this simple form for convenience and more realistic conditions have no great effect on the temporal development. Finally, equation (22) states that the flow q is given by Darcy's law, where the pressure head is the integrated buoyancy generated head resulting from the thermal expansion of the fluid ascending in the fracture. In the case of a single open fracture, K is replaced by $d^2/12$, as in the laboratory Hele-Shaw cell analogy of a permeable medium.

The principal difficulty in solving these equations analytically stems from the non-linearity which is apparent in combining equations (18) and (22). This non-linearity was the reason for resorting to finite difference techniques in Lowell (1975). In order to examine the temporal character of the solutions, however, we need not solve the entire system of equations. We can make use of separation of spatial and temporal variables, as well as the observation that the time dependence enters only through the time dependent character of the heat flux from the rock into the fracture.

The heat conduction across the fracture/rock interface can be looked at simply as conductive cooling of a half-space with initial temperature T_0 . Thus from Carslaw and Jaeger (1959, p. 61), $\lambda \partial T_r / \partial y|_{y=0} = \lambda T_0 (\pi a_r t)^{-1/2}$. Combining this together with equations (18) and (22), and writing

$T_w(x, t) = X(x)\theta(t)$ gives:

$$\rho_f \frac{saKg d}{v h} \int_0^h X(x) \partial x \frac{\partial X}{\partial x} (\theta(t))^2 = 2\lambda T_0 (\pi a_r t)^{-1/2} \quad (23)$$

this gives a time dependence:

$$\theta(t) \propto t^{-1/4} \quad (24)$$

Moreover from (22), it is clear that q , and θ have the same time dependence, thus:

$$q \propto t^{-1/4} \quad (25)$$

Also, the rate of heat transport from the system, H , is

$$H \propto q \theta \propto t^{-1/2} \quad (26)$$

as should be expected. The simple results indicated by (24) and (25) are in fact confirmed by the finite difference calculations which show that T and q fall off with the same time dependence.

Bodvarsson (1978) has also examined the evolutionary aspect of the fracture flow system from similar physical reasoning. He treats the single open fracture case and includes an approximate treatment of time dependent thermal expansion of the fracture aperture. His results are in agreement with the ones presented here, although there is a misprint in his equations (54), (55) and (56). Further work is needed on the evolutionary aspects of these systems, including temporal changes in permeability.

VI. Work Plan for Coming Report Period.

The most important task in the coming period will be to examine the evolutionary aspects of fracture systems in greater detail, possibly by finite difference methods. This will include a closer look at thermoelastic

processes than has been given by Bodvarsson (1978). Some preliminary attempts will be made to relate these results to geothermal systems of the type encountered in the Basin and Range.

VII. Students Supported and Theses.

1. Mr. James K. Fulford has done most of the work regarding the onset of convection in a porous layer bounded above by a thin, but finite, impermeable layer. Mr. Fulford completed his M. S. Thesis recently and currently is a doctoral student in the Atmospheric Sciences program at Georgia Tech.

2. Mr. James Herbert is a new graduate student, has been supported since 9/15/78. He has been doing preliminary studies required before taking a more contributory role in the project.

M. S. Thesis: Mr. James K. Fulford, Thermal Convection in a Porous Media with Application to Hydrothermal Circulation in the Oceanic Crust, 54 pp., 1979.

VIII. Papers and Publications.

1. Lowell, R. P., C. H. Chen, and J. K. Fulford, 1978, On transient temperature inversions in geothermal boreholes, in: Geothermal Resources Council Symposium Proceedings, July, 1978, Hilo, Hawaii, p. 407-409.
2. Lowell, R. P. and T. C. Shyu, The onset of convection in a water-saturated porous box: effect of conducting walls, Letters in Heat and Mass Transfer, 5, 371-378.
3. Lowell, R. P., 1978, Heat transfer Processes Related to Fluid Flow in Fractured Rock, Presented at Penrose Conference on Heat Transport Processes in the Earth, Vail, Colorado, Nov. 12-16, 1978.

Bibliography

- Beck, J. L., 1972, Convection in a box of porous material saturated with fluid, Physics of Fluids, 15, 1377-1383.
- Bodvarsson, G., 1978, Convection and thermoelastic effects in narrow vertical fracture spaces with emphasis on analytical techniques, Final Report, USGS Grant #14-08-0001-G-398., 111p.
- Holst, P. H. and K. Aziz, 1972 Transient three-dimensional natural convection in confined porous media, Int. J. Heat and Mass Transfer, 15, 73-90.
- Hose, R. K. and B. E. Taylor, 1974, Geothermal systems of northern Nevada, U. S. Geological Survey, Open-file report, 74-271, 27 pp.
- Kassoy, D. R. and A. Zebib, 1975, Variable viscosity effects on the onset of convection in porous media, Phys. Fluids, 18, 1649-1671.
- Lapwood, E. R., 1948, Convection of a fluid in a porous medium, Proc. Cambridge Phil. Soc., 44, 508-521.
- Lowell, R. P., 1975, Circulation in fractures, hot springs and convective heat transport on mid-ocean ridge crests, Geophys. J. Roy Astr. Soc., 40, 351-365.
- Lowell, R. P., 1978, Convection and thermoelastic effects in narrow vertical fracture spaces with emphasis on numerical techniques, Final Technical Report, USGS Grant #14-08-0001-G-365, 19p.
- Lowell, R. P. and C. T. Shyu, 1978, On the onset of convection in a water-saturated porous box: effect of conducting walls, Letters in Heat and Mass Transfer, 5, 371-378.

- Nield, D.A., 1968, Onset of thermohaline circulation in a porous medium, Water Resources Res., 4, 553-560.
- Shyu, C. T., 1979, Numerical Analysis of Thermal Convection in Porous Slabs, Ph.D. Thesis, Oregon State University (in preparation).
- Sleep, N. H. and T. J. Wolery, 1978, Egress of hot water from mid-ocean ridge hydrothermal systems: some thermal constraints, J. Geophys. Res., 83, 5913-5922.
- Straus, J.M. and G. Schubert, 1977, Thermal convection of water in a porous medium: effects of temperature and pressure dependent thermodynamic and transport properties, J. Geophys. Res., 82, 325-334.
- White D. E. and D. L. Williams, editors, 1975, Assessment of Geothermal Resources of the United States - 1975, U. S. Geological Survey Circular 726.
- Wooding, R. A. 1976, Influence of anistropy and variable viscosity upon convection in a heated saturated porous layer. Applied Mathematics Division, Tech Report No. 55, Dept. of Scientific and Industrial Research, Wellington, N.Z., 23 p.
- Zebib, A. and D. R. Kassoy, 1977, Onset of natural convection in a box of water-saturated porous media with large temperature variation, Phys. Fluids, 20, 4-9.

APPENDIX

ON THE ONSET OF CONVECTION IN A WATER-SATURATED
POROUS BOX: EFFECT OF CONDUCTING WALLS

Robert P. Lowell¹ and Chuen-Tien Shyu²

1. School of Geophysical Sciences, Georgia Institute of Technology
Atlanta, Georgia 30332
2. School of Oceanography, Oregon State University, Corvallis, Oregon
97331

ABSTRACT

The critical Rayleigh number for the onset of convection in a water-saturated porous box, heated from below, has been determined by the Galerkin method and by an approximate analytical technique. The present problem differs from previous ones which have been published in that we consider the effect of conducting vertical boundaries on the critical number and on the cell pattern at the critical number. Moreover, we emphasize fault or fracture zone-like box geometries; that is, geometries in which one box dimension is much shorter than the other and much shorter than the height.

The results indicate that for fault/fracture zone geometries, in which the long vertical walls are conducting and the short end walls are insulated, the critical Rayleigh number is roughly four orders of magnitude greater than the critical number for a horizontal porous slab. The flow at the onset of convection takes the form of a roll with its axis along the long horizontal dimension of the box. There is, however, little difference between the critical numbers for two and three dimensional cell patterns. These results indicate that convection may occur in naturally occurring faults and fracture zones in the earth's crust only if the permeability is of the order of Darcies. In natural systems, the Rayleigh number would probably not exceed the critical number greatly, and the flow may tend to be fully three dimensional.

The onset of convection in a closed rectangular container of water-saturated porous material with uniform properties has been treated by Beck (1), and the case of a variable viscosity fluid has been treated by Zebib and Kassoy (2). These authors have considered various box geometries, but they have assumed that the vertical walls of the box are insulated. In many practical situations, however, such as in geothermal systems controlled by fault and fracture zones, the assumption of insulated vertical walls is not realistic. We wish to consider the effect of conducting walls on the critical Rayleigh number and on the cell pattern at the critical Rayleigh number. Moreover, we will emphasize a fault or fracture controlled geometry; that is, we will emphasize porous container geometries in which one horizontal dimension is much shorter than the other and much shorter than the height. We will assume that the long walls are conducting but that the short, end-walls are insulated. We will then discuss the possibility of convection taking place in natural faults or fractures in the earth's crust.

Davis (3) and Catton (4) have treated the similar problem of convection in a rectangular container having conducting walls and being filled with viscous fluid.

Analysis

Consider a container of water-saturated porous material of height L and with horizontal dimensions L_1 and L_2 . Let a uniform thermal gradient, β , be applied to the material such that the temperature at the upper surface is $T = T_s$ and the temperature at the lower surface is $T = T_o$ ($T_o > T_s$). The initial state is assumed to be one of pure thermal conduction such that initially

$$\vec{v} = 0, T = T_s + \beta z, dP^*/dz = \rho_f g$$

where \vec{v} is the velocity, P^* the pressure, ρ_f the density of the fluid and g the acceleration due to gravity. The z axis assumed to be positive downwards.

The condition for the onset of convection is found by the principle of exchange of stabilities. That is, infinitesimal perturbation of the initial state leads to a marginally stable state of steady thermal convection. The linearized, non-dimensional, marginal stability equations, using the Boussinesq approximation are (5)

$$\nabla \cdot \vec{q} = 0 \quad (1)$$

$$\vec{q} + R^{\frac{1}{2}} \hat{k} + \nabla P = 0 \quad (2)$$

$$\nabla^2 \theta - R^{\frac{1}{2}} q_z = 0 \quad (3)$$

where $\vec{q} = (q_x, q_y, q_z)$ is the perturbation velocity, θ is the perturbation temperature, P is the perturbation pressure, and \hat{k} is a unit vector in the z direction. R is the dimensionless Rayleigh number given by

$$R = \rho_f s \alpha g K L^2 / \nu \lambda$$

where s is the specific heat of the fluid, α its thermal expansion coefficient, ν its kinematic viscosity, K the permeability of the rock and λ its thermal conductivity. These equations are to be solved with temperature conditions,

$$\partial \theta / \partial x = 0 \text{ at } x = 0, H_1 \quad (4)$$

$$\theta = 0 \quad \text{at } \begin{matrix} y = 0, H_2 \\ z = 0, 1 \end{matrix} \quad (5)$$

where H_1 and H_2 are dimensionless horizontal lengths. Assuming impermeable boundaries, the velocity conditions are

$$\vec{q} \cdot \hat{n} = 0 \quad (6)$$

on all boundaries, where \hat{n} is the unit vector, normal to the wall.

Equations (1) through (3) with conditions (4) through (6) constitute an eigenvalue problem for the Rayleigh parameter, the smallest eigenvalue being the critical Rayleigh number for the onset of convection.

The set of equations and boundary conditions above are not separable, and consequently the normal solution procedures break down. One method of determining the critical Rayleigh number for problems of this type is the Galerkin method. To use this method, we first eliminate \vec{q} and P from the perturbation equations to obtain a single equation for θ . We obtain

$$\nabla^4 \theta + R \nabla_h^2 \theta = 0 \quad (7)$$

where ∇_h^2 is the horizontal Laplacian. We then select a set of trial functions θ_i which satisfy the temperature and the velocity boundary conditions. We substitute

$$\theta = \sum_{i=1}^N c_i \theta_i$$

into (7) and apply the Galerkin criterion. That is,

$$\sum_{i=1}^N \int C_i [\nabla^2 (\nabla^2 \theta_i) + R \nabla_h^2 \theta_i] \cdot \theta_k dV = 0 \quad (9)$$

24

where the integral (9) is carried out over the volume of the box, and θ_k is one component of the set of trial functions θ_i . Substitution of the particular trial functions into (9) gives rise to a matrix equation of the form

$$M_A \vec{C} = R M_B \vec{C} \quad (10)$$

and the condition for a non-trivial solution is that the determinant of the coefficients be zero. That is:

$$|M_A^{-1} M_B - R^{-1} I| = 0$$

Equation (11) represents an eigenvalue problem for the Rayleigh number R ; and the minimum eigenvalue found, $R = R_c$, represents the critical condition for the onset of convection. The results for the critical Rayleigh number, for different box geometries are given in Table 1.

TABLE 1
Critical Rayleigh Numbers 2-D and 3-D Convection
in a Porous Box With Two Vertical Conducting Walls

$H_2 \downarrow$	2-D ($i=0$)	$H_1 \rightarrow$ 1	5	3-D 10	20	50
0.01	446831.6	446835.7	446832.1	446832.1	446832.1	446832.1
0.05	17485.16	17488.8	17485.4	17485.3	17485.26	17485.2
0.1	4327.77	4331.35	4327.92	4327.81	4327.75	4327.78
0.5	212.75	216.34	212.90	212.70	212.68	212.69
1.0	83.22	86.07	83.48	83.36	83.34	83.32
1.5	60.50	61.73	60.58	60.52	60.50	60.50
3	43.57	40.85	40.86	40.61	40.66	40.66
5	41.01	39.61	39.62	39.62	39.60	39.60
10	39.87	39.48	39.48	39.49	39.49	39.49
50	39.48	39.48	39.48	39.48	39.48	39.48

Table 1 shows several interesting features of convection in a box with two conducting walls. First, it is clear that for large box dimensions, the wall conditions become immaterial and the critical number approaches the value $4\pi^2$ given by Lapwood (5) for an infinite slab. Secondly, if the conducting walls are far apart ($H_2 \gg 2$), three dimensional motion is preferred over two dimensional at the onset of convection; and as the separation between the insulated walls increases ($H_1 \rightarrow \infty$), the three-dimensional values of R_c approaches the two-dimensional values. This suggests that in natural systems the motions may tend to be fully three-dimensional rather than roll-like in character. Moreover, these results suggest that at finite amplitude (*i.e.*, $R > R_c$) the two-dimensional solutions may be unstable and the motion at finite amplitude may become three-dimensional. Lastly, in the case of a fault/fracture zone geometry ($H_2 \ll 1$, $H_1 \geq 1$), Table 1 shows that R_c is several orders of magnitude greater than the value $4\pi^2$ for an infinite slab, and the motion at $R = R_c$ takes the form of a roll with its axis parallel to the long horizontal dimension of the box. This is contrary to the results of Beck (1) who showed that, for insulated walls, the rolls were aligned with their axes parallel to the short side of the box.

The results in Table 1 for a fault/fracture zone geometry are in reasonable agreement with an approximate analytical result derived by Lowell (6). The analytical calculations were performed by relaxing the velocity boundary conditions on the vertical walls. If one replaces the condition $q_y = 0$ at $y = 0, H_2$ with $\partial q_z / \partial z = 0$ at $y = 0, H_2$, the eigenfunctions become separable, and equation (7) can be solved by standard methods. In this case, with $H_1 \rightarrow \infty$, $H_2 \ll 1$, Lowell (6) obtains:

$$R_c = 4\pi^2 / H_2^2$$

With $H_2 = 0.01$, $R_c = 4 \times 10^5$, which is about ten percent smaller than the value found by the Galerkin method. This underestimate of R_c is to be expected in view of the fact that the boundary conditions were less restrictive in the analytical calculations than in the Galerkin method. The analytical results also show that the flow at $R = R_c$ takes place as a roll with its axis along the strike of the fault.

Geophysical Implications

Table 1 shows that in a closed container of water-saturated porous material with a fault or fracture zone geometry, *e.g.*, with $H_2 = 0.01$, the

critical Rayleigh number is nearly 4.5×10^5 . Are such high Rayleigh numbers possible in natural systems? Assuming a temperature gradient $\beta = 100^\circ\text{C}/\text{km}$ and a fault depth of 3 km, which are reasonable for a geothermal region, we estimate values of the physical parameters from Straus and Schubert (7): $\rho_f s = 1 \text{ cal}/\text{cm}^3 - ^\circ\text{C}$, $\alpha = 1.5 \times 10^{-3}/^\circ\text{C}$, $\nu = 2 \times 10^{-3} \text{ cm}^2/\text{sec}$, $\lambda = 5 \times 10^{-3} \text{ cal}/\text{cm} - ^\circ\text{C} - \text{sec}$. α, ν, λ are average values over the depth range. Substituting these parameters into the Rayleigh number gives $K \approx 3 \times 10^{-8} \text{ cm}^2$, for the onset of convection in a 30 m wide fault zone. This is quite a high, but not unrealistic value, for the permeability in a fault zone mainly arises from interconnected fractures within the rock volume; and assuming a permeability due to a series of flat parallel fractures of width d and separation h , Bear (8, p. 164) has shown that

$$K = d^3/12h$$

This, if $K = 3 \times 10^{-8} \text{ cm}^2$, $h = 100 \text{ cm}$, then $d = 3.3 \times 10^{-2} \text{ cm}$. Fractures on this scale do not appear unreasonable for a fault or fracture zone in the earth's crust. One might expect, however, that if convection occurs in such systems, that the actual Rayleigh number lies rather close to the critical number.

Finally, we emphasize that the assumption of a uniform thermal gradient along the walls is only appropriate as a condition for the onset of convection in a natural fault or fracture zone. As convection proceeds in time, at values of $R > R_c$, and heat is conducted through the vertical boundaries, the gradient in the adjacent impermeable rock matrix will not be maintained. In time there will be a decrease in the lateral gradient across the walls, and hence the walls will tend to have the appearance of insulated boundaries. For this reason, one might expect convection to become somewhat more vigorous, and perhaps to change its cell pattern, after convection is initiated. At large times, however, the convective flow may decline since the driving temperature gradient is reduced. In summary, the finite-amplitude, time dependent aspects of convection in a porous container with conducting walls may be somewhat more complicated than in containers with insulated walls. An examination of these problems will be a subject of future research.

Acknowledgments

This research was supported by the U. S. Geological Survey, Department of Interior under USGS Grant No. 14-08-0001-G-365.

Nomenclature

27

- \vec{C} - vector of expansion coefficients of trial solutions
- C_i - component expansion coefficients of trial solutions
- d - fracture width
- g - acceleration due to gravity
- h - fracture separation
- H_1, H_2 - dimensionless horizontal box lengths
- K - permeability of rock
- \hat{k} - unit vector in z direction
- L - dimensional box height
- L_1, L_2 - horizontal box dimensions
- M_A, M_B - matrices arising in Galerkin formulation
- \hat{n} - unit vector in z direction
- P - dimensionless perturbation pressure
- P^* - dimensional fluid pressure
- \vec{q}, q_x, q_y, q_z - dimensionless perturbation velocity, and cartesian components
- R - dimensionless Rayleigh number
- R_c - critical Rayleigh number
- s - specific heat of fluid
- T - temperature
- T_o - temperature at base of box
- T_s - temperature at surface
- \vec{v} - Darcy velocity of fluid
- x, y, z - cartesian coordinates, z positive downwards
- α - thermal expansion coefficient
- β - geothermal gradient
- θ - dimensionless perturbation temperature
- θ_i, θ_k - trial temperature function in Galerkin formulation
- λ - thermal conductivity of saturated material
- ν - kinematic viscosity of fluid
- ρ_f - fluid density

REFERENCES

1. J. L. Beck, Phys. Fluids, 15, 1377 (1972).
2. A. Zebib and D. R. Kassoy, Phys. Fluids, 20, 4 (1977).
3. S. H. Davis, J. Fluid Mech. 30, 465 (1967).
4. I. Catton, Jour. Heat Transfer, 92, 186 (1970).
5. E. R. Lapwood, Proc. Cambridge Phil., Soc. 44, 508 (1948).
6. R. P. Lowell, Semi-annual technical letter report no. 1, USGS grant #14-08-0001-G-365, 10p (1977).
7. J. M. Straus and G. Schubert, J. Geophys. Res., 82, 325 (1977).
8. J. Bear, Dynamics of Fluids in Porous Media, Elsevier, New York, 764p (1972).

Semi-Annual Technical Letter Report No. 2

Grant No: 14-08-0001-G-540

Reporting Period Covered: 1/1/79 - 6/30/79

Grantee: Georgia Institute of Technology

Supported by: U.S. Geological Survey
Geothermal Research Program
Reston, Virginia

Grant Amount: \$30,777.00

Start Date: 7/1/78

Expiration Date: 12/31/79

Principal Investigator: Robert P. Lowell

U.S.G.S. Technical Officer: Donald W. Klick

Date Submitted: July 31, 1979

Title of Research Project: Convection in Narrow Vertical Fracture
Spaces

Objectives of Project: The main purpose of this project is to examine thermal convection in long, deep, but very narrow vertical fracture spaces. The initiation and time development of the physical processes are to be studied on the basis of mathematical-physical approximation methods and numerical techniques. The results are to be interpreted with regard to known geothermal systems in the Basin and Range and other areas where faults or fractures are the dominant controlling structures.

I. Introduction

This document represents the second semi-annual technical report on our research on convection in faults and fracture zones and some related problems. This work represents a continuation of the effort which was initiated under the USGS grant number: 14-08-0001-G-365 as part of the Extramural Geothermal Research Program of the U. S. Geological Survey. The initial phase of the work was done in conjunction with Dr. G. Bodvarsson of Oregon State University; however, his group is not directly involved in the present research effort. The present research is being conducted under grant #: 14-08-0001-G-540.

The principal achievements during the past six months have been to:

- (1) expand the work done previously on the effect of anisotropic permeability on the onset of convection in a fault or fracture zone and
- (2) develop further the work on the temporal evolution of convection in fractures, which was outlined briefly in the first technical letter report, to include thermoelastic effects in a series of parallel fractures. The study of anisotropic permeability has culminated in a paper to be included in the transactions of the Geothermal Resources Council Annual Meeting which is to be held in Reno, Nevada, in September, 1979. Preprints of this paper have been sent under separate cover; and, for convenience, one is also attached as an Appendix to this report.

The main body of the report which follows is divided into subsections: II. General Framework and Objectives; III. Convection in a Fault or Fracture Zone; IV. Temporal Evolution of Convective Flow in Fractures: Thermoelastic Effects; V. Bibliography; VI. Work Plan for

the Coming Report Period; VII. Students Supported; VIII. Papers and Publications.

II. General Framework and Research Objectives

The energetics of geothermal systems depend fundamentally upon patterns of heat transport and fluid flow within heated, highly permeable regions of the earth's crust. The ultimate source of heat for many geothermal systems is undoubtedly of magmatic origin; but in some cases, the geothermal fluid is heated at depth as a result of an unusually high geothermal gradient. Most of the systems in the Basin and Range Province are probably of the latter type (White and Williams, 1975).

Of even more importance, however, is the nature and distribution of permeability within the geothermal reservoir. The permeability may either be primary, resulting from interconnected pore spaces within the rock volume or secondary, resulting from fractures and/or fault zones. In all geothermal fields currently under production, the geothermal fluids are withdrawn from discrete fractured regions within the reservoir, yet most mathematical modeling of geothermal systems has assumed a Darcian type of flow through a rock with a bulk permeability. That is not to say that it has been necessarily assumed that the permeability is of a primary type, but rather that one normally assumes the fractures to be on such a fine scale that, for mathematical (or numerical) convenience, the Darcy flow model is appropriate on spatial scales of the order of the reservoir dimensions (or finite element/difference grid spacing).

The mathematical treatment for the onset of thermal convection

under such assumptions follows the method of Lapwood (1948), or some deviant of it; and the treatment of finite amplitude convection uses the same basic perturbation equations with the addition of higher order, non-linear transport terms which are neglected in the linear stability analysis. These models have provided many useful results with regard to the physics of geothermal systems, but often this approach may be quite unrealistic. Geothermal systems in which main permeability is furnished by narrow, discrete, widely separated fault and/or fracture zones imbedded in an otherwise impermeable rock are better handled by somewhat different techniques. Examples of the latter systems are found in Iceland, where dikes provide the main vertical permeability, in the Basin and Range, where long, deep, master faults probably provide the main vertical permeability (Hose and Taylor, 1974), and possibly in the oceanic crust (Lowell, 1975; Sleep and Wolery, 1978).

The principal purpose of this research is to examine thermal convection in long, deep, but very narrow vertical fracture spaces. The initiation and temporal evolution of the physical processes are to be studied on the basis of mathematical-physical approximation methods and finite element and/or finite difference techniques. The results are to be interpreted with regard to known geothermal systems in the Basin and Range and other regions where major faults and fractures are the structures controlling the permeability.

III. Convection in a Fault or Fracture Zone

A. Anisotropic Permeability

The basic equations for the onset of convection in a porous layer

have been derived by Lapwood (1948) and have been reproduced in the case of an anisotropic, porous box by Lowell (1977, 1979b). Only the most essential equations will be given here. In a Cartesian coordinate system with the x axis along the strike of the fault, the y axis perpendicular to it, and the z axis directed positively downward, they are:

$$Rw = \nabla^2 T \quad (1)$$

$$\partial \sigma (\partial w / \partial z) / \partial z + \{ (1/\gamma_1) \partial^2 / \partial x^2 + (1/\gamma_2) \partial^2 / \partial y^2 \} (T + \sigma w) = 0 \quad (2)$$

where w is the dimensionless vertical velocity and T is the dimensionless temperature and where

$$\sigma = (K_0/K_3) (v/v_0); \quad \gamma_1 = K_3/K_1; \quad \gamma_2 = K_3/K_2$$

and the Rayleigh parameter R is

$$R = \rho_f s \alpha \beta g L_z^2 K_0 / v_0 \lambda$$

The symbols are defined in Table 1. Equations (1) and (2) are to be solved subject to the boundary conditions:

$$\vec{u} \cdot \hat{n} = 0 \text{ at all walls} \quad (3)$$

$$T = 0 \text{ at } z = 0, 1 \quad (4)$$

with temperature conditions specified on the vertical walls as:

$$\partial T / \partial x = 0 \text{ at } x = 0, a; \quad a = L_x / L_z \quad (5)$$

$$\partial T / \partial y = 0 \text{ at } y = 0, b; \quad b = L_y / L_z$$

Table 1

Definition of Symbols

g - acceleration of gravity

K_0, K_1, K_2, K_3 - permeability at $z = 0$ and permeability in x, y, z directions respectively.

L_x, L_y, L_z - dimensions of fault zone.

s - specific heat of fluid.

α^* - thermal expansion coefficient.

β^* - applied temperature gradient.

λ - thermal conductivity of rock.

ρ_f - density of fluid.

ν_o, ν - kinematic viscosity of the fluid, o refers to value at $z = 0$.

for insulated walls or

$$\partial T / \partial x = 0 \text{ at } x = 0, a \quad (6)$$

$$T = 0 \text{ at } y = 0, b$$

corresponding to conducting walls on the boundary parallel to the strike of the fault.

Assuming $\sigma = 1$ and combining (1) and (2) into a single equation for T and substituting

$$T = \sin \pi z \cos \alpha x \cos \beta y \quad (7)$$

for conditions (5) or

$$T = \sin \pi z \cos \alpha x \sin \beta y \quad (8)$$

for conditions (6) where $m = \pi a$; $n = \pi b$ leads to an equation for R .

$$R = \left\{ \pi^4 + \pi^2 (\alpha^2 (1 + 1/\gamma_1) + \beta^2 (1 + 1/\gamma_2)) + (\alpha^2/\gamma_1 + \beta^2/\gamma_2)(\alpha^2 + \beta^2) \right\} (\alpha^2/\gamma_1 + \beta^2/\gamma_2)^{-1} \quad (9)$$

The problem is then to determine the minimum value of R for given values of a, b, γ_1, γ_2 and to find the cell patterns for minimum R ($R=R_c$).

The results for $\gamma_1 = \gamma_2$ for insulated or conducting boundaries are discussed in the manuscript which is attached as an Appendix and will not be discussed further here. A few other special cases are discussed here.

1. insulated walls; $\gamma_1 = \gamma, \gamma_2 \rightarrow \infty$.

In this case, the transverse horizontal permeability is negligible compared to the horizontal permeability along the strike of the fault. Since there can be no flow transverse to the fault, the cell pattern must take the form of rolls with axes parallel to the short side. Putting $\beta = 0$ in (9) leads to

$$R = \pi^2 \left\{ \gamma \left(1 + \frac{a^2}{m^2} \right) + \frac{m^2}{a^2} + 1 \right\} \quad (10)$$

which is the same result as obtained for insulated walls with $\gamma_1 = \gamma_2$ (Lowell, 1977). The point is that as long as the walls are insulated, the flow is in the form of two-dimensional rolls, independent of the y direction. Thus, if the walls are insulated, the critical Rayleigh number is independent of the permeability perpendicular to the strike of the fault zone.

2. conducting walls; $\gamma_1 = \gamma, \gamma_2 \rightarrow \infty$.

Even if the walls are conducting, the absence of transverse permeability requires the flow to be two-dimensional rolls with axes along the y direction. The approximate solution procedure based on T given by (8) breaks down. The form for the Rayleigh number cannot be determined by the present methods, although it is expected that R_c should still be much higher in the case of conducting walls than in the case of insulated walls, and probably higher than in the case of finite transverse permeability.

3. insulated walls; $\gamma_1 \rightarrow \infty, \gamma_2 = \gamma$.

The physical situation treated here is offered mainly for completeness; it is not likely to be realized in a natural setting. This case leads to a two-dimensional flow pattern in which the flow is independent of x; that is, the axes of the rolls are along the strike of the fault zone. In this case (9) reduces to

$$R_c = 4\pi^2/b^2\gamma \quad (11)$$

Since $b \ll 1$, this result shows that R_c is much greater in the case of zero longitudinal permeability than in the case of zero transverse permeability. The result (11) also holds for conducting walls.

B. Numerical Modeling

An important aspect of the present research program is to develop numerical models of convection in fault zones using the method of finite differences. The proposed work will follow, in part, the work of Shyu (1979) who treated several two-dimensional models using the finite element method. The emphasis in the current program will be to examine three-dimensional models in order to deduce the most likely form of the cell pattern and its possible temporal evolution. It is hoped that the present conflict, which has arisen in the work of Lowell and Shyu (1978), Shyu (1979), and Murphy (1979), as to the appropriate cell structure will be resolved. This work is still in its formative stages, hence no results are reported here.

IV. Temporal Evolution of Convective Flow in Fractures: Thermoelastic Effects.

In a previous report (Lowell, 1979a), an approximate treatment of the temporal dependence of the temperature and the flow in a convecting fracture was developed. It was shown that the temperature and the flow rate both decreased as $t^{-1/4}$. Bodvarsson (1978) reached a similar conclusion, but he also examined the effect of thermal expansion or contraction on the fracture width. Using a one-dimensional model for a single fracture imbedded in a half-space, Bodvarsson (1978) showed that the fracture width varied as $t^{1/2}$. Since the flow rate is proportional to the cube of the fracture width, one obtains from Lowell (1979a), where the permeability $K = d^2/12$, the result:

$$\theta^2 d^3 \propto t^{-1/2} \quad (12)$$

or

$$\theta \propto t^{-1}$$

and $q \propto d^3 \theta$ (13)

so $q \propto t^{1/2}$

Results (12) and (13) are also in agreement with Bodvarsson (1978).

To represent a natural geothermal system by a single, isolated fracture, however, is a great over simplification in some cases. Even though fractures furnish the main permeability, there may be several closely spaced fractures; and the thermal interference between the fractures substantially alters the thermoelastic behavior. In particular, one would not expect a monotonic, $t^{1/2}$ dependence for the fracture width.

To illustrate the thermal interference effect, consider the conductive heating of a region bounded by two infinite parallel planes separated by a distance $2h$. Let the bounding temperatures be T_0 and the initial temperature be $T = 0$. Then in the region $-h < x < h$, the temperature can be written (Carslaw and Jaeger, 1959 p. 100 and p. 309).

$$T = T_0 - \frac{4T_0}{\pi} \sum_{n=0}^{\infty} \frac{(-1)^n}{2n+1} \cos(2n+1)\pi x/2h \cdot \exp(-a(2n+1)^2 \pi^2 t/4h^2) \quad (14)$$

or

$$T = T_0 \sum_{n=0}^{\infty} (-1)^n \operatorname{erfc} \frac{(2n+1)h-x}{2\sqrt{at}} + T_0 \sum_{n=0}^{\infty} (-1)^n \operatorname{erfc} \frac{(2n+1)h+x}{2\sqrt{at}} \quad (15)$$

where (14) is rapidly convergent at large times and (15) is most rapidly convergent for small times. Using a one-dimensional formalism for the thermal expansion of the slab (Bodvarsson, 1976), the displacement u is:

$$u = \frac{5\alpha^*}{9-h} \int_{-h}^0 T(x,t) dx \quad (16)$$

where α^* is the thermal expansion coefficient, and the factor 5/9 comes about by assuming Poisson's relation between the elastic constants. Substituting the temperature fields (14) and (15) into (16) gives

$$u = 5 \alpha^*/9 \left\{ T_0 h - \frac{8T_0 h}{\pi^2} \sum_{n=0}^{\infty} \frac{1}{(2n+1)^2} \exp(-a(2n+1)^2 \pi^2 t/4h^2) \right\} \quad (17)$$

or

$$u = \frac{5\alpha^* T_0 h}{9} \left(\frac{at}{h^2} \right)^{1/2} \left\{ \pi^{-1/2} + 2 \sum_{n=1}^{\infty} (-1)^n \left[\pi^{-1/2} \exp(-n^2 h^2/at) - (nh/\sqrt{at}) \operatorname{erfc}(nh/\sqrt{at}) \right] \right\} \quad (18)$$

Equation (18) is more suitable for examining the thermoelastic displacement at short times. For short times; i.e., $at/h^2 \ll 1$, the series term is negligible and (18) reduces to Bodvarsson's result of $u \propto t^{1/2}$. This is to be expected, since at short times one surface of the slab does not thermally "feel" the other. Hence at short times the thermal expansion of one boundary should behave as though it were the boundary of a semi-infinite medium.

At long times, (17) is the more appropriate for examining the thermal expansion. Equation (17) shows that the rate of expansion falls off exponentially reaching a steady state value of

$$u_f = 5\alpha^* T_0 h/9$$

Results similar to (17), (18) and (19) hold for contraction due to the cooling of a slab of initial temperature T_0 and bounded by planes at $T = 0$.

The result (19) has useful application as to the maximum closing or

opening of a set of parallel fractures imbedded in impermeable rock. For example, if $\alpha^* = 2 \times 10^{-5}/^{\circ}\text{C}$; $T_0 = 100^{\circ}\text{C}$, the displacements are

$$u \approx 10^{-3} h \text{ meters}$$

Thus fractures of 1 mm width or less and separated by 2 meters or more may close due to thermal expansion (or, conversely, may easily double in size due to thermal contraction). Since the flow rate in convecting fracture systems depends on d^3 , a doubling of the fracture width may increase the flow rate eight fold.

Perhaps just as important as the total displacement is the rate of displacement; that is, on what time scale are thermoelastic effects important in geothermal systems. The rate of thermal displacement should decline once the fractures interfere with one another thermally. The time at which appreciable thermal interaction occurs is given by

$$at/h^2 > 1 \quad (20)$$

Assuming $a = 10^{-6} \text{ m}^2/\text{sec.}$, (20) shows that if:

$$h = 1 \text{ m}; t = 10^6 \text{ sec}$$

$$h = 10 \text{ m}; t = 10^8 \text{ sec}$$

$$h = 100 \text{ m}; t = 10^{10} \text{ sec}$$

Thus in natural undisturbed geothermal systems, thermoelastic effects may be important only on relatively short times scales (i.e. a few hundred years or less) compared to the lifetime of the geothermal system. Once a system is exploited, however, and heat is extracted from the reservoir, the thermal contraction may significantly increase the permeability in that part of the reservoir. Thermoelastic effects may also be extremely important in forced recovery, hot dry rock reservoirs (e.g. the system treated by Gringarten, et al., 1975).

V. Bibliography

- Bodvarsson, G., 1978, Convection and thermoelastic effects in narrow vertical fracture spaces with emphasis on analytical techniques, Final Report, USGS Grant #14-08-0001-G-398., 111p.
- Bodvarsson, G., 1976, Thermoelastic phenomena in geothermal systems, in: Proceedings, 2nd United Nations Symposium on the Development and Use of Geothermal Resources, San Francisco, May 20-29, 1975, p. 903-907.
- Gringarten, A.C., P.A. Witherspoon, and Y. Onishi, 1975, Theory of heat extraction from fractured hot dry rock, J. Geophys. Res, 80, 1120-1124.
- Hose, R.K. and B.E. Taylor, 1974, Geothermal systems of northern Nevada, U. S. Geological Survey, Open-file report, 74-271, 27 pp.
- Lapwood, E.R., 1948, Convection of a fluid in a porous medium, Proc. Cambridge Phil. Soc., 44, 508-521.
- Lowell, R.P., 1979a, Convection in narrow, vertical fracture spaces, Seimi-Annual Technical Letter Report No. 1, USGS Grant No. 14-08-0001-G-540, 28p.
- Lowell, R.P., 1979b, The onset of convection in a fault zone: effect of anisotropic permeability, Geothermal Resources Council Annual Meeting, Reno, September, 1979 (in press).
- Lowell, R.P., 1977, Convection in narrow, vertical fracture spaces, Semi-Annual Technical Letter Report No. 2, USGS Grant No. 14-08-0001-G-365, 16 p.
- Lowell, R.P., 1975, Circulation in fractures, hot springs and convective heat transport on mid-ocean ridge crests, Geophys. J. Roy Astr. Soc., 40, 351-365.

Lowell, R.P. and C.T. Shyu, 1978, On the onset of convection in a water-saturated porous box: effect of conducting walls, Letters in Heat and Mass Transfer, 5, 371-378.

Murphy, H.D., 1979, Convective instabilities in vertical fractures and faults, J. Geophys. Res., (in press).

Shyu, C.T., 1979, Numerical analysis of critical field functions for thermal convection in vertical or quasi-vertical Darcy flow slabs, Ph.D. Thesis, Oregon State University, Corvallis, 190p.

VI. Work Plans for the Coming Report Period

During the coming report period, the principal effort will be focused on developing numerical models of convection in a fault zone. The work on thermoelastic effects will continue also, with particular attention to the effects of transverse temperature gradients in the fracture.

VII. Students Supported

As mentioned in Program Managements Reports, research progress has been slower than anticipated, mainly due to lack of a graduate assistant to help with the computer work. A graduate student, Heroel Hernandez-Cortez, was appointed effective June 15, 1979 to develop the numerical models.

VIII. Papers and Publications

Lowell, R.P., 1979, The onset of convection in a fault zone: effect of anisotropic permeability, Transactions of Geothermal Resources Council Annual Meeting, Reno, Sept., 1979, (in press).

APPENDIX

The Onset of Convection in a Fault Zone:
Effect of Anisotropic Permeability

Robert P. Lowell

School of Geophysical Sciences
Georgia Institute of Technology
Atlanta, Georgia 30332

ABSTRACT

The condition for the onset of convective instability in a water-saturated, fault or fracture zone in which the permeability is anisotropic is derived. For the case in which the walls of the fault are assumed to be insulated, impermeable boundaries the results show that if the permeability ratio, $\gamma = K_v/K_h$ is less than unity, the critical Rayleigh number is substantially less than for an isotropic medium; whereas if γ is greater than unity the critical Rayleigh number is greater than for an isotropic medium. The flow takes the form of rolls with axes parallel to the short side of the box, the number of rolls contained in the fault zone depend upon the fault zone geometry (length/depth ratio) as well as upon the permeability ratio γ . The number of rolls increases as γ increases.

The convection model is applied to the linear, fault-controlled array of hot springs in the Double Hot Springs area of northern Nevada. If the spring system is a manifestation of roll-like convection within the fault, the results suggest that $\gamma > 1$.

INTRODUCTION

Natural geothermal systems consist principally of a sub-surface heat source and a groundwater circulation system. In most cases little is known concerning the details of the ultimate heat source; and, fortunately, this lack of information is not critical to the development of the resource. The energetics of natural geothermal systems, i.e., the amount of energy available and the rate at which it can be extracted, is primarily dependent upon the patterns of convective circulation within the reservoir rock and the mechanism of heat transfer between the heated rock and the circulating groundwaters. The convection patterns are, in turn, largely controlled by the nature and distribution of permeability within the reservoir.

The permeability of crustal rocks is often tectonically controlled; that is, it is due to fractures and faults rather than to interconnected pore spaces within the rock volume. In many known geothermal systems, the permeability is of this type. In the Basin and Range, for example, the

known geothermal systems appear to be controlled by long, deep, nearly vertical fault zones (Hose and Taylor, 1974). These zones of high permeability may have a linear extent of tens of kilometers and depths of several kilometers with widths of only tens or hundreds of meters. Moreover, as a result of the regional stress pattern, the permeability of the fault or fracture zone may be anisotropic. That is, the horizontal and vertical permeabilities may be unequal.

It is important, therefore, to understand the condition for the convective processes in fault and/or fracture zones. The purpose of this paper is to derive the condition for the onset of convection in a long, deep, but narrow, vertical fault zone with anisotropic permeability. The results will be applied to the Double Hot Springs region, of northern Nevada.

ANALYSIS

The condition for the onset of convection in a homogeneous, isotropic, horizontal, fluid-saturated porous slab, heated from below derived by Lapwood (1948) has formed the basis for convective instability analyses in permeable, porous media. Lapwood showed in a slab of thickness h , bounded by impermeable horizontal planes, and in which the bottom temperature was kept higher than the surface temperature, such that a thermal gradient, β , was maintained, convection would occur provided $R = \rho_f g \alpha \beta h^3 K / (\nu \lambda) \geq 4\pi^2$. R is called the Rayleigh parameter and ρ_f, α, ν are the density, specific heat, thermal expansion coefficient, and kinematic viscosity of the fluid, respectively; K, λ are the permeability and thermal conductivity of the rock, respectively; and g is the acceleration due to gravity. Since then, the critical condition for materials with temperature dependent properties (Kassoy and Zebib, 1975; Straus and Schubert, 1977) and analyses of finite amplitude convection systems (e.g. Donaldson, 1962; Wooding, 1963; Straus, 1974) have been carried out. Moreover, there have recently been analyses of the onset of convection in a closed rectangular container of water-saturated permeable materials. Beck (1972) and Holst and Aziz (1972) have assumed insulated walls; Lowell and Shyu (1978), Shyu (1979), and Murphy (1979) have assumed conducting walls. The results indicate that the presence of vertical confining walls significantly affects the critical

condition and the form of the convection cells at the onset of instability. The critical number is particularly high for containers with a fault-like geometry, in which one horizontal dimension is much smaller than the height and the other horizontal dimension, if the long side walls are conducting.

The condition for the onset of convection for a container in which the permeability is anisotropic is carried out below. Both the insulated and conducting wall cases are derived. Wooding (1976) has considered the effect of anisotropic permeability in an infinite horizontal slab.

A. Equations and Boundary Conditions

Consider a model fault zone as a rectangular slab of water-saturated, porous material imbedded in impermeable rock. Let the height of the porous zone be L_z and the horizontal dimensions be L_x and L_y . Let a uniform geothermal gradient, β , be applied to the material such that the temperature at the upper surface is $T = 0$ and at the lower surface $T = T_0$ ($T_0 > 0$).

Assuming a Cartesian coordinate system with the axis defined positively downward, the linearized, steady state perturbation equations are:

$$\lambda \nabla^2 T^* = \rho_f \sigma w^* \beta \quad (1)$$

$$-\nabla P^* - \rho_f \alpha T^* \underline{g} z - \rho_f \underline{v} \underline{K}^{-1} \cdot \underline{u}^* = 0 \quad (2)$$

$$\underline{v} \cdot \underline{u}^* = 0 \quad (3)$$

where the * refers to dimensional perturbation quantities and where all the parameters are defined as previously. w^* is the vertical velocity; P^* the pressure perturbation; \underline{u}^* the velocity vector. Note that \underline{K} is now treated as a tensor. Non-dimensionalizing the above equations by using L as a length scale, T_0 as a temperature scale, and a reference mean flow $q_r = g K_0 \alpha T_0 / \nu_0$, where K_0, ν_0 refer to values at the top of the layer; and eliminating P^* from the equations gives

$$Rw = \nabla^2 T \quad (4)$$

$$\partial \sigma (\partial w / \partial z) / \partial z + \{ (1/\gamma_1) \partial^2 / \partial x^2 + \quad (5)$$

$$(1/\gamma_2) \partial^2 / \partial y^2 \} (T + \sigma w) = 0$$

$$\text{where } \sigma = (K_0/K_3) (\nu/\nu_0); \gamma_1 = K_3/K_1; \gamma_2 = K_3/K_2 \quad 16$$

$$\text{and } R = \rho_f \sigma \alpha \beta L_z^2 K_0 / \nu_0 \lambda$$

Equations (4) and (5) have been derived by Wooding (1976) for the case of an infinite horizontal porous layer. To determine the onset of convection in a box-like region equations (4) and (5) must be solved subject to the boundary conditions:

$$\underline{\hat{u}} \cdot \underline{\hat{n}} = 0 \text{ at all walls} \quad (6)$$

$$T = 0 \text{ at } z = 0, L_z \quad (7)$$

The temperature conditions on the vertical walls will be either

$$\partial T / \partial x = 0 \text{ at } x = 0, a \quad a = L_x / L_z \quad (8)$$

$$\partial T / \partial y = 0 \text{ at } y = 0, b \quad b = L_y / L_z$$

for insulated walls or

$$\partial T / \partial x = 0 \text{ at } x = 0; a \quad (9)$$

$$T = 0 \text{ at } y = 0; b$$

corresponding to conducting walls on the boundary parallel to the strike of the fault.

For convenience it will be assumed that $\sigma = 1$. This corresponds to the situation in which a decrease in viscosity with increasing temperature (depth) is matched by a decrease in permeability with depth, which is not an unrealistic assumption. Furthermore, the horizontal permeabilities will be assumed to be the same. Thus $\gamma_1 = \gamma_2 = \gamma$.

B. Insulated Boundaries

Combining equations (4) and (5) into a single equation for T and substituting a solution of the form

$$T = \hat{T}(z) \cos \alpha x \cos \beta y$$

where $\alpha = m\pi x/a$; $\beta = n\pi y/b$ gives

$$\{ D^4 - D^2(1 + 1/\gamma)(\alpha^2 + \beta^2) + \frac{1}{\gamma}(\alpha^2 + \beta^2)(\alpha^2 + \beta^2 - R) \} \hat{T} = 0 \quad (10)$$

where D represents d/dz . Letting $\hat{T} = \sin \pi z$ in (10) results in an equation for R .

$$R = \pi^2 \{ \gamma^2 + m^2/a^2 + n^2/b^2 \}^2 \quad (11)$$

$$+ (\gamma^2 - 1)^2 (m^2/a^2 + n^2/b^2) \{ m^2/a^2 + n^2/b^2 \}^{-1}$$

The problem is now to find the minimum value of R for a given γ , a , b and to determine the cell pattern at the minimum Rayleigh number. It is noted that (11) reduces to the isotropic case of Beck (1972) by letting $\gamma = 1$ and to the infinite slab case of Wooding (1976) if a, b are allowed to approach infinity.

Rather than treat the full range of box geometries, only the special case of a fault-like geometry will be considered. Then, $a \gg 1$ and $b \ll 1$. In this case a cursory examination of (11) reveals that R_c will occur for $n = 0$. That is, the cell will take the form of rolls with their axes parallel to the shorter side of the container. Setting $n = 0$ in (11) gives

$$R = \pi^2 \{ \gamma (1 + \frac{a^2}{m^2}) + \frac{m^2}{a^2} + 1 \} \quad (12)$$

Table 1 gives the critical Rayleigh number R_c and the number of rolls contained in the fault zone for several values of anisotropy and for fault lengths up to 4 times the depth. The results in Table 1 show that if the horizontal permeability is greater than the vertical ($\gamma < 1$), the critical Rayleigh number is reduced substantially from the isotropic value of $4\pi^2$; and that if $\gamma > 1$, the critical Rayleigh number is increased substantially. Moreover, the results indicate a

remarkable change in aspect ratio as the anisotropy changes from $\gamma < 1$ to $\gamma > 1$. For example, if $a = 2$, there is only one roll present at $R = R_c$ for $\gamma = 0.1$; whereas there are two rolls for isotropic materials, and four rolls for $\gamma = 10$.

C. Conducting Boundaries

If the long sides of the box are conducting, the conditions (9) lead to non-separable solutions. An approximate solution may be found, however, (Lowell, 1977) by assuming a solution of the form

$$T = \hat{T}(z) \cos \alpha x \sin \beta y$$

The equation for the Rayleigh number (11) is identical to the case for insulated walls; however, the solution $n = 0$ is no longer permitted since that would correspond to $T = 0$. The minimum Rayleigh number is now found with $n = 1$ and an appropriate value of m . The solution $(m, n) = (0, 1)$ corresponds to a flow which rises everywhere so one must choose $m > 0$, $n = 1$. An examination of (11) with $b \ll a$ and $n = 1$ is found to be roughly independent of m . Hence the critical number can be found approximately by letting $m = 0$, $n = 1$. This gives

$$R_c \approx \pi^2 \{ \gamma (b^2 + 1) + b^{-2} + 1 \} \quad (13)$$

and since $b^2 \ll 1$, $R_c \approx \pi^2/b^2$, except for exceptionally large values of γ . Thus, if the walls are conducting, the anisotropy has a negligible effect on the critical Rayleigh number. The approximate solution indicates, however, that conducting walls give rise to a rectangular, 3-dimensional cell

TABLE 1. CRITICAL RAYLEIGH NUMBERS AND MODE
FOR SEVERAL VALUES OF ANISTROPY AND FAULT ZONE LENGTH

$a + \gamma +$	0.01	0.1	1	10
1	$R_c = 2.02\pi^2$ $m = 1$	$R_c = 2.2\pi^2$ $m = 1$	$R_c = 4\pi^2$ $m = 1$	$R_c = 17.5\pi^2$ $m = 2$
2	$R_c = 1.3\pi^2$ $m = 1$	$R_c = 1.75\pi^2$ $m = 1$	$R_c = 4\pi^2$ $m = 2$	$R_c = 17.5\pi^2$ $m = 4$
3	$R_c = 1.21\pi^2$ $m = 1$	$R_c = 1.77\pi^2$ $m = 2$	$R_c = 4\pi^2$ $m = 3$	$R_c = 17.4\pi^2$ $m = 5$
4	$R_c = 1.23\pi^2$ $m = 1$	$R_c = 1.75\pi^2$ $m = 2$	$R_c = 4\pi^2$ $m = 4$	$R_c = 17.3\pi^2$ $m = 7$

pattern instead of 2-dimensional rolls. This is because $m, n \neq 0$ implies that all three velocity components are non-zero (but see Murphy, 1979).

DISCUSSION

The application of the highly idealized fault zone convection model derived here to a complex natural geothermal system is indeed difficult. In fact, the thermal boundary conditions may even be erroneous; or to be more precise, the boundary conditions may change in time. That is, if the fault zone is very narrow, conduction through the side walls may be quite important; and the condition of conducting walls may be the most appropriate for calculating the onset of stability. As pointed out by Murphy (1979) most faults may be stable to spontaneous convection due to the high critical number required in the presence of conducting walls. However, convection may be forced by tectonic movement on the fault, by tidal breathing, or by hydraulically driven flow in the fault due to hydrostatic pressure differences. If forced convection occurs, heat transfer across the walls lowers the thermal gradient in time as t (Carslaw and Jaeger, 1959). Hence, in time, the walls take on the appearance of being insulated, and free convection is more likely to occur. A more detailed discussion of delayed free convection is given by Murphy (1979).

Nevertheless, despite these real-world difficulties, it is useful to try to apply the analytical results to observational data. One possible application may be found in the Basin and Range Province where observations indicate that the geothermal systems are often fault-controlled. Hose and Taylor (1974) point out that the Double Hot Springs area west of the Black Rock Range in northern Nevada consists of approximately seven springs (or seeps) which emerge at a rather regular spacing along a linear trend of about 10 km. The springs are spaced at roughly 1.5 km and, based on regional thermal gradient data, geochemical data indicate that the springs have a fairly uniform circulation depth of about 3 km. Thus, if the spring system is a manifestation of roll-like convection within the fault, the somewhat small aspect ratio (cell wavelength vs. depth) suggests that the permeability of the fault zone may be anisotropic: the vertical permeability may be greater than the horizontal.

ACKNOWLEDGMENT

This work was supported by Extramural Geothermal Research Program of the U. S. Geological Survey, Department of the Interior under USGS Grant No. 14-08-0001-G-365 and 14-08-0001-G-540.

REFERENCES

- Beck, J. L., 1972, Convection in a box of porous material saturated with fluid: *Phys. Fluids*, v. 15, p. 1377-1383.
- Carslaw, H.S. and Jaeger, J.C., 1959, *Conduction of heat in solids*, 2nd ed., Oxford, The Clarendon Press, 510 p.
- Donaldson, I.G., 1962, Temperature gradients in the upper layers of the earth's crust due to convective water flows: *J. Geophys. Res.*, v. 67, p. 3449-3460.
- Holst, P.H. and Aziz, K., 1972, Transient three-dimensional natural convection in confined porous media: *Int. J. Heat and Mass Trans.*, v. 15, p. 73-90.
- Hose, R.K. and Taylor, B.E., 1974, *Geothermal systems of northern Nevada*: U.S. Geol. Survey, Open-file Rept. 74-271, 27 p.
- Kassoy, D.R. and Zebib, A., 1975, Variable viscosity effects on the onset of convection in porous media: *Phys. Fluids*, v. 18, p. 1649-1651.
- Lapwood, E.R., 1948, Convection of a fluid in a porous medium: *Proc. Cambridge Phil. Soc.*, v. 44, p. 508-521.
- Lowell, R.P., 1977, Convection and thermoelastic effects in narrow, vertical fracture spaces: Semi-annual Technical Letter Rept. No. 1, USGS Grant No. 14-08-0001-G-365, 10 p.
- Lowell, R.P. and Shyu, C.-T., 1978, On the onset of convection in a water-saturated porous box: effect of conducting walls: *Lett. Heat and Mass Trans.*, v. 5, p. 371-378.
- Murphy, H.D., 1979, Convective instabilities in vertical fractures and faults: *J. Geophys. Res.* (in press).
- Shyu, C.-T., 1979, Numerical Analysis of Critical Field Functions for Thermal Convection in Vertical or Quasi-Vertical Darcy Flow Slabs: Ph.D. Dissertation, Oregon State University, Corvallis, 190 p.
- Straus, J.M., 1974, Large amplitude convection in porous media: *J. Fluid Mech.*, v. 64, p. 51-63.
- Straus, J.M. and Schubert, G. 1977, Thermal convection of water in a porous medium: effects of temperature and pressure dependent thermodynamic and transport properties: *J. Geophys. Res.*, v. 82, p. 325-334.
- Wooding, R.A., 1963, Convection in a saturated porous medium at large Rayleigh number or Peclet number: *J. Fluid Mech.* v. 15, p. 527-544.
- Wooding, R.A., 1976, Influence of anisotropy and variable viscosity upon convection in a heated saturated porous layer: Applied Math Division, Tech. Rept. No. 55, DSIR, Wellington, N.Z., 23 p.

Semi-Annual Technical Letter Report No. 3

Grant No: 14-08-0001-G-540

Reporting Period Covered: 7/1/79 - 12/31/79

Grantee: Georgia Institute of Technology

Supported by: U. S. Geological Survey
Geothermal Research Program
Reston, Virginia

Grant Amount: \$30,777.00

Start Date: 7/1/78

Expiration Date: 7/31/80

Principal Investigator: Robert P. Lowell

U.S.G.S. Technical Officer: Donald W. Klick

Date Submitted: January 31, 1980

Title of Research Project: Convection in Narrow Vertical Fracture
Spaces

Objectives of Project: The main purpose of this project is to examine thermal convection in long, deep, but very narrow vertical fracture spaces. The initiation and time development of the physical processes are to be studied on the basis of mathematical-physical approximation methods and numerical techniques. The results are to be interpreted with regard to known geothermal systems in the Basin and Range and other areas where faults or fractures are the dominant controlling structures.

I. Introduction

This document represents the third semi-annual technical report on our research on convection in faults and fracture zones and some related problems. This work represents a continuation of the effort which was initiated under the USGS grant number: 14-08-0001-G-365 as part of the Extramural Geothermal Research Program of the U. S. Geological Survey. The initial phase of the work was done in conjunction with Dr. G. Bodvarsson of Oregon State University; however, his group is not directly involved in the present research effort. The present research is being conducted under grant number: 14-08-0001-G-540.

The principal achievements during the past six months have been to: (1) continue the work on the temporal evolution of convection in fractures to include a parabolic velocity profile across the fracture aperture and (2) initiate the development of a finite-difference model for time dependent convection in a fault/fracture zone.

The main body of the report which follows is divided into subsections: II. General Framework and Objectives; III. Convection in a Fluid-Filled Fracture; IV. Convection in a Fault or Fracture Zone; V. Bibliography; VI. Work Plans for the Coming Report Period; VII. Students Supported.

II. General Framework and Research Objectives

The energetics of geothermal systems depend fundamentally upon patterns of heat transport and fluid flow within heated, highly

permeable regions of the earth's crust. The ultimate source of heat for many geothermal systems is undoubtedly of magmatic origin; but in some cases, the geothermal fluid is heated at depth as a result of an unusually high geothermal gradient. Most of the systems in the basin and Range Province are probably of the latter type (White and Williams, 1975).

Of even more importance, however, is the nature and distribution of permeability within the geothermal reservoir. The permeability may either be primary, resulting from interconnected pore spaces within the rock volume or secondary, resulting from fractures and/or fault zones. In all geothermal fields currently under production, the geothermal fluids are withdrawn from discrete fractured regions within the reservoir, yet most mathematical modeling of geothermal systems has assumed a Darcian type of flow through a rock with a bulk permeability. This is not to say that it has been necessarily assumed that the permeability is of a primary type, but rather that one normally assumes the fractures to be on such a fine scale that, for mathematical (or numerical) convenience, the Darcy flow model is appropriate on spatial scales of the order of the reservoir dimensions (or finite element/difference grid spacing).

The mathematical treatment for the onset of thermal convection under such assumptions follows the method of Lapwood (1948), or some deviant of it; and the treatment of finite amplitude convection uses the same basic perturbation equations with the addition of higher order, non-linear transport terms which are neglected in the linear stability analysis. These models have provided many useful results with regard to the physics of geothermal systems, but often this approach may be quite

unrealistic. Geothermal systems in which main permeability is furnished by narrow, discrete, widely separated fault and/or fracture zones imbedded in an otherwise impermeable rock are better handled by somewhat different techniques. Examples of the latter systems are found in Iceland, where dikes provide the main vertical permeability, in the Basin and Range, where long, deep, master faults probably provide the main vertical permeability (Hose and Taylor, 1974), and possibly in the oceanic crust (Lowell, 1975; Sleep and Wolery, 1978).

The principal purpose of this research is to examine thermal convection in long, deep, but very narrow vertical fracture spaces. The initiation and temporal evolution of the physical processes are to be studied on the basis of mathematical-physical approximation methods and finite element and/or finite difference techniques. The results are to be interpreted with regard to known geothermal systems in the Basin and Range and other regions where major faults and fractures are the structures controlling the permeability.

III. Convection in a Fluid-Filled Fracture

The first models of convection in which the reservoir permeability was assumed to be controlled by a few narrow, widely-spaced, deep, vertical fractures were developed by Bodvarsson and Lowell (1972) and Lowell (1975) and the results have been extended recently (Bodvarsson, 1978; Lowell, 1979a, 1979b) to include some aspects of temporal evolution and thermoelastic phenomena. However, although the discrete fracture models are conceptually quite simple and potentially very useful, they are not nearly so well developed as their porous medium-Darcy flow counterpart.

One aspect of the fracture models which has not been treated in the earlier models involves a more careful examination of the fluid flow within the fracture and the heat transfer across the fracture walls. In previous models, the velocity across the aperture of the fracture was assumed to be constant, and given by the average velocity between two parallel plates; and the temperature across the aperture was assumed to be uniform. These assumptions are suitable for determining the average heat transfer rate by the moving fluid; however, geochemical effects such as clogging of fractures by precipitation from solution and deposition of chemical species and other rock-fluid interactions, may depend significantly on the detailed temperature and velocity structure across the fracture opening. Temperature and velocity variations across the fracture width may become increasingly important as the fracture width increases beyond several millimeters or so, since convection within the fracture may occur. On the other hand, as the fracture width increases, turbulent flow may develop which would tend to smooth and temperature and velocity variations across the fracture opening.

A. Basic equations

The basic equations are the equations for the conservation of mass, momentum and energy. Assuming the fluid to be incompressible, conservation of mass requires

$$\nabla \cdot \vec{v} = 0 \quad (1)$$

whereas conservation of momentum requires

$$\rho d\vec{v}/dt = -\nabla P + \eta \nabla^2 \vec{v} + \rho \vec{g} \quad (2)$$

for a viscous fluid or

$$1/\phi \partial \vec{v} / \partial t = -\nabla P - \eta K^{-1} \cdot \vec{v} + \rho \vec{g} \quad (3)$$

for Darcian flow in a porous medium. In the above equations \vec{v} is the fluid velocity (or Darcian velocity where applicable), t the time, ρ is the fluid density, η the dynamic viscosity, K the permeability tensor, ϕ the porosity, P the pressure, and \vec{g} the acceleration due to gravity. The conservation of energy equation for fluid in a fracture, or porous rock is:

$$\rho s (\partial T / \partial t + \vec{v} \cdot \nabla T) = \lambda \nabla^2 T \quad (4)$$

where T is the temperature, s the specific heat of the fluid, λ the thermal conductivity of the fluid (or solid rock matrix in the case of a porous medium); and in impermeable rock the heat transfer equation reduces to the heat conduction equation

$$\partial T_r / \partial t = a^* \nabla^2 T_r \quad (5)$$

where a^* is the thermal diffusivity of the rock and T_r refers to the rock temperature. In addition to the basic equations one must apply boundary and initial conditions as well as the matching conditions that the temperature and heat flux across the fracture walls are continuous.

These conditions combined with the above equations represents a rather formidable mathematical problem which can only be solved in special cases. One can consider two broad categories of problems: (1) forced flow-in which the velocity field is specified a priori and the temperature field is determined from the given velocity field; (2) natural convective flow--in which flow derives from thermo-gravitational instability. One example of a forced flow problem is given below. Section IV will discuss some recent work on convective flow.

B. Forced flow in a narrow, open fracture.

Consider a model fracture as a rectangular, open, vertical, flat-walled channel of width $2h$ in a semi-infinite, impermeable rock slab of height H and length $2L$. Assume a Cartesian coordinate system with its origin at the top of the slab and mid-way between the fracture walls and oriented with its z axis vertically downward, y axis along the strike of the fracture and the x axis in the horizontal direction perpendicular to the fracture aperture.

As an initial state, assume steady heat transport by thermal conduction in the slab with conditions

$$\begin{aligned} T^0(x, y, 0) &= 0 \\ T^0(x, y, H) &= T_0 \end{aligned} \quad (6)$$

and let the thermal diffusivity of the rock and fluid to be equal. Then the initial steady-state condition is given by

$$T^0(x, y, z) = \beta z \quad (7)$$

where β is the geothermal gradient. At time $t = 0$ a specified fluid velocity distribution is initiated in the region $-h \leq x \leq h$; $0 \leq z \leq H$; $-\infty < y < \infty$; the pertinent heat transport equation is then given by (4) and (5) where $\lambda/\rho s = a = a^*$. As a first order approximation, let the velocity \vec{v} be a small perturbation. Then writing T as

$$T = T^0 + T'$$

where T' is a perturbed temperature, equations (4) and (5) reduce to

$$\partial T' / \partial t - v_z \beta = a \nabla^2 T' \quad (8)$$

in the fracture; and

$$\partial T' / \partial t = a \nabla^2 T' \quad (9)$$

in the rock, where v_z is the vertical velocity component and second order terms are neglected. In the first order approximation with v_z specified (8) takes on the form of a heat conduction equation with a temperature source (or sink) of magnitude $-v_z\beta$; (8) and (9) can then be combined into a single equation.

The most convenient method of solution is by the Green's function method, the formal solution being given by:

$$T'(x,y,z,t) = -\beta \iiint v_z(x',y',z') G(x,x',y,y',z,z',t-\tau) dx' dy' dz' d\tau \quad (10)$$

where G is the Green's function. With boundary conditions

$$T'(x,y,0) = (T'(x,y,H) = 0 \quad (11)$$

$$\partial T'(0,y,z)/\partial x = T'(L,y,z) = 0$$

and anticipating a period solution in y , the Green's function is found to be

$$G(x,x',z,z',t) = \frac{4}{LH} \sum_{\substack{m=0 \\ n=1}}^{\infty} \cos(m+1/2) \pi x/L \cos(m+1/2) \pi x'/L \cdot \\ \sin n\pi z/H \sin n\pi z'/H \cdot \exp[-a\pi^2 t((m+1/2)^2/L^2 + n^2/H^2)] \quad (12)$$

The velocity distribution is assumed to arise from convective instability and to take the form of a two-dimensional roll with its axis perpendicular to the strike of the aperture of the fracture. The vertical velocity must vanish at the top and bottom of the fracture as well as at the side walls. A velocity distribution which satisfies the boundary conditions and the continuity equation is

$$\begin{aligned} v_y &= -C(x^2-h^2) \sin \pi y/H \cos \pi z/H \\ v_z &= C(x^2-h^2) \cos \pi y/H \sin \pi z/H \end{aligned} \quad (13)$$

where C is assumed to be constant given roughly by

$$C = (1/2\eta)(dP'/dz) \quad (14)$$

where dP'/dz is a mean perturbation pressure gradient.

As can be seen from (8), v_y does not enter the first order solutions; and substituting (12) and (13) into (10) gives

$$T'(x,y,z,t) = \frac{4C\beta L^4}{a\pi^5} \cos\pi y/H \sin\pi z/H \sum_{m=0}^{\infty} (m+1/2)^{-3} [(m+1/2)^2 + L^2/H^2]^{-1}.$$

$$\begin{aligned} & [(m+1/2)\pi h/L \cos(m+1/2)\pi h/L - \sin(m+1/2)\pi h/L] \cos (m+1/2)\pi x/L \quad (15) \\ & \cdot \{ 1 - \exp[-a\pi^2 t ((m+1/2)^2/L^2 + 1/H^2)] \} \end{aligned}$$

The solution (15) may be simplified considerably by noting that h is much less than L . Physically one would expect the temperature perturbation to fall to zero at a distance $L \sim H$, the depth of the fracture system. Since $h \sim 10^{-2}m$ and $L \sim 10^3m$, $h/L \sim 10^{-5}$. Since a reasonable approximation may be expected by summing only a few terms in the series, one can expand the factors in h/L in a Maclaurin series. Thus,

$$\begin{aligned} T'(x,y,z,t) = & - \frac{4C\beta L h^3}{3a\pi^2} \cos\pi y/H \sin\pi z/H \sum_{m=0}^{\infty} [(m+1/2)^2 + L^2/H^2]^{-1} \cos(m+1/2)\pi x/L \cdot \\ & \{ 1 - \exp(-a\pi^2 t [(m+1/2)^2/L^2 + 1/H^2]) \} \quad (16) \end{aligned}$$

The result (16) shows several interesting features. First of all, the temperature anomaly is extremely sensitive to the fracture width, being proportional to h^3 . Secondly, the temperature anomaly at the fracture is dominated by the factor multiplying the series, particularly for large times. Inserting C from (14) gives roughly

$$|T'_{\text{Max}}| = 2(dP/dz) \beta L h^3 / 3a\pi^2 n \quad (17)$$

in the steady state.

Most important, however, is the variation in temperature across the fracture aperture. For $h/L \sim 10^{-5}$, the $\cos (m+1/2)\pi x/L \sim 1 - [(m+1/2)\pi x/L]^2$ which is approximately $1 - 10^{-10}$; so for a single narrow fracture the temperature variation across the fracture is extremely small and should be negligible in geologic situations.

C. Forced flow in a closely spaced system of fractures.

On the other hand, suppose one considers a set of narrow, but closely spaced fractures. As a result of thermal interaction between fractures, an approximate treatment can be given by considering a single fracture, but with the condition $\partial T' / \partial x = 0$ at $x = L$, where L is a plane mid-way between adjacent fractures. In this case, the solution (15) remains unchanged, except that $m + 1/2$ is replaced by m . The maximum temperature anomaly can be found more rigorously, since the series is summable for $L/H \ll 1$. Thus, maintaining the assumption that $h/L \ll 1$ gives

$$|T'_{\text{Max}}| = (dP/dz) \beta L h^3 / 9a n \quad (18)$$

which is formally of the same order of magnitude as (17). Perhaps a more significant change is that the ratio h/L , though still considerably less than unity, is not nearly as small as in the case of a single fracture. For a set of fractures one might expect $h/L \sim 10^{-2}$ instead of 10^{-5} . The temperature variation across an individual fracture in the set may be one part in 10^{-4} or so. A variation of this magnitude, though still small, may be potentially significant. In addition, one

can estimate the horizontal temperature gradient near the fracture wall

$$dT'/dx|_{\max, x=L} \cong [2(dP/dz) h^4/3anL]\beta \quad (19)$$

D. Comparison with results assuming a uniform flow velocity.

If instead of a parabolic velocity profile, a uniform, average velocity across the fracture is assumed, the temperature perturbation takes on a slightly different form. The average velocity between parallel plates separated by a distance $2h$ is

$$\bar{v}_z = -((h^2/3\eta)dP/dz)\cos\pi y/H \sin\pi z/H \quad (20)$$

Using this form in the Green's function formulation, instead of (13) gives

$$\begin{aligned} T'(x,y,z,t) = & \frac{2C^*\beta}{a\pi} L^2 \cos\pi y/H \sin\pi z/H \cdot \\ & \sum_{m=1}^{\infty} m^{-1} [m^2 + L^2/H^2]^{-1} \sin m\pi h/L \cos m\pi x/L \\ & \cdot [1 - \exp(-a\pi^2 t(m^2/L^2 + 1/H^2))] \end{aligned} \quad (21)$$

$$\text{where} \quad C^* = -(h^2/3\eta)(dP/dz) \quad (22)$$

and expanding for $m\pi h/L \ll 1$ yields a solution identical to (16). Thus to first order in smallness of h/L , the parabolic velocity profile and the average velocity profile give the same result. Therefore, the horizontal temperature variations across the fracture appear to be negligible, especially for widely spaced fractures, regardless of the velocity profile used. Details of the velocity profile should be unimportant except for chemical processes which are sensitive to temperature variations of the order of one part in 10^4 or less. The result derived here may break down if the fracture width is great enough for convection cells to form across the aperture of the fracture. It

seems unlikely that such fractures would exist at depth in geologic systems.

IV. Convection in a Fault Zone

A major goal of this research program is to develop models of convection in a fault or fracture zone. Results to date have been reported previously (Lowell, 1977a, b, 1979a, b; Lowell and Shyu, 1978). These results have addressed criteria for various stability problems, but they have not been concerned with transient effects due to lateral heat conduction between the fault zone and the adjacent impermeable rock. This problem is essentially of a numerical nature, and we are currently developing a finite-difference model. The work will follow the three-dimensional approach outlined by Holst and Aziz (1972), but with the additional complications arising from the presence of conducting boundaries. Results of this work will be given in a future report.

V. Bibliography

- Bodvarsson, G. 1978, Convection and thermoelastic effects in narrow vertical fracture spaces with emphasis on analytical techniques, Final Report, USGS Grant 14-08-0001-G-398, 111 p.
- Holst, P. H. and K. Aziz, 1972, Transient three-dimensional natural convection in confined porous media, Int. J. Heat and Mass Transfer, 15, 73-90.
- Hose, R. K. and B. E. Taylor, 1974, Geothermal systems of northern Nevada, U. S. Geological Survey, Open-file report, 74-271, 27 pp.
- Lapwood, E. R., 1948, Convection of a fluid in a porous medium, Proc. Cambridge Phil. Soc., 44, 508-521.

- Lowell, R. P., 1979a, Convection in narrow, vertical fracture spaces, Semi-Annual Technical Report No. 1, USGS Grant No. 14-08-0001-G-540, 28 p.
- Lowell, R. P., 1979b, Convection in narrow, vertical fracture spaces, Semi-Annual Technical Report No. 2, USGS Grant No. 14-08-0001-G-540, 18 p.
- Lowell, R. P., 1977a, Convection in narrow, vertical fracture spaces, Semi-Annual Technical Report No. 1, USGS Grant No. 14-08-0001-G-365, 10 p.
- Lowell, R. P., 1977b, Convection in narrow, vertical fracture spaces, Semi-Annual Technical Report No. 2, USGS Grant No. 14-08-0001-G-365, 16 p.
- Lowell, R. P., 1975, Circulation in fractures, hot springs and convective heat transport on mid-ocean ridge crests, Geophys. J. Roy Astr. Soc., 40, 351-365.
- Lowell, R. P. and C. T. Shyu, 1978, On the onset of convection in a water-saturated porous box: effect of conducting walls. Letters in Heat and Mass Transfer, 5, 371-378.
- Sleep, N. H. and T. J. Wolery, 1978, Egress of hot water from mid-ocean ridge hydrothermal systems: some thermal constraints, J. Geophys. Res., 83, 5913-5922.
- White, D. E. and D. L. Williams, eds., 1975, Assessment of geothermal resources of the United States - 1975, U. S. Geological Survey Circular, 726, 155 p.

VI. Work Plan for the Coming Report Period

The principal effort over the next six months will be on the development of the finite-difference model. The programming is now underway and results may be available in time for the Spring Annual Meeting of AGU. In addition to the numerical work, some further analytical modeling will be done, particularly on narrow, open fracture systems.

VII. Students Supported

Mr. Heroel Hernandez-Cortez will be completing his Masters thesis under this program. His thesis will be on finite difference modeling of three-dimensional transient convection in a fault zone.

505-622

GEORGIA INSTITUTE OF TECHNOLOGY
SCHOOL OF GEOPHYSICAL SCIENCES

Atlanta, Georgia 30332
(404) 894-2857

July 16, 1980

U. S. Army Corps of Engineers
Mobile District
P. O. Box 2288
Mobile, Alabama 36628

Subject: Annual Summary Report covering the period 1 May, 1979 to
1 June, 1980

Re: Contract DACW01-78-C-0153 "Microearthquake instrumentation
and analysis at Carter's Dam, Georgia"

Dear Sirs:

Microearthquake monitoring for the period 1 May 1979 to 1 June 1980 was accomplished with a coverage of 81.6 percent of the total available recording time. The percent coverage for each month is given in Table I. (Of this coverage, approximately 25 percent of the coverage was not readable due to noise from the pumpback operation.)

During the recording period several seismic events have been recorded at the Carter's Dam station. Some of these events are given in Table II along with their location. Numerous quarry blasts occurring within a distance range of 14 to 250 km were identified from their arrival times and seismic characteristics. A few teleseisms were also recorded by the Carter's Dam station. These events have been catalogued, and their arrival times are available if desired.

The impulsive disturbances which were described in our special report of 11 September, 1979 continued to occur but at a reduced level of activity. No additional information on their origin, spatial or temporal distribution has been forthcoming. The impulsive disturbances are believed to be local to the immediate geophone area.

During the recording period of 1 May, 1979 to 1 June, 1980, no earthquake of natural origin has been detected within 10 km of the Carter's Dam seismic station.

Installation of a new seismic station in the eastern portion of the reservoir is complete at the field site. The signal should be connected to the communication system in mid July. Figure 1 and Figure 2 show its location. The station, CRG (Coosawattee River, Georgia), is in an area that appears to receive little, if any, traffic from hikers, hunters, and campers. The installation should be secure and quiet, allowing recording at increased gain. This will allow recording during pumpback operation, location capability for nearby events, and improved coverage of the backwater area of the reservoir.

As requested in a telephone conversation on 13 August 1979 we are attaching an analysis of data we obtained for the southeastern Tennessee earthquake and its aftershock sequences.

Respectfully submitted,



Leland T. Long
Associate Professor

LTL/dh

Attachment

TABLE I

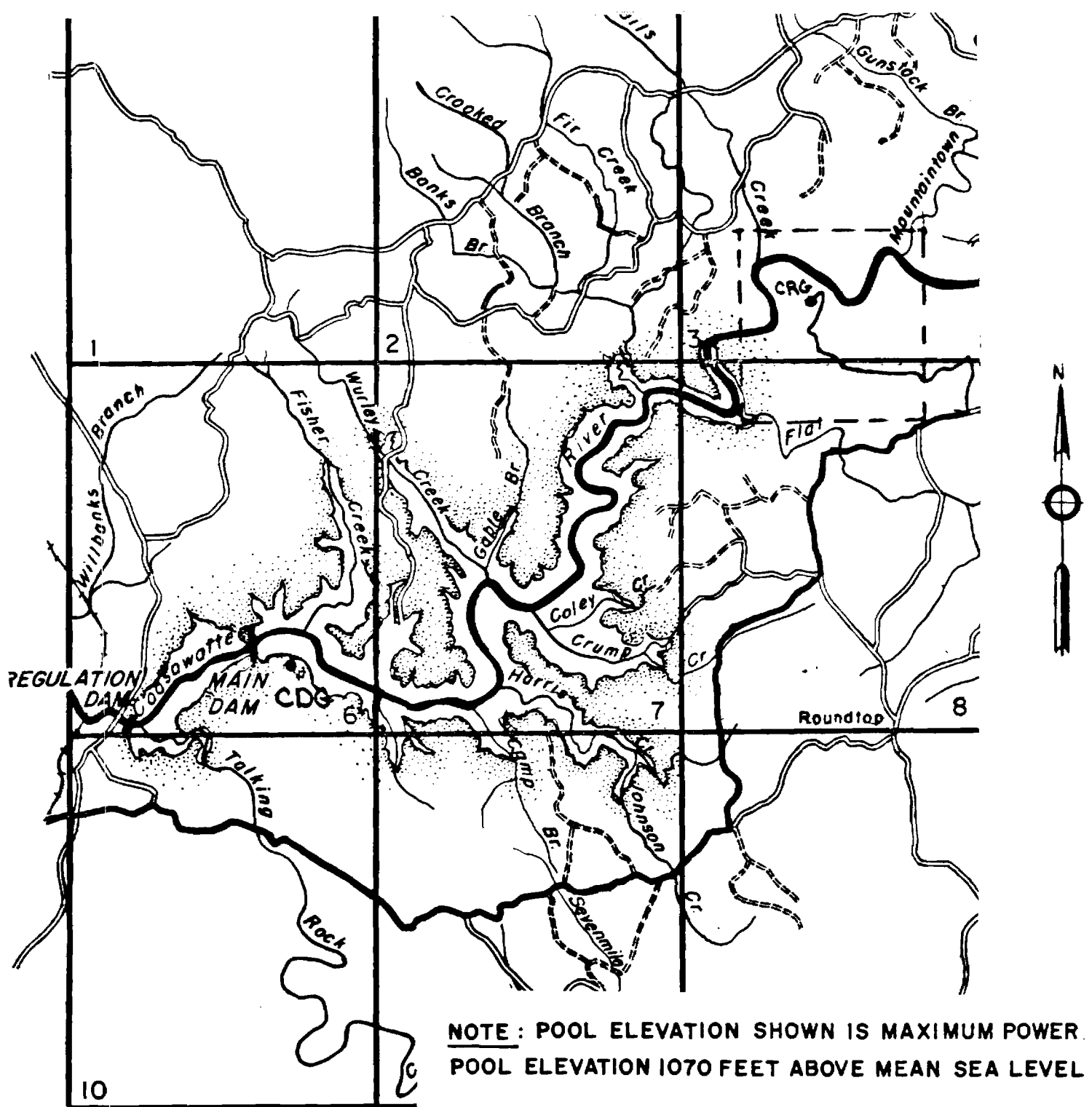
Monthly Seismic Recording/Percentage Coverage

<u>Month - year</u>	<u>Percent Seismic Recording Coverage</u>
May 1979	99%
June 1979	76%
July 1979	99%
August 1979	93%
September 1979	98%
October 1979	96%
November 1979	87%
December 1979	63%
January 1980	89%
February 1980	90%
March 1980	53%
April 1980	35%
May 1980	75%

TABLE II

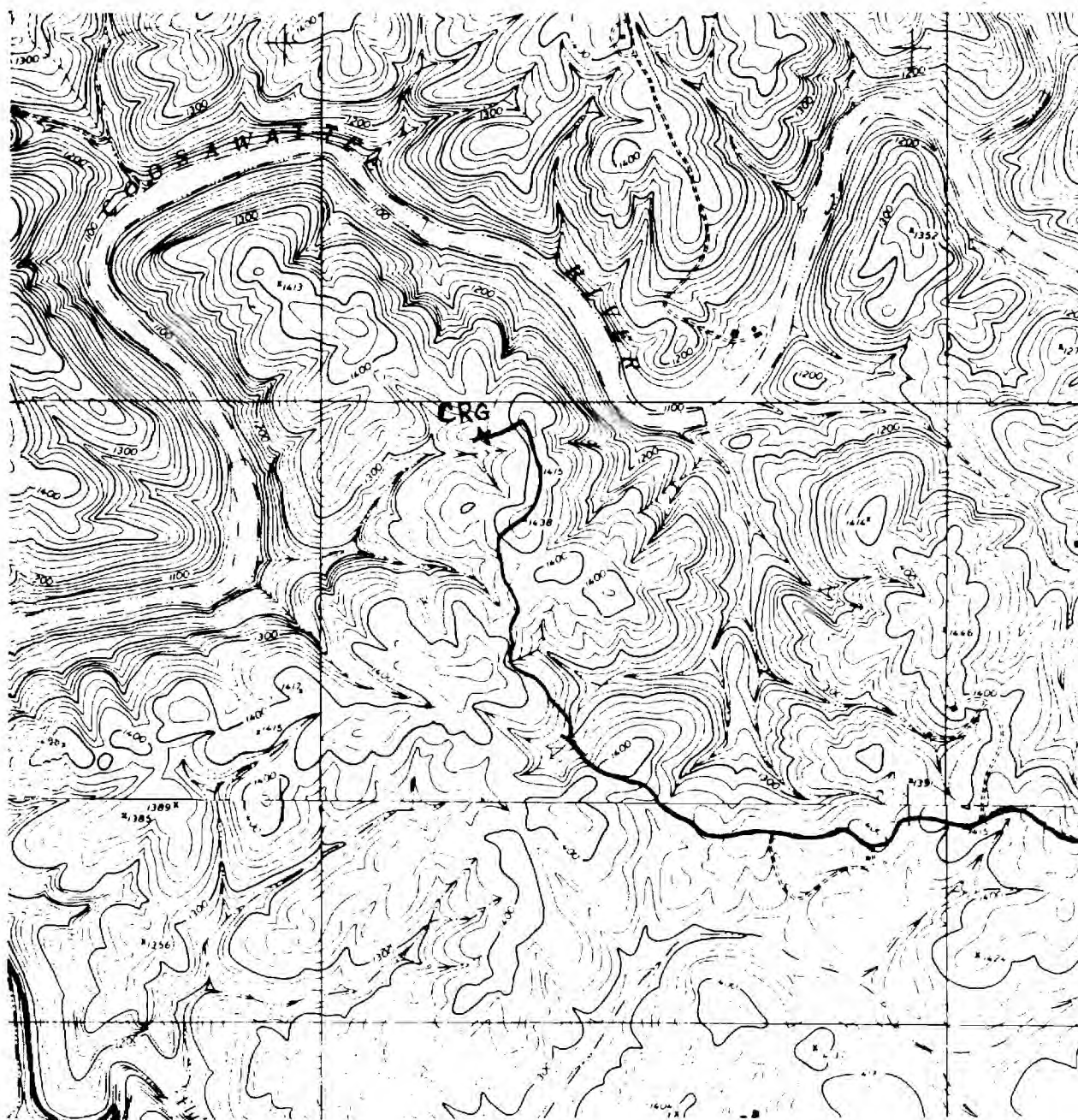
Some Events Recorded by the Carter's Dam Station

19 July 1979	10:27:16.52	35.146N	84.755W
S. E. Tennessee, Cleveland			
13 August 1979	05:19:08.89	35.220N	84.390W
S. E. Tennessee event, Tellico Plains			
13 August 1979	05:27:34.55		
Tellico Plains event aftershock			
13 August 1979	05:30:09.10		
Tellico Plains event aftershock			
13 August 1979	05:36:41.9		
Tellico Plains event aftershock			
13 August 1979	05:39:36.9		
Tellico Plains event aftershock			
25 August 1979	01:32:12.95	34.8471N	82.9467W
Lake Jocassee			
12 September 1979	06:24:24.7	35.5151N	83.8927W
Near Fontana Reservoir			
29 October 1979	20:28:02.0	35.3196N	84.8423W
North of Cleveland, Tennessee			
10 January 1980	19:18:48.9	27.0944N	85.8713W
Gulf of Mexico			
24 January 1980	04:12:27.2	35.5581N	84.2652W
Tellico Plains, Tennessee			
20 April 1980	23:20:43.70	35.5537N	83.9864W
South Knoxville			
21 April 1980	20:44:01.90	35.8882N	83.9828W
South Knoxville			

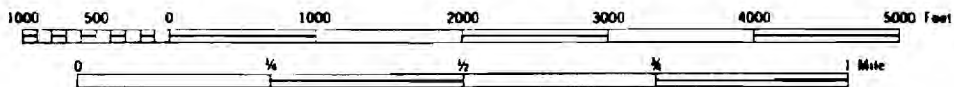


COOSAWATTEE RIVER, GEORGIA
RESERVOIR MAPPING
CARTERS DAM RESERVOIR PROJECT
INDEX MAP

Figure 1. Carter's Dam reservoir project index map showing seismic station locations CDG and CRG.



Scale 1:12,000



CONTOUR INTERVAL 20 FEET
 DATUM IS MEAN SEA LEVEL 1929 ADJUSTMENT
 POLYCONIC PROJECTION
 1927 NORTH AMERICAN DATUM

Figure 2. Site location map for seismic station CRG.

The August 13, 1979, Southeast Tennessee Earthquake

by L. T. Long, J. Musser, Gordon Smith, Anton Dainty and Andy Binford

Introduction

On August 13, 1979 at 05:18:56.6 UT an earthquake of approximate magnitude 3.3 occurred in southeastern Tennessee about 20 km SSW of Tellico Plains. Immediately following detection of the event, investigators from Georgia Tech and the Tennessee Earthquake Information Center placed portable seismic equipment near the estimated epicenter. A four station aftershock survey was initiated August 14, 1979 and was extended to September 18, 1979 with assistance from the Tennessee Valley Authority. Following the survey additional regional seismic recordings for the main event were obtained and analyzed. The objectives of this report are to present the results of Georgia Tech's investigation of the data for the main event and from the aftershock survey.

Regional Seismicity

The epicenter of the August 13, 1979 event is located in the Valley and Ridge Province of the Appalachian Mountains near its boundary with the Blue Ridge Province (Figure 1). The area is underlain by strongly folded and faulted Precambrian to Pennsylvanian sediments. The area of southeastern Tennessee within an approximate radius of 100 km of the epicenter of the August 13, 1979 earthquake has experienced a moderate level of seismic activity. The epicenter falls within the southern Appalachian Seismic Zone of Bollinger (1973). From 1829 to 1976 there were 38 events felt in southeastern Tennessee within a radius of 100 km of the August 13, 1979 event. The largest of these occurred in March 1913 and had a maximum epicentral intensity of VII (MM) (see Figure 2).

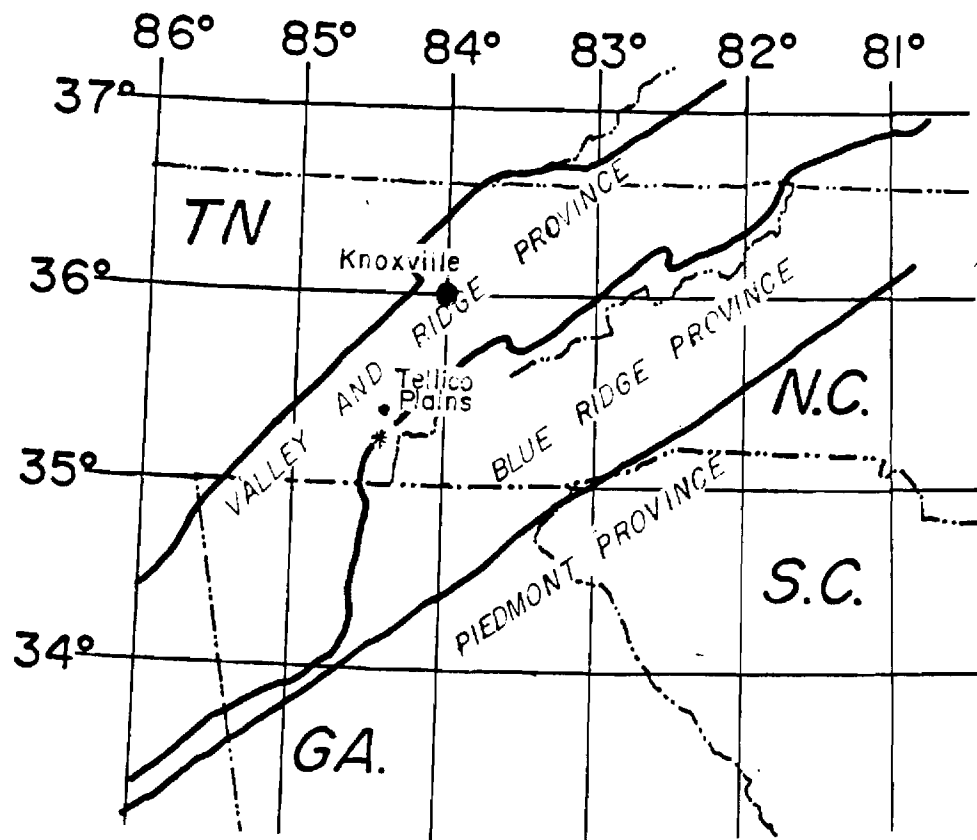


Figure 1. Location map for southeastern Tennessee.

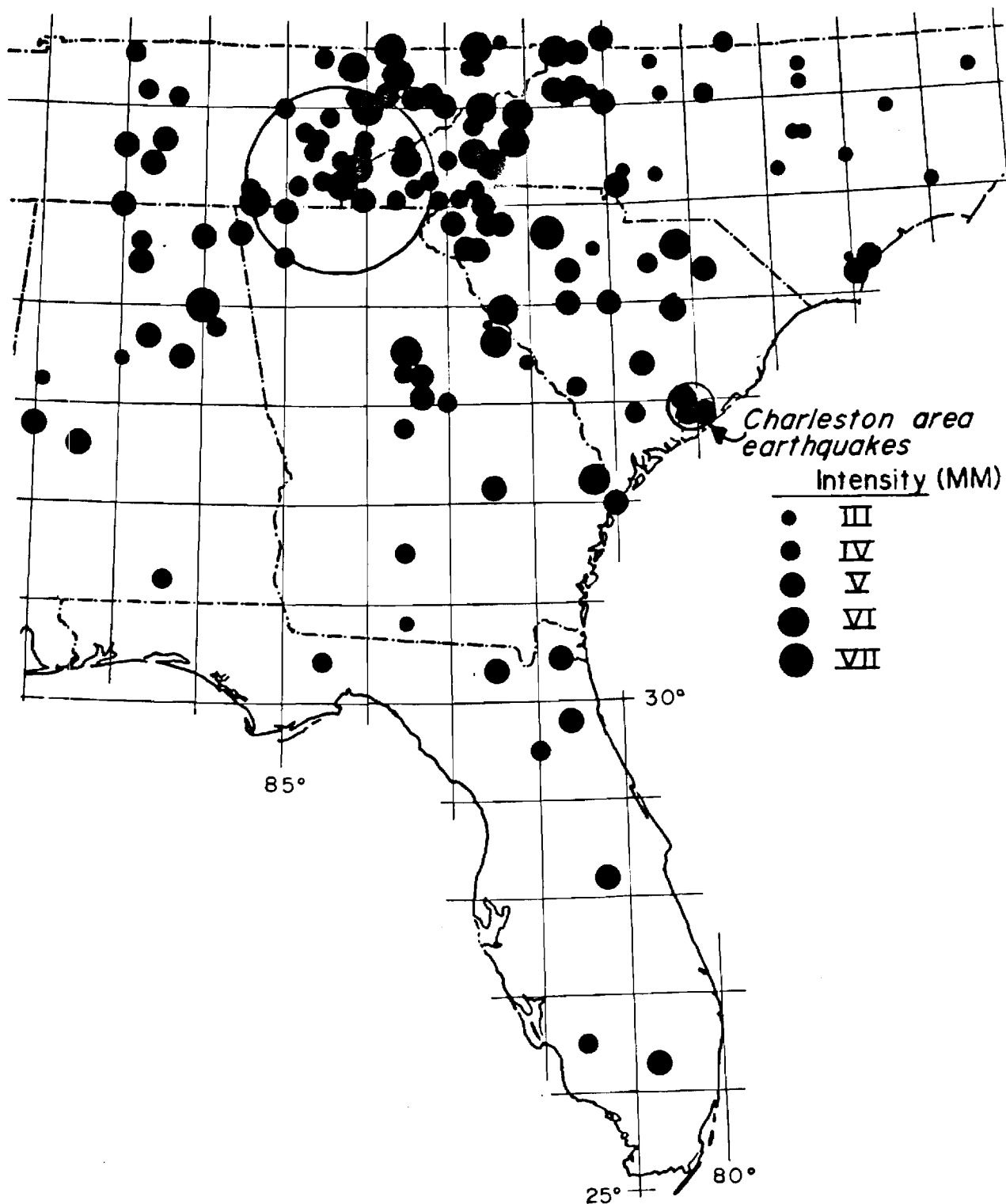


Figure 2. Regional Seismicity map. Circle denotes 100 km radius from the location of August 13, 1979 earthquake.

Intensity Survey

Immediately following the August 13, 1979 event Georgia Tech initiated an intensity survey in the immediately vicinity of the epicenter. Over 45 individual responses were obtained in the field or subsequently mailed to Georgia Tech. In addition the U.S. Geological Survey initiated a survey of post masters covering a considerably wider area. From these two sets of questionnaires, intensities were evaluated according to the Modified Mercalli scale and the felt reports are summarized in Figure 3. Table 1 is a summary of the intensity data showing the distribution of observed intensities at each community. The Intensity IV area has an approximate radius of 40 km and Intensity IV (MM) is considered the maximum intensity for the event. There were only a very few indications of Intensity V in the central area and these were not sufficient to justify a maximum intensity rating above IV. The total felt area was approximately $15,000 \text{ km}^2$ and the intensity IV area was about $5,000 \text{ km}^2$.

Location

Usable records for the East Tennessee event of August 13, 1979 were obtained from 15 regional seismic stations (see Table 2 for arrival times). The hypocenter determined from these arrival times is $35^{\circ}13.20'N \pm 1.91 \text{ km}$ and $84^{\circ}23.43'W \pm 1.63 \text{ km}$ with an error ellipse with an area of 12.8 km^2 (see Table 2 for details). The depth of focus was $5.0 \text{ km} \pm 4.5 \text{ km}$. However, the depth of focus computation requires knowledge of the Moho depth near the epicenter. If the Moho depth is deeper than that of the model used for location (i.e. 33 km) the event may appear to be located above the surface. Hence, we modified the model in the location program to correspond to a depth of 49.6 km which

MODIFIED MERCALLI INTENSITY
AUGUST 13, 1979

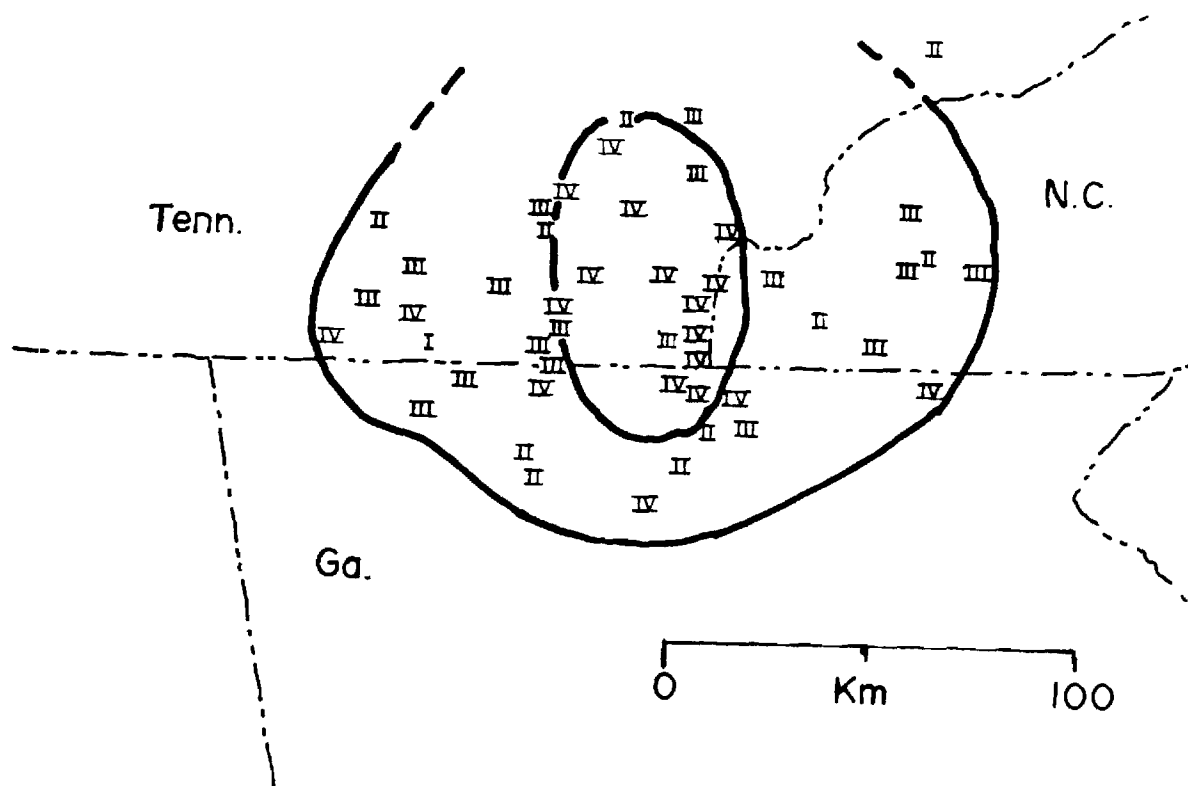


Figure 3. Distribution of Intensity Data (Modified Mercalli) for the August 13, 1979 earthquake in southeastern Tennessee.

Table 1. Summary of Intensity Data for the southeastern Tennessee event of August 13, 1979

<u>City</u>	<u>County</u>	<u>State</u>	<u>Avg.</u>	I	II	III	IV	V
<u>Intensity(ies)</u>								
Copperhill	Polk	TN	III			1		
Old Fort	Polk	TN	III			1		
Murphy	Cherokee	NC	III		1	1	3	
Blue Ridge	Fannin	GA	III			1	1	
Unaka	Cherokee	NC	III			1		
Cherrylog	Gilmer	GA	II		1			
Hiawasse	Towns	GA	IV				1	
Epworth	Fannin	GA	IV				1	
Ooltewah	Hamilton	TN	IV				1	
Townsend	Blount	TN	II		1			
Benton	Polk	TN	IV				1	
Ducktown	Polk	TN	IV				6	1
Postelle	Polk	TN	III			1		
McCaysville	Fannin	GA	IV				1	
Tobbinsville	Monroe	TN	III			1		
Mt. Vernon	Monroe	TN	III			1		
Farner	Polk	TN	IV				1	
Apison	Hamilton	TN	I	1				
Cisco	Murray	GA	IV				1	
Ellijay	Gilmer	GA	IV				1	
Daisy	Hamilton	TN	II		1			
Varnell	Whitfield	GA	III			1		
Andrews	Cherokee	NC	III			1		
Harrison	Hamilton	TN	III			1		
Brasstown	Caly	NC	III			1		
Chattanooga	Hamilton	TN	IV				1	
Madisonville	Monroe	TN	III			2	2	
Cleveland	Bradley	TN	III		1	2	3	
Mineral Bluff	Fannin	GA	IV				1	
Charleston	Bradley	TN	III			1		
Telico Plains	Monroe	TN	IV			3	8	2
Delano	Polk	TN	IV			1	3	
Ocoee	Polk	TN	IV				1	
Reliance	Polk	TN	IV				1	
Marietta	Cobb	GA	I	1				
Cohutta	Whitfield	GA	III			1		
Chatsworth	Murray	GA	II		1			
Eton	Murray	GA	II		1			
Etowah	McMinn	TN	IV				1	
Aquone	Macon	NC	III			1		
Niota	McMinn	TN	II		1			
Shelbyville	Bedford	TN	II		1			
Riceville	McMinn	TN	IV				1	
Topton	Cherokee	NC	II		1			
Decatur	Meigs	TN	I	1				
Calhoun	McMinn	TN	IV				1	
Tenngo	Murray	GA	III			1		
Coker Creek	Monroe	TN	IV		1	3	3	1
Athens	McMinn	TN	IV				2	
Conasauga	Polk	TN	III			1		
Morganton	Fannin	GA	III			1		
Mixson	Hamilton	TN	III			1		
Turtletown	Polk	TN	IV				2	

Table 2. Arrival times at regional seismic stations and location data for the August 13, 1979 earthquake.

	PHASE	STATION	ARRIVAL		ERROR ± SEC.
			HR	MIN SEC	
1	PLG	CDG }	5	19 8.800	.100
2	SLG-PLG	CDG }	0	0 8.800	.100
3	PLG	TUG }	5	19 17.060	.100
4	PN	REG }	5	19 31.100	.500
5	SN-PN	REG }	0	0 25.040	.500
6	PN	CH6 }	5	19 31.200	.500
7	PN	EP1 }	5	19 31.150	.500
8	SN-PN	EP1 }	0	0 25.100	.500
9	PN	ETG }	5	19 32.960	.500
10	PN	WDG }	5	19 33.000	.500
11	SN-PN	WDG }	0	0 25.560	.500
12	PLG	TKL }	5	19 9.200	.100
13	SLG	TKL }	5	19 18.200	.100
14	SLG-PLG	CPD }	0	0 14.800	.100
15	PLG	SRN }	5	19 50.500	1.000
16	SLG	SRN }	5	20 28.300	1.000
17	PLG	SRW }	5	19 51.800	1.000
18	SLG	SRW }	5	20 32.000	1.000
19	PLG	SRI }	5	19 50.000	1.000
20	SLG	SRI }	5	20 30.800	1.000
21	PLG	SRN }	5	19 52.000	1.000
22	SLG	SRN }	5	20 28.200	1.000
23	PN	HBFB }	5	19 58.550	5.000
24	PN	SGS }	5	19 54.950	5.000
25	PN	MIT }	5	19 40.050	5.000
26	PN	LHS }	5	19 45.400	5.000
27	PN	PRM }	5	19 31.650	5.000
28	PN	CHF }	5	19 29.950	5.000
29	PN	JSC }	5	19 41.750	5.000
30	PN	SH1 }	5	20 4.500	5.000
31	SLG	SH1 }	5	21 11.300	5.000
32	PN	SH2 }	5	20 4.300	5.000
33	SLG	SH2 }	5	21 10.200	5.000
34	PN	SH3 }	5	20 5.700	5.000
35	SLG	SH3 }	5	21 12.100	5.000
36	PLG	BG3 }	5	19 20.170	1.000
37	PLG	LPM }	5	19 18.900	1.000
38	PLG	SMT }	5	19 20.140	1.000
39	PN	SRN }	5	19 44.000	1.000
40	PN	SRW }	5	19 45.300	1.000
41	PN	SRI }	5	19 44.400	1.000
42	PN	SRN }	5	19 43.400	1.000

Table 2. (Continued....)

STATION	PHASE	HR	MIN	SEC	+OR-SEC	DIST	AZ
CDG	PLG	5	19	8.80	.10	72.24	200.5
CDG	SLG-PLG	0	0	8.80	.10	72.24	200.5
TVG	PLG	5	19	17.06	.10	125.03	221.9
REG	PN	5	19	31.10	.50	219.27	153.6
REG	SN-PN	0	0	25.04	.50	219.27	153.6
CH6	PN	5	19	31.20	.50	224.72	130.6
EP1	PN	5	19	31.15	.50	221.41	129.0
EP1	SN-PN	0	0	25.10	.50	221.41	129.0
ETG	PN	5	19	32.96	.50	233.93	155.6
WDG	PN	5	19	33.00	.50	231.02	150.9
WDG	SN-PN	0	0	25.56	.50	231.02	150.9
TKL	PLG	5	19	9.20	.10	74.22	48.9
TKL	SLG	5	19	18.20	.10	74.22	48.9
CP0	SLG-PLG	0	0	14.80	.10	115.19	291.2
HRF	PN	5	19	58.55	1.00	444.96	124.0
SGS	PN	5	19	54.95	1.00	418.61	121.9
JSC	PN	5	19	41.75	1.00	303.64	109.9
LRS	PN	5	19	45.40	1.00	336.31	104.0
PR6	PN	5	19	31.45	1.00	223.50	124.0
CHI	PN	5	19	29.95	1.00	211.05	128.9

ERROR ELLIPSE IS AS FOLLOWS:

SEMINOR AXIS LENGTH = 1.5248 KM.
 SEMIMAJOR AXIS LENGTH = 2.6873 KM.
 AZIMUTH OF MAJOR AXIS = 143.7282 DEG.
 AREA OF ELLIPSE = 12.8731 SQ.KM.
 ECCENTRICITY = .8234

MEAN RESIDUAL : .30749 STANDARD DEVIATION : .57611

is equivalent to subtracting exactly 2.0 seconds from the arrival times of the Pn phases. The depth of the Moho in the vicinity of the August 13, 1979 event varies from 40 to 55 km deep on the basis of data from Kean and Long (1980). The depth computed for an assumed Moho at 49.6 km was $9.7 \text{ km} \pm 4.5 \text{ km}$. Interpolation of the Moho depth from Kean and Long (1980) on the basis of the revised epicenter indicate a 45 km Moho depth. Then correcting the 9.7 km depth of focus for the difference between a 45 and 49.6 km deep Moho gives $5.0 \text{ km} \pm 4.5 \text{ km}$ depth. This estimate is consistent with a 6.0 km depth of focus found for one of the aftershocks (see discussion below). If one assumes a 6 km depth of focus for the main shock, then the method of Kean and Long (1980) implies a 46.5 km deep Moho which is consistent with their data for the north Georgia area.

Magnitude

The magnitude of the event was determined from duration data from ten stations. For these stations the duration ranged from 240 to 270 seconds. Using Bollinger's (1979) formula

$$m_b = 2.44 \log_{10} D - 2.87$$

a magnitude of 3.0 was found. Using a similar formula from the U. S. Geological Survey which they apply to the South Carolina seismic network

$$m(D) = 2.0 \log_{10}(D) - 1.5$$

the magnitude was 3.6. We will assume an average magnitude of $M(D) = 3.3 \pm 0.3$ as a reasonable estimate for the August 13, 1979 main event.

Focal Mechanism

A study of the directions of first motion was made for 16 stations (Table 3). The first motions were then evaluated for the domain of valid focal mechanisms using a computer technique developed in Guinn and

Table 3. First Motion data for southeastern Tennessee earthquake of August 13, 1979.

AZIMUTH-----	TOA-----	1ST MOTION-->
44.400	65.000	1.00
204.900	65.000	1.00
151.400	42.000	-1.00
156.200	42.000	-1.00
154.100	42.000	-1.00
130.500	42.000	-1.00
292.300	65.000	1.00
123.700	42.000	-1.00
128.400	42.000	-1.00
123.900	42.000	-1.00
121.700	42.000	-1.00
11.000	65.000	1.00
84.400	42.000	-1.00
85.400	42.000	-1.00
84.900	42.000	-1.00
221.100	65.000	1.00

TYPE 1: SPACE TO TOP OF PAGE AND PRESS RETURN

T 1

Long (1977). The distribution of first motions is given in Figure 4. The valid P T and B axes for these first motions are shown in Figure 5. The P-axis is constrained by the data distribution to (S45°E, 70° dip) within 20°. Two dominant zones of B and T axis are allowed. These indicate fault plains as given in Table 4.

Table 4. Fault plains for focal mechanism solutions

<u>Strike</u>	<u>Dip</u>
Solution 1 N65W	25 S
N80E	65N
Solution 2 N70W	50NE
N10W	55W

We interpret the data in table 4 to imply normal faulting on northwest trending faults. The normal faulting mechanisms differs from previous focal mechanism for southeastern Tennessee which indicate thrust faulting (see Guinn 1977). This event and previous events indicate faulting which is normal to the dominant trend of the near surface faults and geologic units which represent Paleozoic deformation.

Aftershock Study

Associated with this event were four aftershocks recorded at regional stations within four hours of the main event. The third of these was recorded at four stations in the Georgia Tech network and was independently located at 35°17.8'N, 84°30.7°W. Its origin time was at 5:36:28.6 ± 0.9 sec on August 13, 1979.

Within one day after the main event on August 13, 1979 the Tennessee Earthquake Information Center and Georgia Institute of Technology established a joint aftershock monitoring network consisting of four smoked paper recorders. Records were changed daily by Georgia

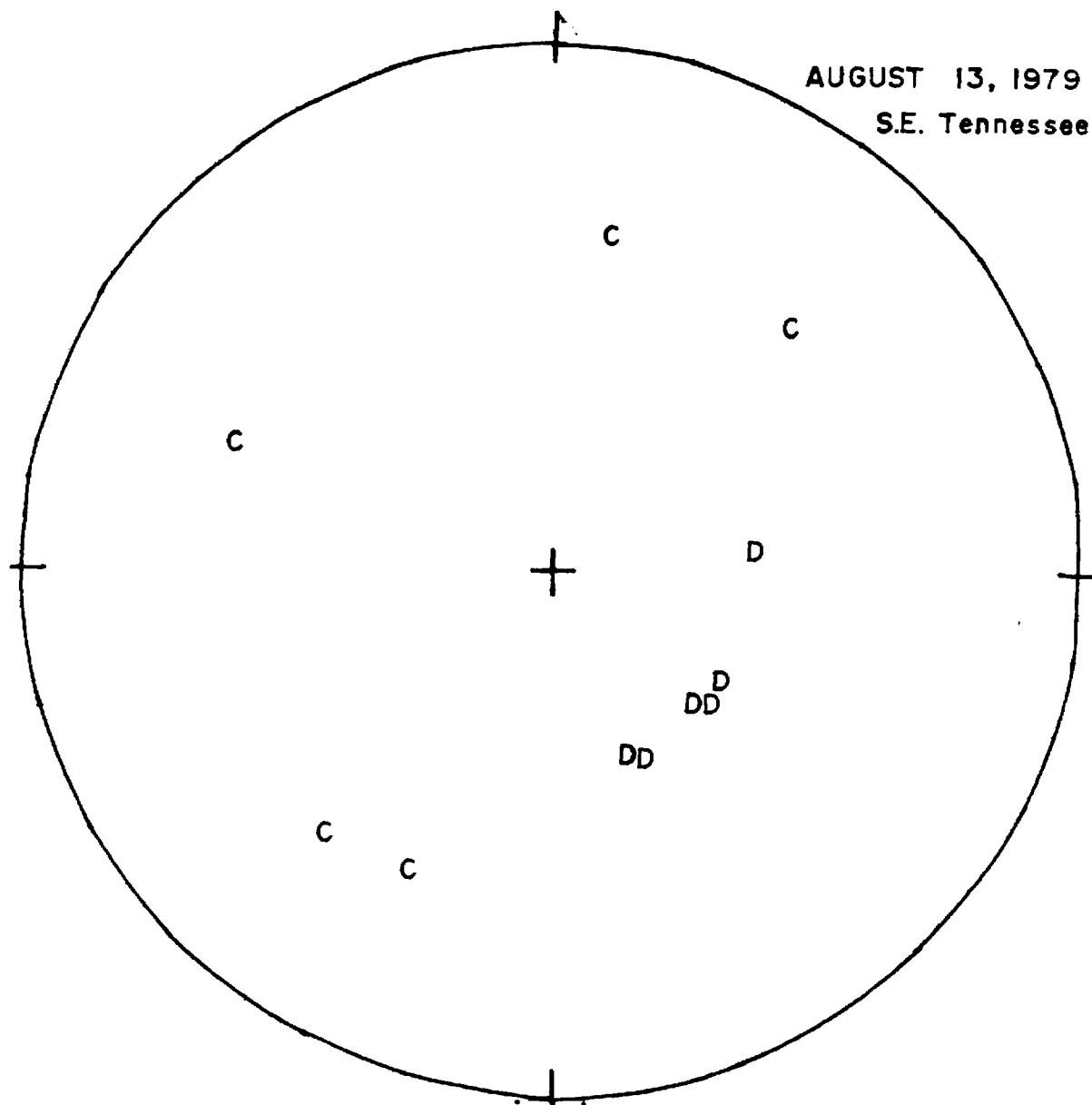


Figure 4. Lower hemisphere plot of first Motion data for the August 13, 1979 southeastern Tennessee earthquake.

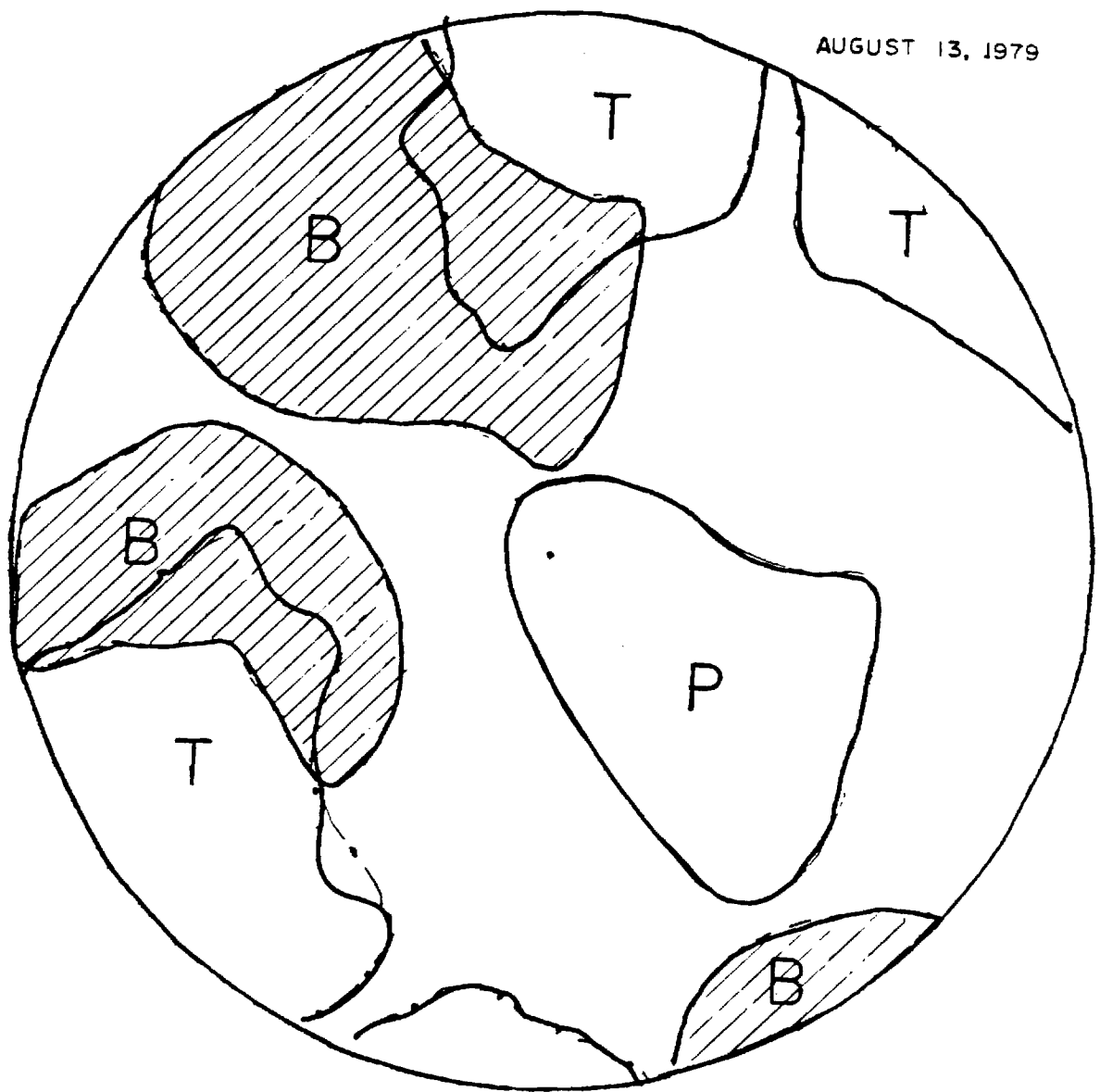


Figure 5. Lower hemisphere projection of valid P, T, and B, axis for the August 13, 1979 southeastern Tennessee earthquake.

Tech and Tennessee Valley Authority personnel for a period of one month and the timing was correlated with WWV daily. The stations were placed at locations surrounding the epicenter of the main event (see Table 6).

From August 14 to August 15, three possible aftershocks were recorded by these stations. One was recorded at only one station and was not located. The other two were located (see Table 5). The depth of focus for the aftershock occurring at 8:14:14.7 on August 15, 1979 was at 6.5 km. This value was used earlier to confirm the depth of the main event. After this aftershock, the temporary recording stations were relocated in order to better surround the epicenters of the recorded aftershocks (see Table 5).

These stations were operated for one month and during that time eleven possible aftershocks were recorded (see Table 6). Of these only

Table 6.

PLT 35°13'12.0"N, 84°27'37.5"W 1120 ft.

IVY 35°17'25.5"N, 84°26'43.5"W 1280 ft.

FCT 35°16'18.0"N, 84°22'18.0"W 1625 ft.

DRT 35°12'37.5"N, 84°21'45.0"W 1850 ft.

two were recorded at more than one station. During the aftershock monitoring period a magnitude 3.2 event was recorded on September 12, 1979. The event occurred near Maryville, TN. In addition, several teleseismic events and regional blasts were recorded.

Discussion of Results

The depth of focus of the events indicates a source in the basement rocks of the underthrust crust as interpreted from COCORP data (Cook). The focal mechanism deviates from past data and may indicate a highly non-uniform stress field in the crust. The depth of focus also may

Table 5. Listing of events recorded during the aftershock monitoring of the August 13, 1979 earthquake in southeastern Tennessee.

EVENTS RECORDED : GEORGIA TECH EAST TENNESSEE NETWORK (TEMPORARY)
AUGUST - SEPTEMBER, 1979

DATE	STA.	A.T.	S-P	T	D.T.	DIST.	LOCATION/COMMENTS
08/14	SMC	08:21:36.43	11.87	16.28	08:21:20.15	95.04	NOT LOCATED
08/15	SMC	02:27:54.10	1.76	2.94	02:27:51.16	15.12	LATITUDE=35.0153 (35D+00.92M) +/-3.43KM. NO DEPTH SEQUENCE
08/15	REL	02:27:54.30	2.68	3.14	02:27:51.16	18.24	LONGITUDE=84.4285 (84D+25.70M) +/-1.075
08/15	SMC	02:39:47.00	.85	1.17	02:39:45.83	6.83	NOT LOCATED; POSSIBLE BLAST
08/15	SMC	08:09:17.40	2.28	2.66	08:09:14.74	18.75	STATION NOT USED IN LOCATION ROUTINE
08/15	LB2	08:09:17.74	2.22	3.02	08:09:14.74	16.62	LATITUDE=35.1519 (35D+09.11M) +/-0.043KM. NO DEPTH SEQUENCE
08/15	REL	08:09:17.75	2.19	3.01	08:09:14.74	16.51	LONGITUDE=84.3322 (84D+19.93M) +/-0.056KM.
08/22	DRT	02:53:34.10	2.36	3.25	02:53:30.87	18.86	NOT LOCATED
08/22	DRT	05:30:18.45	2.49	3.41	05:30:15.04	19.88	NOT LOCATED
08/26	IVY	01:32:09.62	19.50	24.61	01:31:45.01	150.88	JOCASSEF, S.C. EVENT (MAGNITUDE 3.7)
08/26	FCT	01:32:09.38	18.60	24.37	01:31:45.01	142.94	LATITUDE=34.8471 (34D+50.80M) NO DEPTH SEQUENCE
08/26	DRT	01:32:08.13	19.00	23.12	01:31:45.01	139.12	LONGITUDE=82.9467 (82D+56.80M)
08/26	IVY	03:40:04.45	3.70	1.70	03:40:02.75	24.82	LATITUDE=35.4946 (35D+29.67M) +/-11.07KM.
08/26	DRT	03:40:06.70	3.85	3.95	03:40:02.75	30.77	LONGITUDE=84.4026 (84D+24.15M) +/-2.739KM.
08/29	FCT	01:15:46.45	2.36	3.23	01:15:43.2	18.86	NOT LOCATED; POSSIBLE AFTERSHOCK
08/30	DRT	06:14:53.98	2.93	4.02	06:14:49.96	23.45	NOT LOCATED; POSSIBLE AFTERSHOCK
08/31	DRT	06:26:18.79	2.38	3.27	06:26:15.52	19.07	NOT LOCATED
09/01	FCT	23:16:30.06	3.00	4.11	23:16:25.95	23.99	NOT LOCATED
09/04	PLT	04:18:36.54	3.01	4.12	04:18:32.42	24.07	NOT LOCATED
09/09	FCT	16:57:26.42	3.44	4.71	16:57:21.71	27.53	NOT LOCATED
09/09	DRT	12:11:19.80	.47	.65	12:11:19.15	3.77	NOT LOCATED
09/11	IVY	03:43:30.88	?	?	?	?	NOT LOCATED; APPARENT TIMING ERRORS;
09/11	PLT	03:43:38.13	?	?	?	?	ONLY ONE POSSIBLE PG PHASE OBSERVED
09/11	DRT	03:43:48.36	.80	1.01	03:43:55.35	5.91	
09/11	FCT	03:43:53.28	?	?	?	?	
09/11	IVY	04:25:31.13	10.50	12.05	04:25:18.28	77.35	LATITUDE=35.9428 (35D+56.57M) +/-15.235KM. DEPTH=8.00KM.
09/11	FCT	04:25:31.47	11.00	13.19	04:25:18.28	82.74	LONGITUDE=84.7256 (84D+43.54M) +/-5.189KM.
09/11	FCT	04:25:32.74	10.75	14.46	04:25:18.28	84.15	
09/11	DRT	04:25:32.87	12.00	14.59	04:25:18.28	88.21	
09/12	IVY	06:24:14.00	6.60	8.17	06:24:05.19	48.78	LATITUDE=35.4938 (35D+29.62M) NO DEPTH SEQUENCE
09/12	FCT	06:24:13.46	?	7.63	06:24:05.19	43.89	LONGITUDE=83.9175 (83D+55.05M)
09/12	PLT	06:24:16.59	7.15	10.76	06:24:05.19	55.03	STATIONS FCT, DRT SATURATED
09/12	DRT	06:24:14.58	?	8.75	06:24:05.19	50.57	MARYVILLE EVENT

NOTES:

1. ALL DISTANCES ARE IN KILOMETERS.
2. S-P, T ARE GIVEN IN SECONDS.
3. IF AN EVENT WAS NOT LOCATED, T, DIST. ARE ARRIVED UPON AS FOLLOWS:
T-1.37(S-P) DIST-8.015(-P)

explain why the maximum intensity was limited to IV(MM). Additional data are needed to clarify these results.

Acknowledgments

The Tennessee Earthquake Information Center provided coordination and assistance in establishing the aftershock monitoring program and also provided one of the portable instruments used in the monitoring. The aftershock monitoring was largely made possible by a grant from the Tennessee Valley Authority. Don Reinbolt of TVA assisted generously in the field work.

List of Tables

- Table 1. Summary of Intensity data for the southeastern Tennessee event of August 13, 1979.
- Table 2. Arrival times at regional seismic stations and location data for the August 13, 1979 earthquake.
- Table 3. First Motion data for southeastern Tennessee earthquake of August 13, 1979.
- Table 4. Fault planes for focal mechanism solutions for the southeastern Tennessee earthquake of August 13, 1979.
- Table 5. Listing of events recorded during the aftershock monitoring of the August 13, 1979 earthquake in southeastern Tennessee.
- Table 6. Listing of locations and station designations used in the aftershock survey.

List of Figures

- Figure 1. Location map for southeastern Tennessee.
- Figure 2. Regional Seismicity map. Circle denotes 100 km radius from the location of August 13, 1979 earthquake.
- Figure 3. Distribution of Intensity Data (Modified Mercalli) for the August 13, 1979 earthquake in southeastern Tennessee.
- Figure 4. Lower hemisphere plot of first Motion data for the August 13, 1979 southeastern Tennessee earthquake.
- Figure 5. Lower hemisphere projection of valid P, T, and B. axis for the August 13, 1979 southeastern Tennessee earthquake.

LOCATED ON: 80/07/07. 14.37.26.

THE EVENT OCCURED ON AUG 13, 1979

AT ORIGIN TIME 5:18:56.60 +/- .247

EAST TENNESSEE MAIN EVENT

MAGNITUDE: 3.3

THE WEIGHTS ARE

WX= 1.000 WY= 1.000 WZ= 0.000 WT= 1.000

IT WAS LOCATED AT

LATITUDE 35.2200 +/- 1.908 KM. (35D,13.20M)

LONGITUDE 84.3904 +/- 1.634 KM. (84D,23.43M)

DEPTH 6.00 +/- 0.000 KM.

STATION	PHASE	HR	MIN	SEC	+OR-SEC	DIST	AZ	ORC-TIME
CDG	PLG	5	19	8.80	.10	72.24	200.5	-.109
CDG	SLG-PLG	0	0	8.80	.10	72.24	200.5	-.292
TVG	PLG	5	19	17.06	.10	125.03	221.9	-.575
REG	PN	5	19	31.10	.50	219.27	153.6	.711
REG	SN-PN	0	0	25.04	.50	219.27	153.6	.016
CH6	PN	5	19	31.20	.50	224.72	130.6	.148
EP1	PN	5	19	31.15	.50	221.41	129.0	.502
EP1	SN-PN	0	0	25.10	.50	221.41	129.0	-.113
ETG	PN	5	19	32.96	.50	233.93	155.6	.786
WDG	PN	5	19	33.00	.50	231.02	150.9	1.178
WDG	SN-PN	0	0	25.56	.50	231.02	150.9	-.513
TKL	PLG	5	19	9.20	.10	74.22	48.9	-.037
TKL	SLG	5	19	18.20	.10	74.22	48.9	-.348
CPG	SLG-PLG	0	0	14.80	.10	115.19	291.2	.750
HBG	PN	5	19	58.55	1.00	444.96	124.0	.651
SGS	PN	5	19	54.95	1.00	418.61	121.9	.263
JSC	PN	5	19	41.75	1.00	303.64	109.9	1.076
LHS	PN	5	19	45.40	1.00	336.31	104.0	.742
PRM	PN	5	19	31.65	1.00	223.50	124.0	.738
CHF	PN	5	19	29.95	1.00	211.05	129.5	.565

DIAGONAL ELEMENTS

1.5200 1.3424 .1695

COVARIANCE MATRIX:

12.948	5.491	-1.293
5.491	9.495	-.942
-1.293	-.942	.217

ERROR ELLIPSE IS AS FOLLOWS:

SEMINOR AXIS LENGTH = 1.5248 KM.

SEMAJOR AXIS LENGTH = 2.6873 KM.

AZIMUTH OF MAJOR AXIS = 143.7282 DEG.

AREA OF ELLIPSE = 12.8730 SQ.KM.

ECCENTRICITY = .8234

MEAN RESIDUAL : .30748 STANDARD DEVIATION : .53015
NO DEPTH COMPUTATION

LOCATED ON: 80/07/07. 14.53.39.

THE EVENT OCCURED ON AUG 13, 1979

AT ORIGIN TIME 5:18:56.61 +/- .163

EAST TENNESSEE MAIN EVENT

MAGNITUDE: 3.3

THE WEIGHTS ARE

WX= 1.000 WY= 1.000 WZ= 1.000 WT= 1.000

IT WAS LOCATED AT

LATITUDE 35.1808 +/- 2.043 KM. (35D,10.85M)

LONGITUDE 84.3407 +/- 1.775 KM. (84D,20.44M)

DEPTH 15.53 +/- 4.201 KM.

STATION	PHASE	HR	MIN	SEC	+OR-SEC	DIST	AZ	OBS-T
CDG	PLG	5	19	8.80	.10	69.98	205.3	.321
CDG	SLG-PLG	0	0	8.80	.10	69.98	205.3	.097
TUG	PLG	5	19	17.06	.10	124.97	224.8	-.509
REG	PN	5	19	29.10	.50	213.40	154.2	.166
REG	SN-PN	0	0	23.64	.50	213.40	154.2	-.285
CH6	PN	5	19	29.20	.50	218.50	130.5	-.354
EP1	PN	5	19	29.15	.50	215.21	128.9	-.002
EP1	SN-PN	0	0	23.70	.50	215.21	128.9	-.385
ETG	PN	5	19	30.96	.50	228.14	156.2	.232
WDG	PN	5	19	31.00	.50	225.06	151.4	.644
WDG	SN-PN	0	0	24.16	.50	225.06	151.4	-.906
TKL	PLG	5	19	9.20	.10	73.93	44.1	.067
TKL	SLG	5	19	18.20	.10	73.93	44.1	-.094
CP0	SLG-PLG	0	0	14.80	.10	121.06	292.4	.188
HBF	PN	5	19	56.55	1.00	438.89	123.9	.130
SGC	PN	5	19	52.95	1.00	412.59	121.7	-.264
JSC	PN	5	19	39.75	1.00	298.03	109.4	.500
LHS	PN	5	19	43.40	1.00	331.02	103.5	.127
PRM	PN	5	19	29.65	1.00	217.38	123.7	.225
CHF	PN	5	19	27.95	1.00	204.85	128.4	.061

DIAGONAL ELEMENTS

1.8783 1.6245 .1707 4.6240

COVARIANCE MATRIX:

34.072	24.079	-.416	56.131
24.079	25.713	-.143	49.822
-.416	-.143	.216	1.859
56.131	49.822	1.859	144.059

ERROR ELLIPSE IS AS FOLLOWS:

SEMINOR AXIS LENGTH = .8908 KM.
SEMAJOR AXIS LENGTH = 2.8115 KM.
AZIMUTH OF MAJOR AXIS = 139.9233 DEG.
AREA OF ELLIPSE = 7.8680 SQ.KM.
ECCENTRICITY = .9485

MEAN RESIDUAL : .00293 STANDARD DEVIATION : .35001

WOULD YOU BELIEVE IT CONVERGED

VELOCITY RATIO COMPUTATION COMPLETE

LOCATED ON: 80/07/07, 15.12.07.

THE EVENT OCCURED ON AUG 13, 1979

AT ORIGIN TIME 5:36:28.57 +/- .850

EAST TENNESSEE EVENT AFTERSHOCK #3

MAGNITUDE: /

THE WEIGHTS ARE

WX= 1.000 WY= 1.000 WZ= 0.000 WT= 1.000

IT WAS LOCATED AT

LATITUDE 35.2959 +/- 5.557 KM. (35E+17.75N)

LONGITUDE 84.5093 +/- 4.554 KM. (84E+39.56N)

DEPTH 1.00 +/- 0.000 KM.

STATION	PHASE	HR	MIN	SEC	40R-SEC	DIST	AZ	OBS-
TUG	PLG	5	36	50.05	.10	124.85	215.6	.453
TUG	SLG-PLG	0	0	15.50	.10	124.85	215.6	.275
CDG	PLG	5	36	41.90	.10	77.46	190.7	.134
CDG	SLG	5	36	50.50	.10	77.46	190.7	-1.012
TKI	PLG	5	36	42.00	.10	78.01	58.9	.144
TKI	SLG	5	36	51.00	.10	78.01	58.9	-.667
CH5	PN	5	37	10.35	.30	244.55	130.4	2.091
CH5	SN	5	37	40.00	.30	244.55	130.4	2.372
ET6	PN	5	37	5.10	.30	246.04	154.1	-.903
ET6	SN	5	37	32.00	.30	246.04	154.1	-.711

DIAGONAL ELEMENTS

1.8796 1.5466 .2509

COVARIANCE MATRIX:

118.387	77.660	3.319
77.660	53.671	3.110
3.319	3.110	.010

ERROR ELLIPSE IS AS FOLLOWS:

SEMINOR AXIS LENGTH = 2.9782 KM.

SEMAJOR AXIS LENGTH = 15.6343 KM.

AZIMUTH OF MAJOR AXIS = 139.2509 DEG.

AREA OF ELLIPSE = 183.7074 SQ.KM.

ECCENTRICITY = .9884

MEAN RESIDUAL : .21737 STANDARD DEVIATION : 1.186

NO DEPTH COMPUTATION

LOCATED ON: 80/07/07. 15.21.32.

THE EVENT OCCURED ON AUG 13, 1979
AT ORIGIN TIME 5:36:29.04 +/- .776
EAST TENNESSEE EVENT AFTERSHOCK #3
MAGNITUDE: /
THE WEIGHTS ARE

WX= 1.000 WY= 1.000 WZ= 1.000 WT= 1.000

IT WAS LOCATED AT

LATITUDE 35.2475 +/- 11.458 KM. (35D,14.85N)
LONGITUDE 84.4351 +/- 9.148 KM. (84D,26.10W)
DEPTH 11.15 +/- 17.657 KM.

STATION	PHASE	HR	MIN	SEC	10R-SEC	DIST	AZ	GBS-THE
TVB	PLG	5	36	50.05	.10	124.70	219.6	.064
TVB	SLG-PLG	0	0	15.50	.10	124.70	219.6	.417
CDG	PLG	5	36	41.90	.10	73.84	196.7	.320
CDG	SLG	5	36	50.50	.10	73.84	196.7	-.284
TKL	PLG	5	36	42.00	.10	75.45	52.7	.155
TKL	SLG	5	36	51.00	.10	75.45	52.7	-.234
CH5	PN	5	37	8.35	.30	256.02	130.5	1.447
CH5	SN	5	37	36.60	.30	256.02	130.5	1.706
ETG	PN	5	37	3.10	.30	238.36	155.0	-1.651
ETG	SN	5	37	29.60	.30	238.36	155.0	-1.566

DIAGONAL ELEMENTS

3.4958 2.7712 .2392 5.7869

COVARIANCE MATRIX:

111.405	84.532	-5.468	156.380
84.532	71.018	-4.453	124.438
-5.468	-4.453	.511	-5.754
156.380	124.438	-5.754	264.556

ERROR ELLIPSE IS AS FOLLOWS:

SEMINOR AXIS LENGTH = 2.7592 KM.
SEMAJOR AXIS LENGTH = 17.7563 KM.
AZIMUTH OF MAJOR AXIS = 141.7177 DEG.
AREA OF ELLIPSE = 153.9153 SQ.KM.
ECCENTRICITY = .9879

MEAN RESIDUAL : .03733 STANDARD DEVIATION : 1.08559
WOULD YOU BELIEVE IT CONVERGED
VELOCITY RATIO COMPUTATION COMPLETE

LOCATED ON: 80/07/07, 15.47.46.

THE EVENT OCCURED ON AUG 15, 1979

AT ORIGIN TIME 2:27:51.72 +/- .323

EAST TENNESSEE AFTERSHOCK #6

MAGNITUDE: /

THE WEIGHTS ARE

WX= 1.000 WY= 1.000 WZ= 0.000 WT= 1.000

IT WAS LOCATED AT

LATITUDE 35.2471 +/- 2.761 KM. (SED:14.82M)

LONGITUDE 84.3891 +/- 2.230 KM. (RAD:22.35M)

DEPTH 5.00 +/- 6.000 KM.

STATION	PHASE	HR	MIN	SEC	40K-SEC	DIST	AZ	OBS-THE
SMD	PLG	2	27	54.10	.50	11.05	196.9	.184
SMD	SLG-PLG	0	0	1.76	.50	11.05	196.9	-.262
REL	PLG	2	27	54.30	.50	14.49	230.9	-.184
REL	SLG-PLG	0	0	2.68	.50	14.49	230.9	.262

DIAGONAL ELEMENTS

7.4642 6.0301 .8724

COVARIANCE MATRIX:

121.782	45.875	4.030
45.875	63.633	-4.439
4.030	-4.439	1.434

ERROR ELLIPSE IS AS FOLLOWS:

SEMINOR AXIS LENGTH = 2.9070 KM.

SEMAJOR AXIS LENGTH = 5.4928 KM.

AZIMUTH OF MAJOR AXIS = 151.1828 DEG.

AREA OF ELLIPSE = 48.4393 SQ.KM.

ECCENTRICITY = .8596

MEAN RESIDUAL : -.00000 STANDARD DEVIATION : .26154
NO DEPTH COMPUTATION

LOCATED ON: 80/07/07. 16.24.55.

THE EVENT OCCURED ON AUG 15, 1979

AT ORIGIN TIME 8: 9:15.26 +/- .142

EAST TENNESSEE EVENT AFTERSHOCK #7

MAGNITUDE: /

THE WEIGHTS ARE

WX= 1.000 WY= 1.000 WZ= 1.000 WT= 1.000

IT WAS LOCATED AT

LATITUDE 35.2334 +/- .961 KM. (35D,14.01M)

LONGITUDE 84.3930 +/- .854 KM. (84D,23.58M)

DEPTH 6.49 +/- 1.004 KM.

STATION	PHASE	HR	MIN	SEC	+OR-SEC	DIST	AZ	OBS-THE
REL	PG	8	9	17.80	1.00	14.93	235.0	-.174
REL	SP1	0	0	2.25	.10	14.93	235.0	-.209
LG2	PG	8	9	17.77	1.00	14.48	57.9	-.123
LG2	SP1	0	0	2.25	.10	14.48	57.9	-.136
UGT	PG	8	9	17.22	1.00	8.84	344.2	.352
UGT	SP1	0	0	1.53	.10	8.84	344.2	.074
SMC	PG	8	9	17.35	1.00	11.80	197.5	-.055
SMC	SP1	0	0	2.10	.10	11.80	197.5	.157

DIAGONAL ELEMENTS

2.1950 1.9421 .5286 1.6773

COVARIANCE MATRIX:

24.532	13.768	-.313	6.063
13.768	19.375	-.421	4.718
-.313	-.421	.535	-2.739
6.063	4.718	-2.739	26.803

ERROR ELLIPSE IS AS FOLLOWS:

SEMINOR AXIS LENGTH = .7256 KM.

SEMAJOR AXIS LENGTH = 1.5437 KM.

AZIMUTH OF MAJOR AXIS = 140.3040 DEG.

AREA OF ELLIPSE = 3.5190 SQ.KM.

ECCENTRICITY = .8826

MEAN RESIDUAL : -.01437 STANDARD DEVIATION : .19398

WOULD YOU BELIEVE IT CONVERGED

VELOCITY RATIO COMPUTATION COMPLETE

LOCATED ON: 80/07/07, 16.33.05.

THE EVENT OCCURED ON AUG 26, 1979

AT ORIGIN TIME 3:40: .86 +/- .588

EAST TENNESSEE EVENT AFTERSHOCK #10

MAGNITUDE: /

THE WEIGHTS ARE

WX= 1.000 WY= 1.000 WZ= 0.000 WT= 1.000

IT WAS LOCATED AT

LATITUDE 35.4829 +/- 12.773 KM. (35D,28.97M)

LONGITUDE 84.4372 +/- 3.217 KM. (84D,26.23M)

DEPTH 6.00 +/- 0.000 KM.

STATION	PHASE	HR	MIN	SEC	10R-SEC	DIST	AZ	ORS-THE
IUY	PLG	3	40	4.45	.50	21.54	181.5	-.335
IUY	SLG-PLG	0	0	3.70	.50	21.54	181.5	.479
DRT	PLG	3	40	6.70	.50	31.10	166.5	.335
DRT	SLG-PLG	0	0	3.85	.50	31.10	166.5	-.479
DIAGONAL ELEMENTS								
		18.9427	4.7713	.8724				

COVARIANCE MATRIX:

717.530	-71.969	-.557
-71.969	44.532	-5.861
-.557	-5.861	1.462

ERROR ELLIPSE IS AS FOLLOWS:

SEMINOR AXIS LENGTH = 5.0181 KM.

SEMAJOR AXIS LENGTH = 22.2387 KM.

AZIMUTH OF MAJOR AXIS = 6.0361 DEG.

AREA OF ELLIPSE = 350.5928 SQ.KM.

ECCENTRICITY = .9742

MEAN RESIDUAL : -.00000 STANDARD DEVIATION : .47680
NO DEPTH COMPUTATION

LOCATED ON: 80/07/07. 16.56.25.

THE EVENT OCCURED ON SEP 12, 1979

AT ORIGIN TIME 6:24: 4.86 +/- .354

MARYVILLE, TENNESSEE EVENT

MAGNITUDE: 3.2

THE WEIGHTS ARE

WX= 1.000 WY= 1.000 WZ= 0.000 WT= 1.000

IT WAS LOCATED AT

LATITUDE 35.5151 +/- 1.991 KM. (35D,30.90M)

LONGITUDE 83.8927 +/- 2.386 KM. (83D,53.56M)

DEPTH 5.00 +/- 0.000 KM.

STATION	PHASE	HR	MIN	SEC	FOR-SEC	DIST	AZ	OBS-
IVY	PLG	6	24	14.00	.10	55.91	243.4	-.471
IVY	SLG-PLG	0	0	6.60	.10	55.91	243.4	-.607
PLT	PLG	6	24	15.59	.10	61.01	237.6	.277
PLT	SLG-PLG	0	0	7.15	.10	61.01	237.6	-.646
FCT	PLG	6	24	13.46	.10	48.62	236.3	.194
DRT	PLG	6	24	14.85	.10	54.04	231.4	.687
GBG	PN	6	24	41.30	.40	231.95	164.2	1.032
GBG	PLG	6	24	42.30	.20	231.95	164.2	-1.267
GBG	SN	6	25	5.30	.50	231.95	164.2	-1.184
GBG	SLG	6	25	10.70	.20	231.95	164.2	-.423
CH6	PN	6	24	39.00	.40	218.66	145.0	.355
CH6	PLG	6	24	41.60	.30	218.66	145.0	.230
CH6	SLG	6	25	9.30	.30	218.66	145.0	1.911
ETG	PN	6	24	43.70	.20	251.50	168.4	1.050
ETG	PLG	6	24	46.20	.30	251.50	168.4	-.598
WDG	PN	6	24	42.90	.50	244.42	164.2	1.110
WDG	PLG	6	24	45.10	.30	244.42	164.2	-.529
EP1	PLG	6	24	39.90	.10	213.88	143.7	-.681
EP1	SLG	6	25	6.30	.20	213.88	143.7	.251
CDG	PLG	6	24	24.70	.10	122.55	215.3	-.785
CDG	SLG	6	24	40.40	.20	122.55	215.3	.001
DRT	PLG	6	24	13.30	.20	59.15	320.1	-1.701
BLA	PN	6	24	56.00	.20	366.90	59.6	-.761
CPD	PLG	6	24	33.00	.20	152.44	273.3	2.577
PRM	PN	6	24	38.20	.20	210.87	138.4	.496

DIAGONAL ELEMENTS

.7710 1.0432 .1524

COVARIANCE MATRIX:

4.570	-.134	-.679
-.134	7.293	-1.698
-.679	-1.698	.760

ERROR ELLIPSE IS AS FOLLOWS:

SEMIMINOR AXIS LENGTH = 2.2379 KM.

SEMIMAJOR AXIS LENGTH = 2.8302 KM.

AZIMUTH OF MAJOR AXIS = 87.1850 DEG.

AREA OF ELLIPSE = 19.8975 SQ.KM.

ECCENTRICITY = .6122

MEAN RESIDUAL : .02056 STANDARD DEVIATION : 1.0027

NO DEPTH COMPUTATION

LOCATED ON: 80/07/07. 17.04.17.

THE EVENT OCCURED ON SEP 12, 1979

AT ORIGIN TIME 6:24: 4.79 +/- .415

MARYVILLE, TENNESSEE EVENT

MAGNITUDE: 3.2

THE WEIGHTS ARE

WX= 1.000 WY= 1.000 WZ= 1.000 WT= 1.000

IT WAS LOCATED AT

LATITUDE 35.5287 +/- 2.113 KM. (35D,31.72M)

LONGITUDE 83.8848 +/- 2.383 KM. (83D,53.09M)

DEPTH 28.44 +/- 5.830 KM.

STATION	PHASE	HR	MIN	SEC	+OR-SEC	DIST	AZ	OBS-THE
IVY	PLG	6	24	14.00	.10	57.23	242.4	-.482
IVY	SLG-PLG	0	0	6.60	.10	57.23	242.4	-.472
PLT	PLG	6	24	15.59	.10	62.43	236.8	.250
PLT	SLG-PLG	0	0	7.15	.10	62.43	236.8	-.522
FCT	PLG	6	24	13.46	.10	50.06	235.3	.163
DRY	PLG	6	24	14.85	.10	55.55	230.6	.645
GBG	PN	6	24	39.30	.40	233.21	164.5	.768
GBG	PLG	6	24	42.30	.20	233.21	164.5	-1.268
GBG	SN	6	25	1.90	.50	233.21	164.5	-1.548
GBG	SLG	6	25	10.70	.20	233.21	164.5	-.282
CH4	PN	6	24	37.00	.40	219.49	145.4	.144
CH4	PLG	6	24	41.60	.30	219.49	145.4	.300
CH4	SLG	6	25	9.30	.30	219.49	145.4	2.173
ETG	PN	6	24	41.70	.20	252.84	168.7	.777
ETG	PLG	6	24	46.20	.30	252.84	168.7	-.612
WDG	PN	6	24	40.90	.50	245.69	164.5	.946
WDG	PLG	6	24	45.10	.30	245.69	164.5	-.530
EP1	PLG	6	24	39.90	.10	214.68	144.0	-.604
EP1	SLG	6	25	6.30	.20	214.68	144.0	.524
CDG	PLG	6	24	24.70	.10	124.20	215.1	-.850
CDG	SLG	6	24	40.40	.20	124.20	215.1	.037
ORT	PLG	6	24	13.30	.20	58.47	318.7	-1.385
BLA	PN	6	24	54.00	.20	365.46	58.7	-.695
CPO	PLG	6	24	33.00	.20	153.06	272.7	2.678
PRM	PN	6	24	36.20	.20	211.52	138.8	.307

DIAGONAL ELEMENTS

.8298 1.0490 .1770 3.0820

COVARIANCE MATRIX:

4.513	-1.583	.327	4.270
-1.583	5.739	-.735	-1.307
.327	-.735	.174	1.280
4.270	-1.307	1.280	34.355

ERROR ELLIPSE IS AS FOLLOWS:

SEMIMINOR AXIS LENGTH = 1.9691 KM.

SEMAJOR AXIS LENGTH = 2.7781 KM.

AZIMUTH OF MAJOR AXIS = 55.5801 DEG.

AREA OF ELLIPSE = 17.1859 SQ.KM.

ECCENTRICITY = .7054

MEAN RESIDUAL : .01453 STANDARD DEVIATION : .99472
WOULD YOU BELIEVE IT CONVERGED

VELOCITY RATIO COMPUTATION COMPLETE

Final Technical Letter Report

Grant No: 14-08-0001-G-540

Reporting Period Covered: 7/1/78 - 7/31/80

Grantee: Georgia Institute of Technology

Supported by: U. S. Geological Survey
Geothermal Research Program
Reston, Virginia

Grant Amount: \$30,777.00

Start Date: 7/1/78

Expiration Date: 7/31/80

Principal Investigator: Robert P. Lowell

U.S.G.S. Technical Officer: Donald W. Klick

Date Submitted: October 15, 1980

Title of Research Project: Convection in Narrow Vertical Fracture
Spaces

Objectives of Project: The main purpose of this project is to examine thermal convection in long, deep, but very narrow vertical fracture spaces. The initiation and time development of the physical processes are to be studied on the basis of mathematical-physical approximation methods and numerical techniques. The results are to be interpreted with regard to known geothermal systems in the Basin and Range and other areas where faults or fractures are the dominant controlling structures.

Summary

This report is the product resulting from a theoretical investigation of thermal convective processes in the earth's crust with relevance to geothermal systems. The work involved three main divisions: 1) convection in a fault or fracture zone; 2) convection in fluid-filled fractures; 3) convection in porous layer with a radiative condition on the upper boundary. The principal effort contained in this report concerns division 1); divisions 2) and 3) have been treated fully in earlier, semi-annual reports and have been described in less detail here. The principal results from each of these divisions are:

1. Convection in a fault or fracture zone. Under finite amplitude conditions with $5R_c < R < 10R_c$, in a homogeneous, isotropic porous material with fault-like geometry, and bounded by either perfectly conducting or imperfectly conducting walls, the cell pattern is weakly three-dimensional. The geometry is such, however, that the velocity perpendicular to the fracture aperture is significantly less than in the other two directions. The pattern thus approximates that of two-dimensional transverse rolls. The results obtain regardless of initial perturbation or aspect ratio. Comparison with field data tends to confirm the theoretical cell pattern results.

In fault zones with anisotropic permeability conditions, the critical Rayleigh number is less than or greater than that for an isotropic medium, depending on whether the horizontal permeability is less than or greater than the vertical. For a given fault aspect ratio, the cell aspect ratio increases as the vertical permeability increases with respect to the horizontal.

2. Convection in fluid-filled fractures. In a single fixed-width fracture, the outlet temperature and flow rate decreases in time as $t^{-1/4}$. If the fracture is allowed to undergo thermal expansion, the flow rate increases as $t^{1/2}$ and the temperature falls as t^{-1} . In a system of fractures, however, the thermal expansion effects are bounded, having a lessened influence on a time scale $> h^2/a$, where h is the distance between adjacent fractures and a is the thermal diffusivity. In a single fracture, temperature and velocity variations across the fracture aperture are negligible. For a closely spaced system of fractures, however, such temperature variations may be important with regard to some geochemical processes.

3. Convection in a porous layer with a radiative condition on the upper boundary. As the heat transfer coefficient decreases, the critical Rayleigh number increases, and the cell wavelength decreases. These effects are small and are not likely to be important in natural geothermal systems.

I. INTRODUCTION

This document represents the final technical report on the research on thermal convection in fault and fracture zones which has been conducted under grant 14-08-00001-G-540. This work has been a continuation of an effort initiated under USGS grant 14-08-00001-G-365 as part of the Extramural Geothermal Research program. The initial phase of the work was done in conjunction with Dr. Gunnar Bodvarsson of Oregon State University; however, his group has not been involved in the present effort.

The principal research tasks which have been performed over the duration of the current project have been:

(a) a determination of the critical Rayleigh number for the onset of convective instability in a slab of porous material with a mixed (radiative) thermal condition on the upper boundary.

(b) an investigation of the temporal evolution of convection in narrow, open, fluid-filled fractures, including thermoelastic effects as well as a non-uniform velocity and temperature profile across the fracture aperture.

(c) an investigation of convection in a permeable fault or fracture zone, including the effects of anisotropic permeability on the critical Rayleigh number as well as finite amplitude convection in a porous zone imbedded in an impermeable layer of rock having a finite thermal conductivity.

The research performed under current project has formed the basis of one M.S. thesis and has served as an important section of a second M.S.thesis, both of which have been completed. There have also been two

presentations and three papers published; however some of the material for these papers was developed under the initial phase of the research (under G365). A paper containing the finite-amplitude studies is currently in preparation.

The research tasks performed under items (a) and (b) above, have been thoroughly presented in earlier technical reports and the results will only be briefly summarized here. The emphasis in this report will be on the study of finite-amplitude convection in a fault zone, which has not been reported on earlier. The main body of the report which follows will be divided into subsections: II. General Framework and Objectives; III. Convection in a Fault or Fracture Zone - Finite Difference Models; IV. Convection in a Fault or Fracture Zone - Anisotropic Permeability; V. Convection in a Fluid-Filled Fracture; VI. Convection in a Porous Slab with a Radiative Upper Boundary Condition; VII. Bibliography; VIII. Students Supported and Theses; IX. Papers and Publications.

II. GENERAL FRAMEWORK AND RESEARCH OBJECTIVES

The energetics of geothermal systems depends fundamentally upon patterns of heat transport and fluid flow within heated, highly permeable regions of the earth's crust. The ultimate source of heat for many geothermal systems is undoubtedly of magmatic origin, but, in some cases the geothermal fluid is heated at depth as a result of an unusually high geothermal gradient. Most of the systems in the Basin and Range province are probably of the latter type (White and Williams, 1975).

Of even more importance, however, is the nature and distribution of permeability within the geothermal reservoir. The permeability may

either be primary, resulting from interconnected pore spaces within the rock volume or secondary, resulting from fractures and/or fault zones. In all geothermal fields currently under production, the geothermal fluids are withdrawn from discrete fractured regions within the reservoir, yet most mathematical modeling of geothermal systems has assumed a Darcian type of flow through a rock with a bulk permeability. That is not to say that it has been necessarily assumed that the permeability is of a primary type, but rather than one normally assumes the fractures to be on such a fine scale that, for mathematical (or numerical) convenience, the Darcy flow model is appropriate on spatial scales of the order of the reservoir dimensions.

The mathematical treatment for the onset of thermal convection under such assumptions follows the method of Lapwood (1948), or some deviant of it; and the treatment of finite amplitude convection uses the same basic perturbation equations with the addition of higher order, non-linear transport terms which are neglected in the linear stability analysis. These models have provided many useful results with regard to the physics of geothermal systems, but often this approach may be quite unrealistic. Geothermal systems in which main permeability is furnished by narrow, discrete, widely separated fault and/or fracture zones imbedded in an otherwise impermeable rock are better handled by somewhat different techniques. Examples of the latter systems are found in Iceland, where dikes provide the main vertical permeability, in the Basin and Range, where long, deep, master faults probably provide the main vertical permeability (Hose and Taylor, 1974), and possibly in the oceanic crust (Lowell, 1975; Sleep and Wolery, 1978).

The principal purpose of this research has been to examine thermal convection in long, deep, but very narrow vertical fracture spaces. The initiation and temporal evolution of the physical processes have been studied on the basis of mathematical-physical approximation methods and finite difference techniques. The results have been interpreted with regard to known geothermal systems in the Basin and Range and other regions where major faults and fractures are the structures controlling the permeability.

III. CONVECTION IN A FAULT OR FRACTURE ZONE

The initial work on thermal convection in permeable material was done by Lapwood (1948), who assumed an infinite isotropic, homogeneous porous slab with plane horizontal boundaries and heated from below. Since Lapwood's original paper, much work has been done on convective instability in a porous medium, including determination of a critical number in the case of temperature dependent fluid properties (Straus and Schubert, 1977; Kassoy and Zebib, 1975), and anisotropic permeability (Wooding, 1976). Finite amplitude results have also been obtained (e.g. Straus, 1974; Ribando et al., 1976). Of particular interest, however, are the recent results on convection in a closed porous container (Beck, 1972; Holst and Aziz, 1972; Zebib and Kassoy, 1977; Murphey, 1979; Straus and Schubert, 1978; Lowell and Shyu, 1978; Lowell, 1979b, c; Shyu, 1979).

The results to date have several shortcomings with regard to an analysis of convection in a fault zone. The different model assumptions made by the various investigators as regards the condition for the onset of instability have led to a somewhat confused picture as to the cell pattern at the onset of instability and possible modifications of the

cell pattern under finite amplitude conditions. The only finite-amplitude results (Holst and Aziz, 1972; Straus and Schubert, 1978) have been for steady-state systems with insulated vertical walls, which is not a realistic condition for a natural system. Moreover, the models have not considered containers with a fault-like geometry (i.e. a container with one horizontal dimension much shorter than the vertical and the other horizontal dimension). The particular questions which have been addressed in the present research are: (1) Is the cell pattern three-dimensional or two-dimensional? (2) If two-dimensional, are rolls aligned with axes across the fracture aperture (as in Murphy, 1979, Beck, 1972) along the strike of fracture (as in Lowell and Shyu, 1978; Shyu, 1979)? (3) Does the cell pattern at finite-amplitude depend upon initial and/or boundary conditions, or aspect ratio? (4) Does the cell pattern change in time?

We have tried to answer those questions by developing finite-difference models of thermal convection in rectangular boxes with fault-like geometry. The fluid motion was assumed to be three-dimensional and the Rayleigh number supercritical, based on the critical value for perfectly conducting walls given by Shyu (1979). For all models, the short walls of the box were assumed to be insulated; the long walls were assumed either to be perfectly conducting or to be bounded by a block of impermeable rock having a finite thermal conductivity. The top and bottom planes were assumed to be impermeable and at constant temperature. Various initial perturbations and aspect ratios were used and the system was allowed to evolve in time, the final output being a representation of the velocity field at representative planes and the conductive heat flow field through the upper surface of the container.

The results were interpreted with regard to known geothermal systems in which fractures and faults are dominant controlling structures.

A. Basic Equations

Figure 1 depicts a simple model of a porous fault zone imbedded between two impermeable blocks, and inclined at an angle θ to the vertical. In the cases discussed below, θ was assumed to be 90° so that the acceleration due to gravity, g , acted in the negative x direction. The pertinent equations of conservation of mass, momentum and energy for the porous zone were respectively:

$$\nabla \cdot \vec{v} = 0 \quad (1)$$

the fluid being assumed to be incompressible;

$$\vec{v} = -(K/\eta)(\nabla P - \rho_f \vec{g}) \quad (2)$$

inertial terms being neglected;

$$(\rho c)_m \partial T / \partial t = \lambda_m \nabla^2 T - \rho_f c_f \vec{v} \cdot \nabla T \quad (3)$$

In the impermeable material, heat was transferred by conduction only.

Thus,

$$\nabla^2 T = (\rho_s c_s / \lambda_s) \partial T / \partial t \quad (4)$$

The symbols are defined in Table 1.

Solutions to equations (1) through (4) were subject to boundary conditions:

$$\vec{v} \cdot \hat{n} = 0 \quad (5)$$

at the boundaries of the porous zone, where \hat{n} is a unit vector normal to the walls;

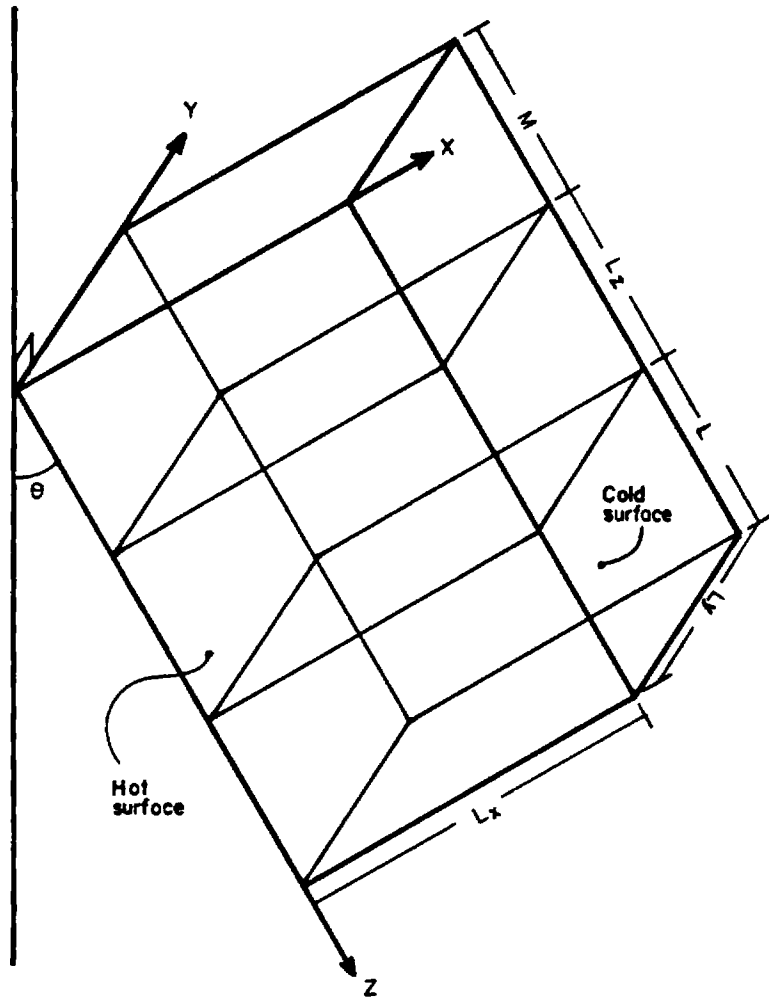


Figure 1. Basic physical system with its dimensions and boundary conditions of the temperature

TABLE 1. LIST OF SYMBOLS

a	thermal diffusivity; cell wavelength (Ch. VI.)
A	aspect ratio L_z/L_x
B	aspect ratio L_z/L_y
c	specific heat
d	fracture width
g	gravitational acceleration
h	fracture spacing; slab thickness (Ch. VI.)
k	permeability
L	dimension of porous zone in direction of subscript
M	horizontal dimension of impermeable material
P	pressure
q	mass flow rate in fracture
R, Ry	Rayleigh number
R_c	critical Rayleigh number
$R_{c, iso}$	critical Rayleigh of isotropic permeability
t	time
T	temperature
T_0	temperature at cold boundary; boundary temperature (Ch. V.)
T_1	temperature at hot boundary
ΔT_0	temperature difference between hot and cold boundaries
u	x component of Darcian fluid velocity; displacement of fracture wall (Ch. V.)
v	y component of Darcian fluid velocity

w z component of Darcian fluid velocity

\vec{v} Darcian velocity vector

x,y,z Cartesian coordinates

GREEK LETTERS

α^*, β thermal expansion coefficient

∇ DEL operator

$\bar{\nabla}^2$ modified Laplacian operator present in the dimensionless equations

$$= A \partial^2 / \partial x^2 + B \partial^2 / \partial y^2 + \partial^2 / \partial z^2$$

γ ratio of vertical to horizontal permeability

ζ heat transfer coefficient

η viscosity

θ angle of inclination (Figure 1), fluid temperature in open fracture system (Ch. V.)

λ thermal conductivity

ρ density

τ thermal interference time

$\vec{\psi}$ vector potential (ψ_1, ψ_2, ψ_3)

SUBSCRIPTS

f fluid

m solid-fluid mixture

s solid

o cold surface

SUPERSCRIPITS

' dimensionless quantity

$$T = T_1 \text{ at } x = 0 \quad (6)$$

$$T = T_0 \text{ at } x = L_x$$

where $T_1 > T_0$;

$$\begin{aligned} \partial T / \partial y = 0 \text{ at } & y = 0, \\ & y = L_y \end{aligned} \quad (7)$$

and

$$\begin{aligned} T = T_1 - (T_1 - T_0)(x/L_x) \text{ at } & z = 0 \\ & z = M + L_z + L \end{aligned} \quad (8)$$

In cases in which the impermeable rock was ignored (8) was applied to the appropriate boundaries of the porous zone.

Finally, the fluid density was governed by an equation of state

$$\rho_f = \rho_0(1 - \beta(T - T_0)) \quad (9)$$

which was substituted into the buoyancy term in (2) (i.e., the Boussinesq approximation).

Following Holst and Aziz (1972), the equations were simplified by:

a) introducing a vector potential $\vec{\psi} = (\psi_1, \psi_2, \psi_3)$ defined by

$$\begin{aligned} \vec{v} &= \nabla \times \vec{\psi} \\ \nabla \cdot \vec{\psi} &= 0 \end{aligned} \quad (10)$$

b) taking the curl of equation (2) to eliminate the pressure

c) non-dimensionalizing the resulting equations as well as the heat transport equations (3) and (4) by introducing

$$Q = \frac{\lambda_m}{L_z c_f \rho_0}, \quad T = T_0 + \Delta T_0 T', \quad t = \frac{L_z^2 (\rho c)_m t'}{\lambda_m}$$

$$x = x' L_x, \quad y = L_y y', \quad z = L_z z'$$

$$u = Qu', \quad v = \frac{L_y}{L_x} Qv', \quad w = \frac{L_z}{L_x} Qw'$$

$$\psi_1 = \frac{L_y L_z}{L_x} Q\psi_1', \quad \psi_2 = L_z Q\psi_2', \quad \psi_3 = L_y Q\psi_3'$$

The final, dimensionless equations were, in the porous zone

$$\bar{\nabla}^2 T' - A[u'(\partial T'/\partial x') + v'(\partial T'/\partial y') + w'(\partial T'/\partial z')] = \partial T'/\partial t' \quad (11)$$

$$\bar{\nabla}^2 \psi_2' = -AR \partial T'/\partial z' \quad (12)$$

$$\bar{\nabla}^2 \psi_3' = AB^2 R \partial T'/\partial y' \quad (13)$$

$$u' = \partial \psi_3' / \partial y' - \partial \psi_2' / \partial z' \quad (14)$$

$$v' = -\partial \psi_3' / \partial x' \quad (15)$$

$$w' = \partial \psi_2' / \partial x' \quad (16)$$

where

$$R = \rho_0^2 g \beta c_f \Delta T_0 L_x K / \lambda_m \eta$$

is the Rayleigh number; whereas in the conducting regions

$$\bar{\nabla}^2 T' = D \partial T'/\partial t' \quad (17)$$

held, where

$$D = \rho_s c_s \lambda_m / \rho_m c_m \lambda_s \quad (18)$$

Equations (11) through (17) were solved numerically using the method of finite-differences. Details of the numerical procedure are given in Hernandez (1980).

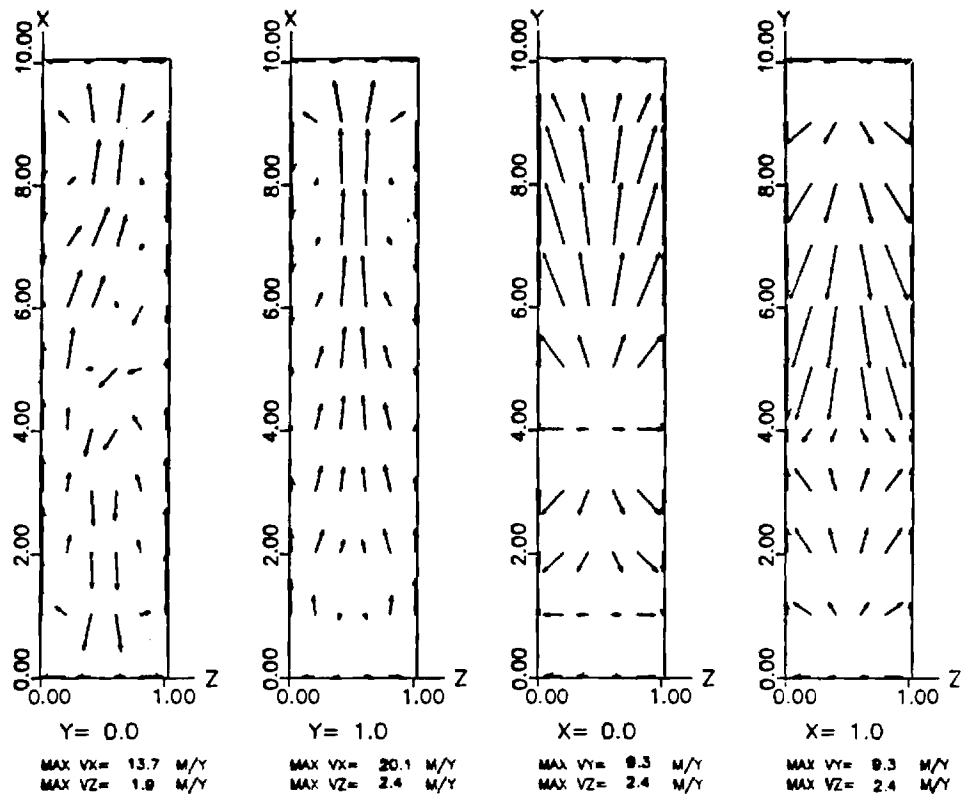
B. Results

For the purpose of this study, the aspect ratios A and B were assumed to be equal. The procedure was to first select a wall boundary condition and aspect ratio, then for a fixed Rayleigh number to choose a variety of initial velocity perturbations. The temperature distribution and velocity components were sampled at time intervals so that the temporal evolution of the cell pattern could be monitored as a function of the initial velocity perturbation. The velocity field was depicted as a vector at each grid point on the six exterior surfaces of the porous zone and a computer subroutine was used to print out the results. Occasionally, the velocity field at some interior plane was also so depicted. In addition, a three-dimensional representation of the surface heat flow was made for each model in order to compare the fault zone model with observed heat flow patterns associated with fault controlled natural geothermal systems.

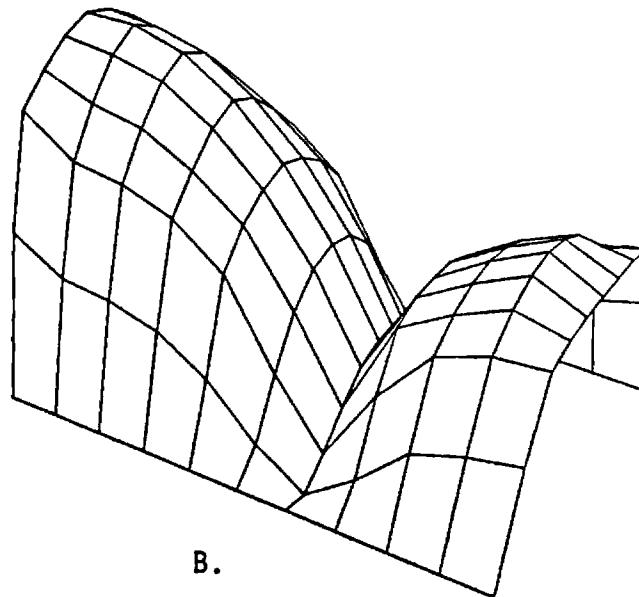
In the results presented below, the circulation velocities are given assuming fault zone widths of 1 km and 100 meters for assumed aspect ratios of $A = B = 0.1$ and 0.01 , respectively. For all models the Rayleigh numbers were chose to be $R = 5R_c$ or $R = 10R_c$, where R_c was assumed to be the critical number for perfectly conducting walls of the proper aspect ratio as calculated by Shyu (1979).

B.1 Conducting Walls

As a first step, the conducting wall model with aspect ratio $A = B = 0.1$ and $R = 5R_c$ was chosen. Figures 2 and 3 show the flow patterns

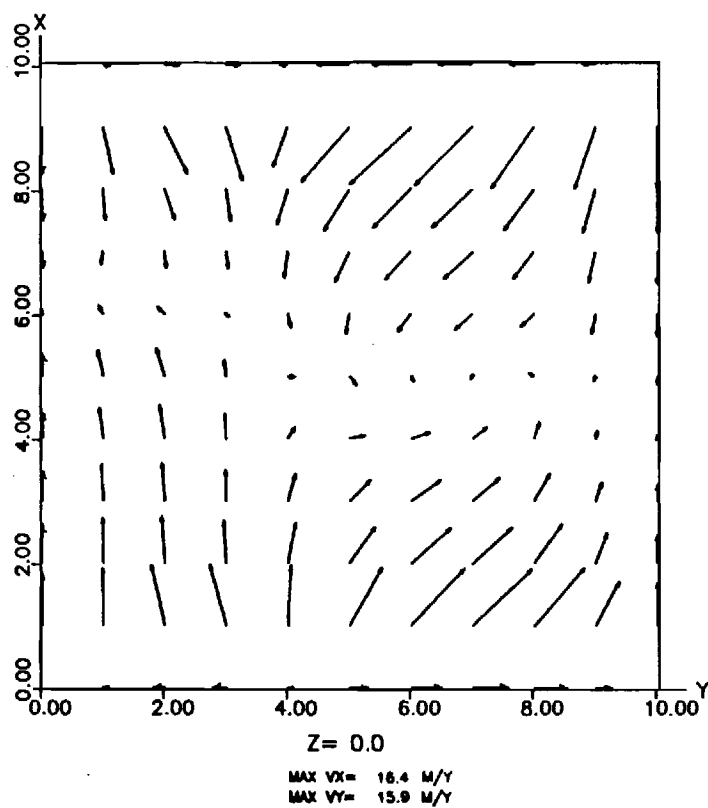


A.

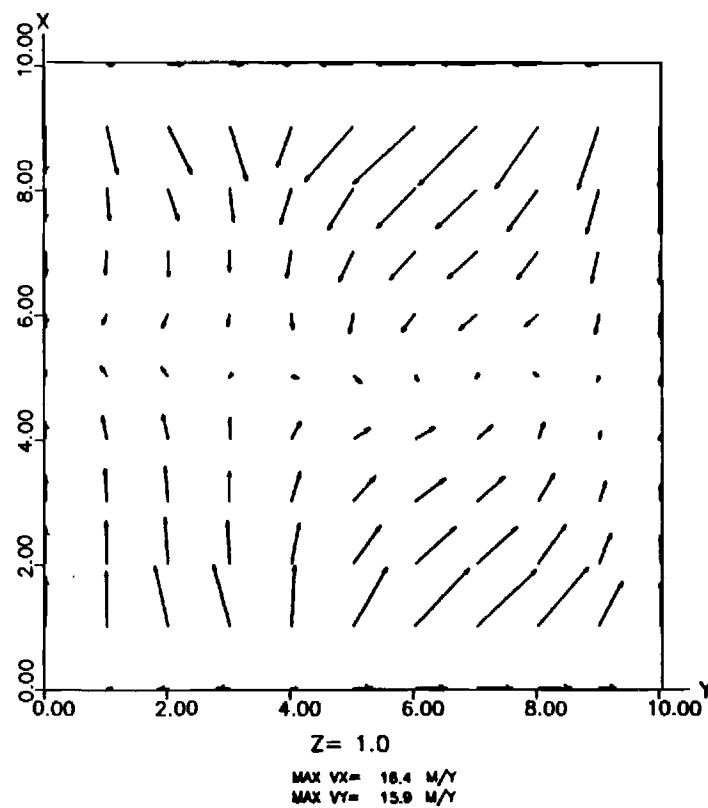


B.

Figure 2. a), c) and d) shows the flow vectors at the faces of a porous box. The faces at $z=0, 1.0$ are perfect conductors. b) shows a 3-D plot of the heat flow at the upper surface. $A=B=0.1$, $R=5R_c$ and $t=5,000$ years. Initial condition: fluid was caused to rise in the corner $x=y=z=0$.

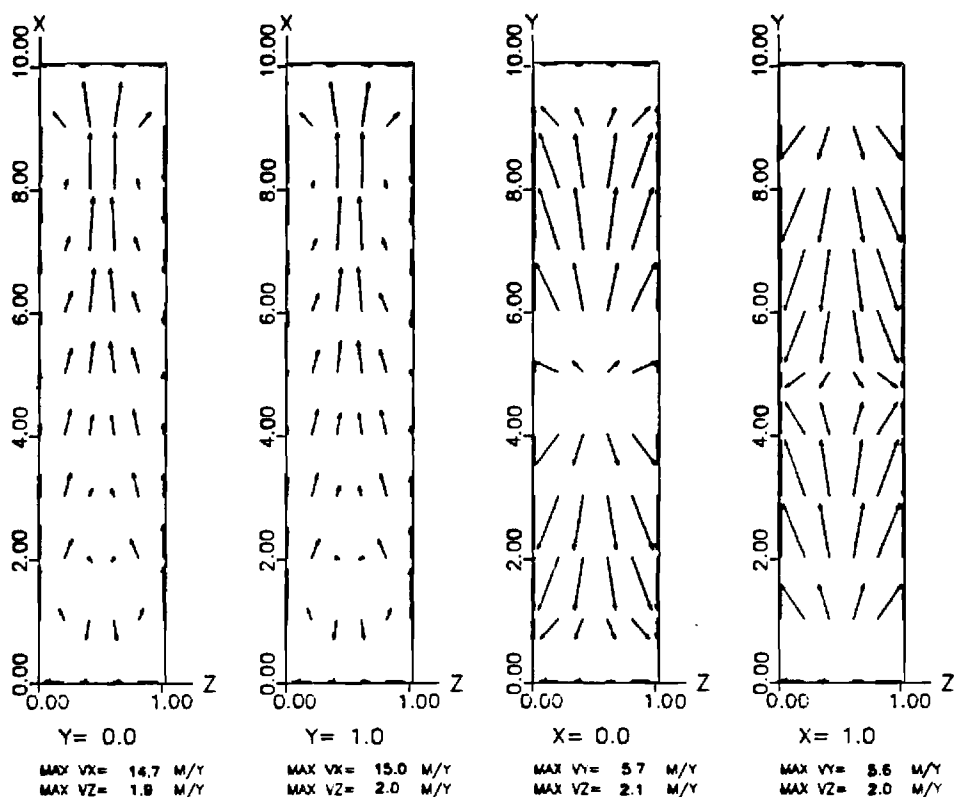


C.

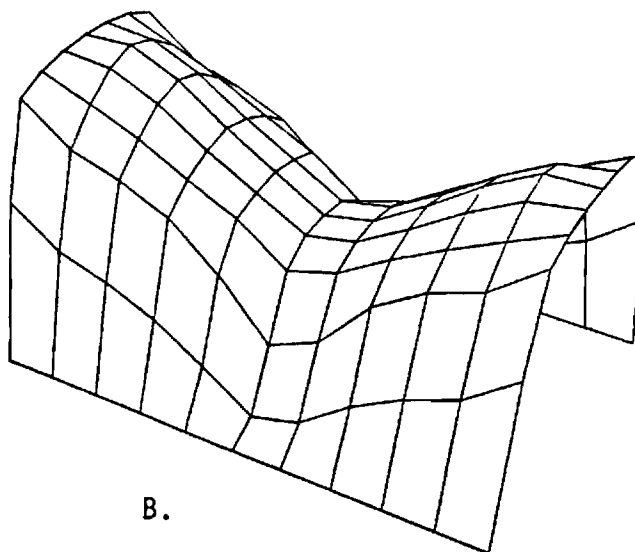


D.

Figure 2. (Continued)

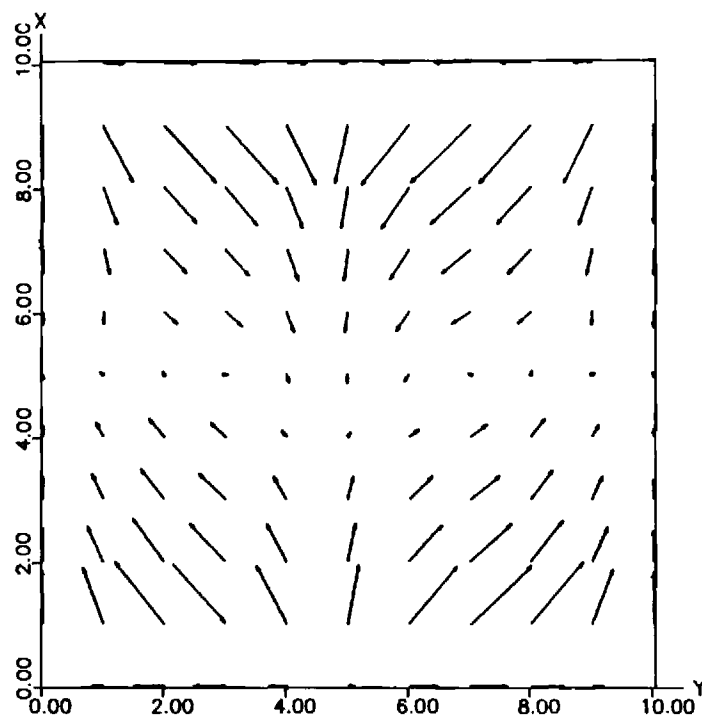


A.



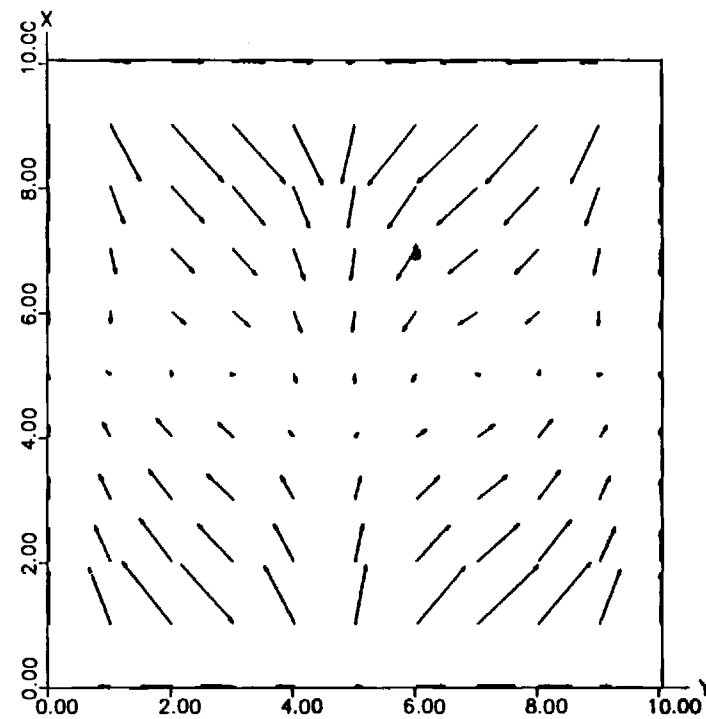
B.

Figure 3. a), c) and d) show the flow vectors at the faces of a porous box. The faces at $z=0, 1.0$ are perfect conductors. b) shows a 3-D plot of the heat flow at the upper surface. $A=B=0.1$, $R=5R_c$ and $t=12,000$ years. Initial condition: fluid was caused to rise in corner $x=y=z=0$.



Z= 0.0
MAX VX= 15.0 M/Y
MAX VY= 9.4 M/Y

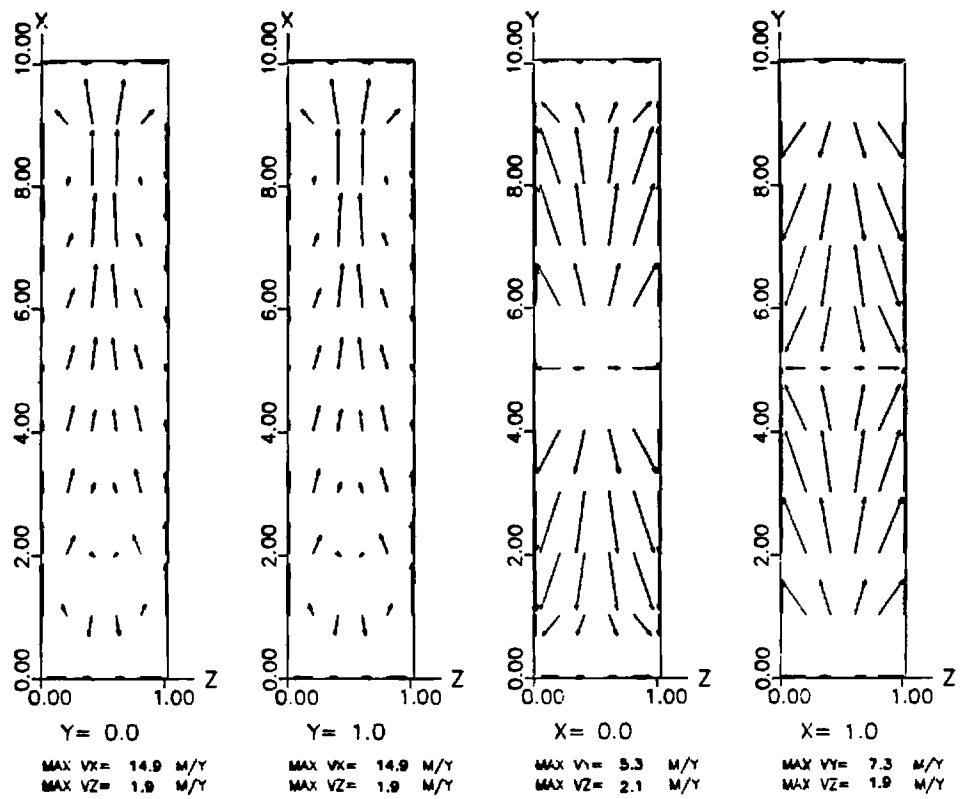
C.



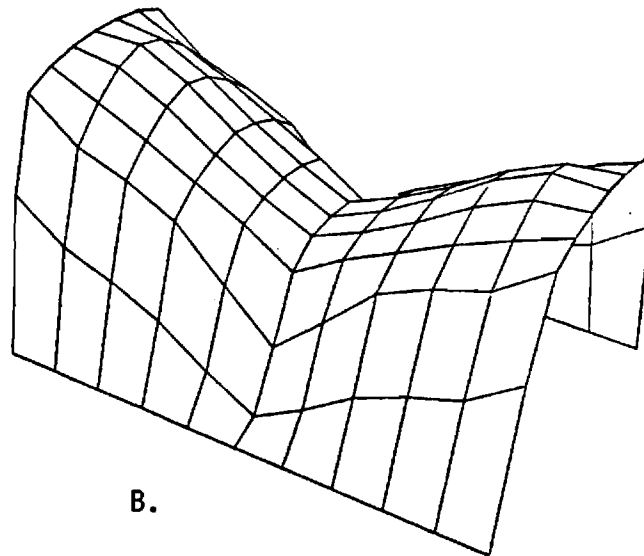
Z= 1.0
MAX VX= 15.0 M/Y
MAX VY= 9.4 M/Y

D.

Figure 3. (Continued)

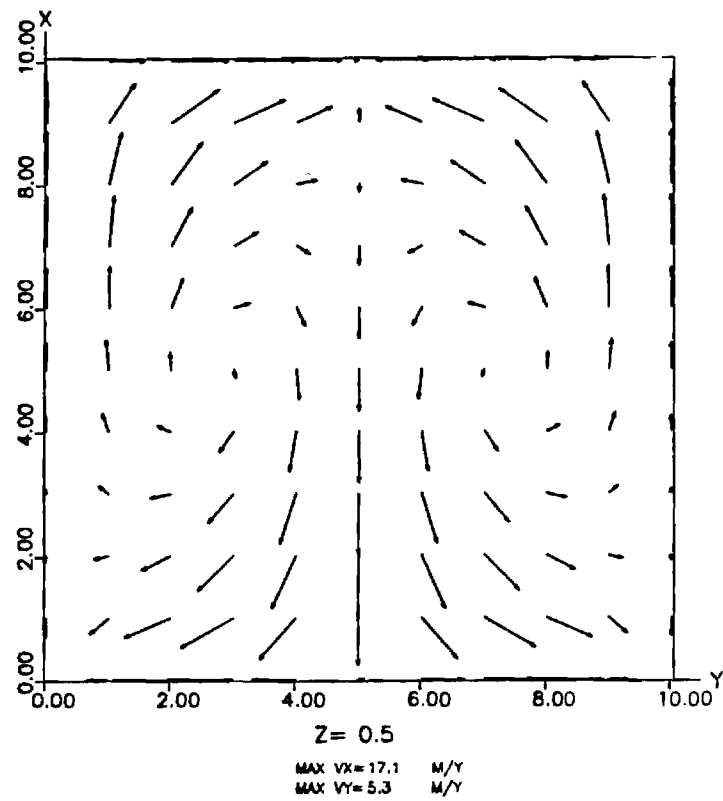


A.



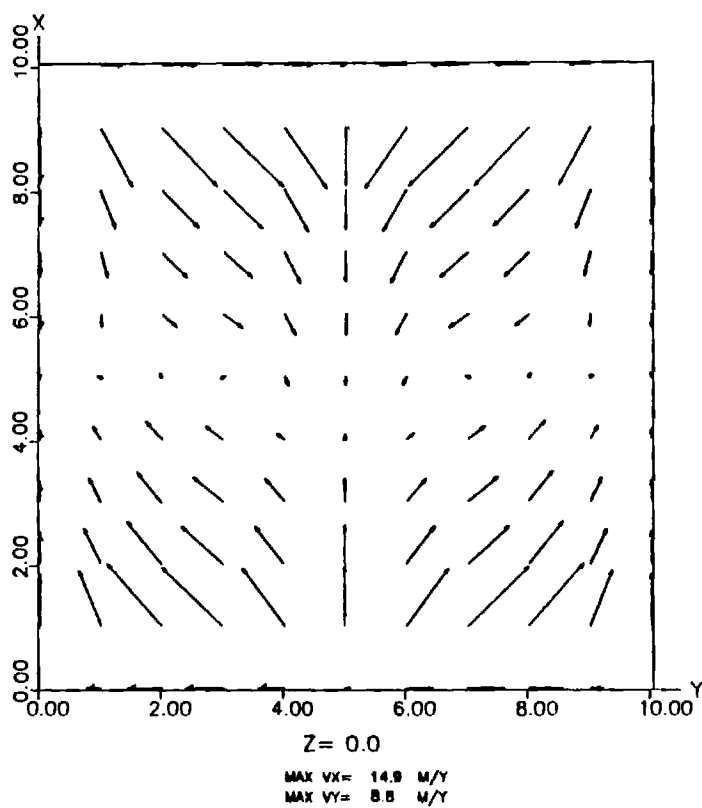
B.

Figure 4. a), c), d) and e) show the flow vectors at the faces of a porous box. The faces at $z=0, 1.0$ are perfect conductors. b) shows a 3-D plot of the heat flow at the upper surface. $A=B=0.1$, $R=5R_c$ and $t=12,000$ years. Initial condition: fluid was caused to rise along $x=z=0$.

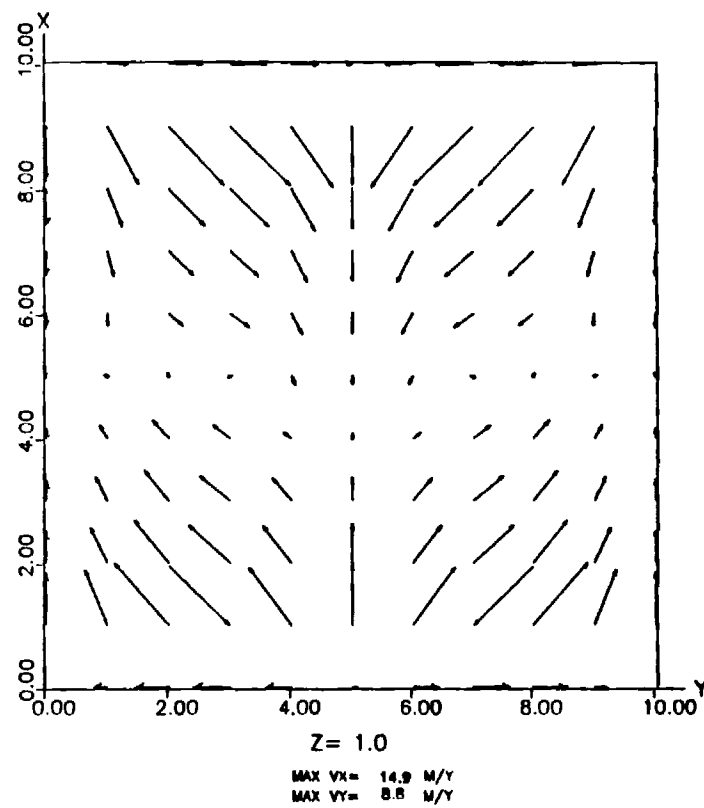


C.

Figure 4. (Continued)

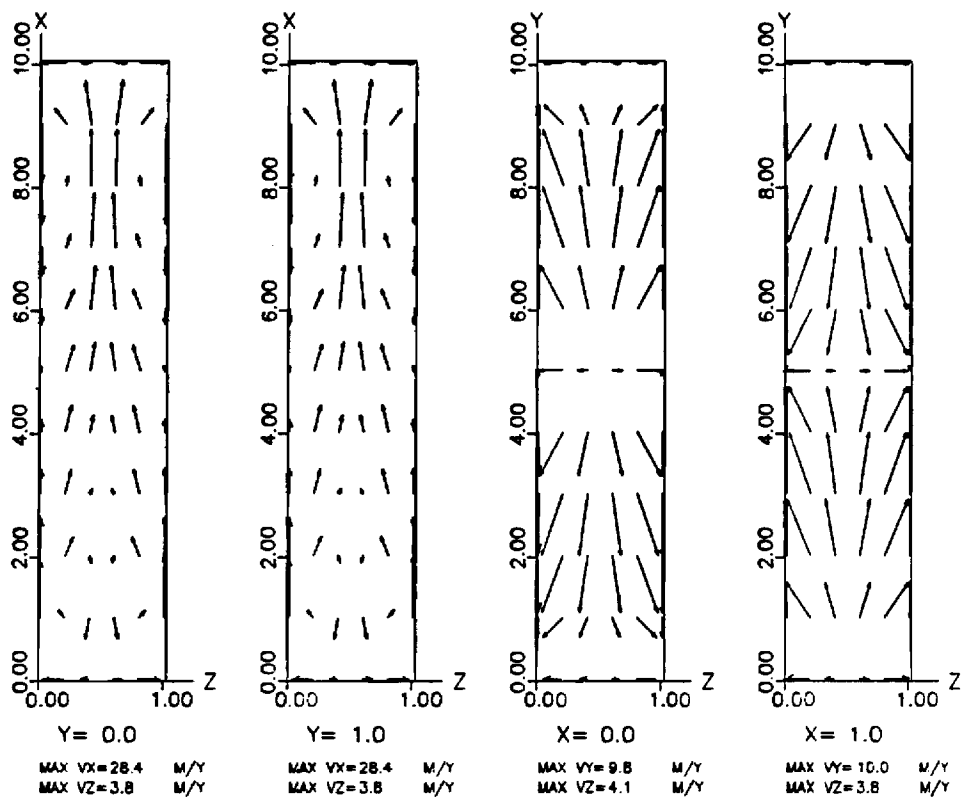


D.

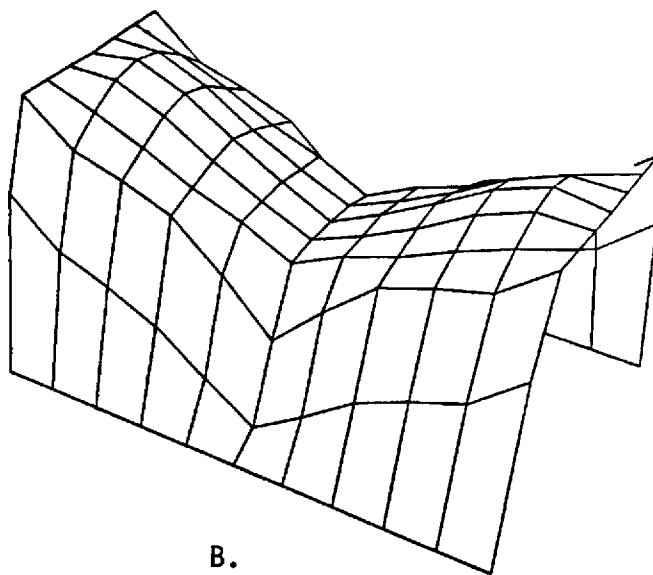


E.

Figure 4. (Continued)

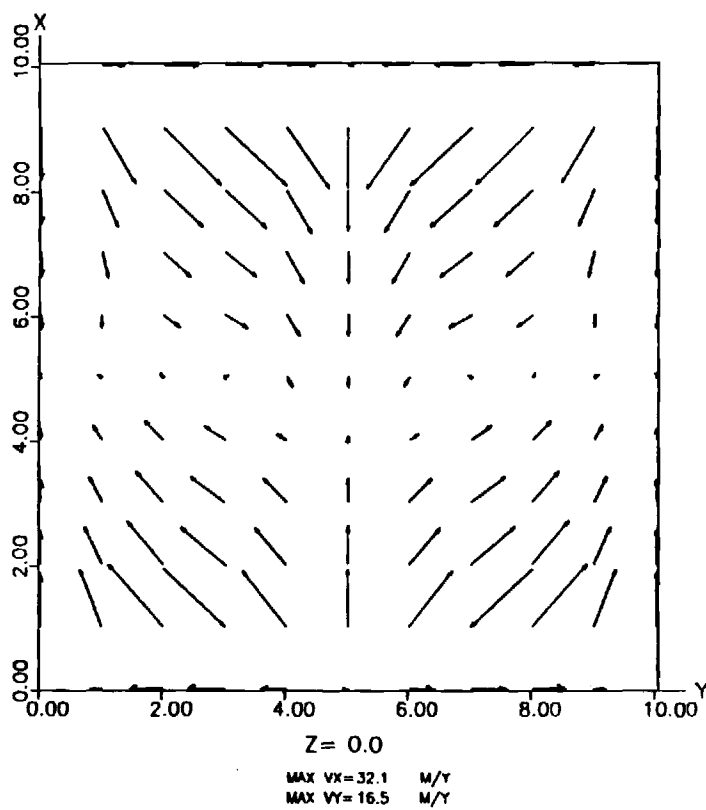


A.

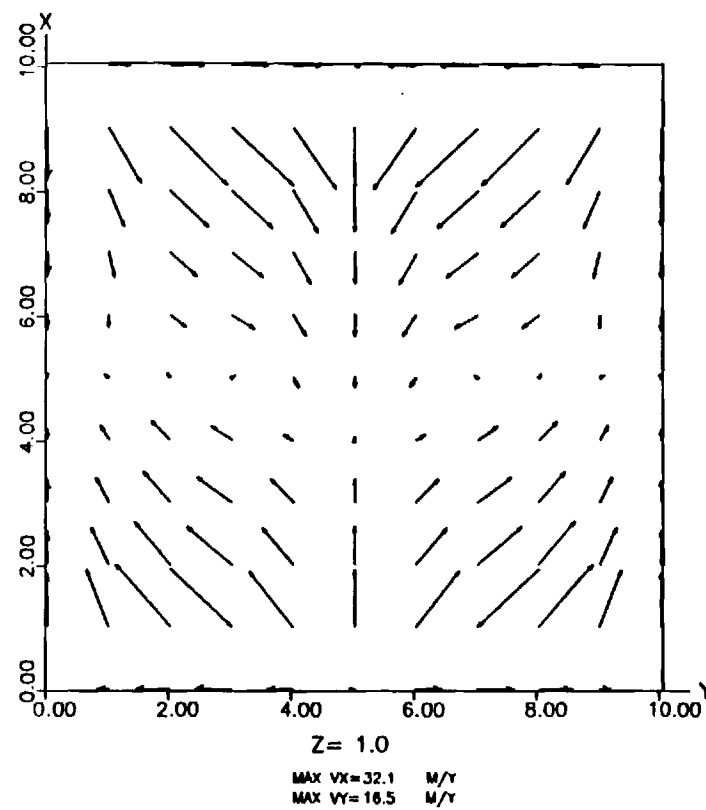


B.

Figure 5. a), c) and d) show the flow vectors at the faces of a porous box. The faces at $z=0, 1.0$ are perfect conductors. b) shows a 3-D plot of the heat flow at the upper surface. $A=B=0.1$, $R=10R_c$ and $t=2,000$ years. Initial condition: steady flow shown in Figure 4 was used as initial condition



C.



D.

Figure 5. (Continued)

in the exterior planes and the heat flow through the upper surface at time $t = 5,000$ and $12,000$ years, respectively. The initial perturbation was in the form of a small upward velocity in the corner $x = y = z = 0$. The velocity field indicates a three-dimensional convection pattern; however, the velocity in the z direction (across the fracture aperture) is considerably smaller than in the other two directions. The pattern generally resembles two dimensional rolls with axes parallel with the z direction, hereafter termed 'transverse rolls'. The fluid rises along the insulated walls and sinks at the center. The heat flow pattern further corroborates the suggested flow pattern. It may be observed that the asymmetry which is apparent at $t = 5,000$ years (Fig. 2) has disappeared at the later time (Fig. 3). The early asymmetry is presumably due to the asymmetry in the initial perturbation.

Figure 4 shows the flow pattern, and heat flow, at $12,000$ years for the identical system as in Figs. 2 and 3, except that the initial perturbation velocity was directed upward along the line $x = z = 0$. Such a perturbation would tend to lead to rolls oriented with axes parallel to the y direction, hereafter termed 'longitudinal rolls'. The system, however, rapidly evolved into transverse rolls, as in the case shown in Figs. 2 and 3.

Figure 5 shows the development after $2,000$ years of a system with $A = B = 0.1$ and $R = 10R_c$. The initial condition was the velocity field at $R = 5R_c$ at $t = 12,000$ years. The principal of effect of the doubling the Rayleigh number was to double the fluid velocity.

B.2 Imperfectly Conducting Walls

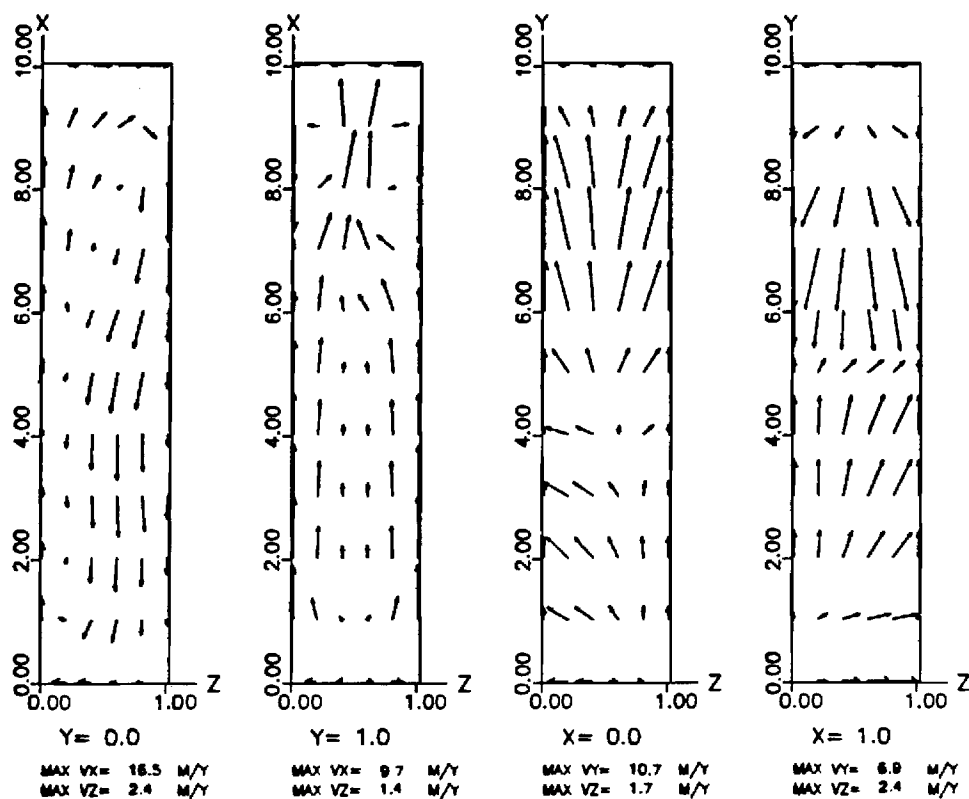
For these cases, the vertical conducting walls were replaced by blocks of impermeable material of finite thermal conductivity. Figures

6 and 7 show the temporal development of the convection pattern under the same conditions as given for the system depicted in Figs. 2 and 3, ($A = B = 0.1$, $R = 5R_c$, initial perturbation at front lower left-hand corner). The flow pattern is much more irregular than in the case with conducting walls. There is a pronounced tendency towards the development of transverse rolls, the roll at the end of the porous zone far from the location of the initial perturbation being more clearly formed. It is clear that the impermeable, conducting material bounding the porous zone substantially influences the development of the cell pattern. Because of the finite conductivity of the boundary material, the effect of the initial condition is not as readily dissipated by the convective circulation as in the case of perfectly conducting boundaries.

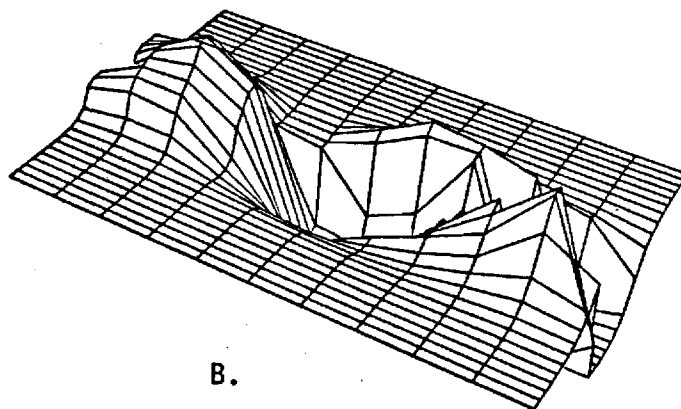
Figures 8 and 9 show the cell pattern and heat flow for systems with $R = 5R_c$ and $R = 10R_c$, respectively, in which the initial perturbation was a small upward velocity placed at the base of zone and along the two insulated end walls. Such a perturbation was expected to lead to transverse rolls; and in fact such was the case, as Figs. 8 and 9 show.

Figure 10 shows the pattern for $R = 10R_c$ for an initial perturbation placed at the base of the porous zone, and along a wall contacting the permeable and impermeable zone (in an attempt to induce a longitudinal roll). The cell pattern is somewhat complicated, but basically depicts transverse rolls. The heat flow pattern is quite asymmetric, and even after 13,600 years, the influence of the initial condition is still apparent.

Finally, two cases were modeled in which the aspect ratio was changed to $A = B = 0.01$. Figures 11 and 12 show the situation at

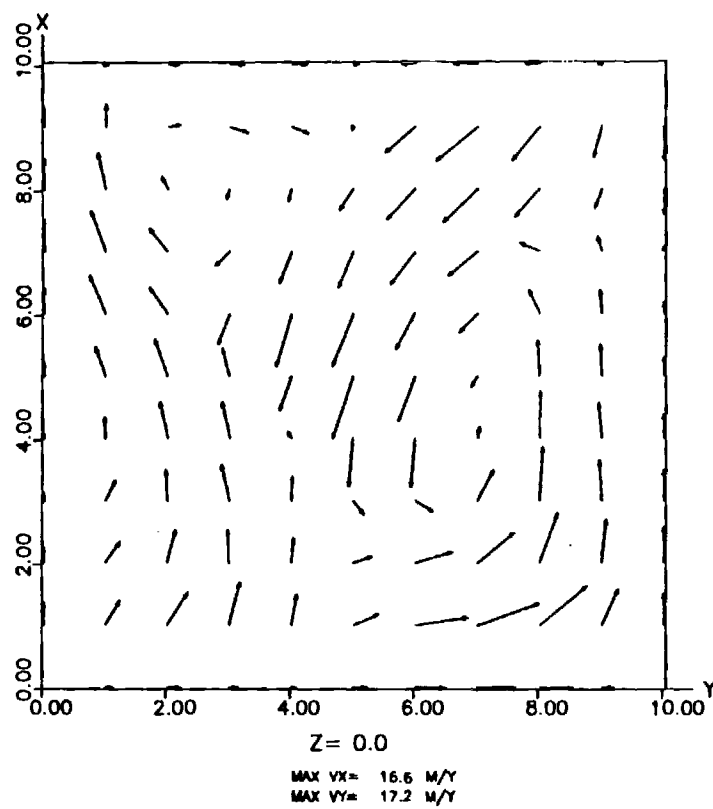


A.

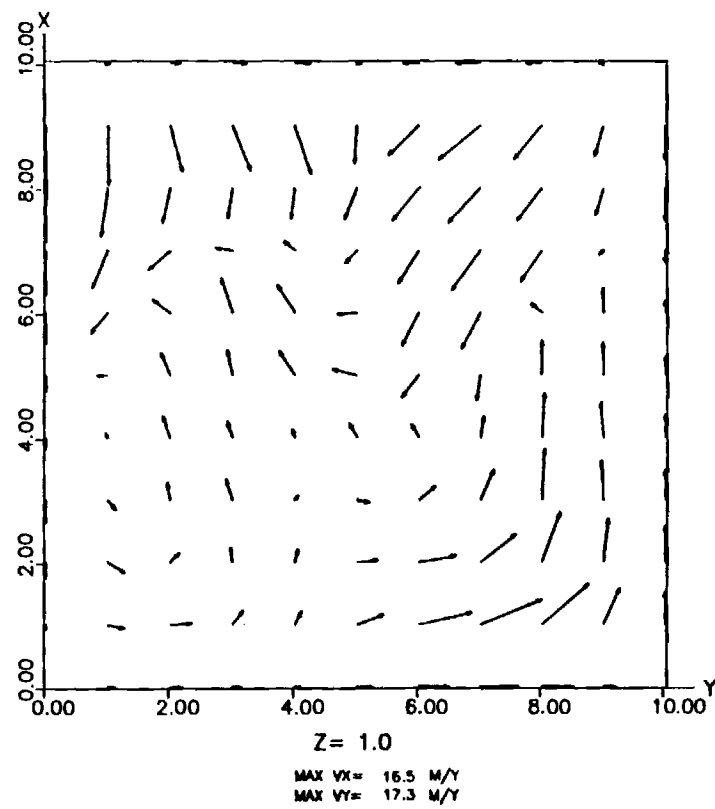


B.

Figure 6. a), c) and d) show the flow vectors at the faces of a porous box in contact with material of finite heat conductivity. b) shows a 3-D plot of the heat flow at the upper surface. $A=B=0.1$, $R=5R_c$ and $t=5,000$ years. Initial condition: fluid was caused to rise in lower, left-hand corner at $y=0$.

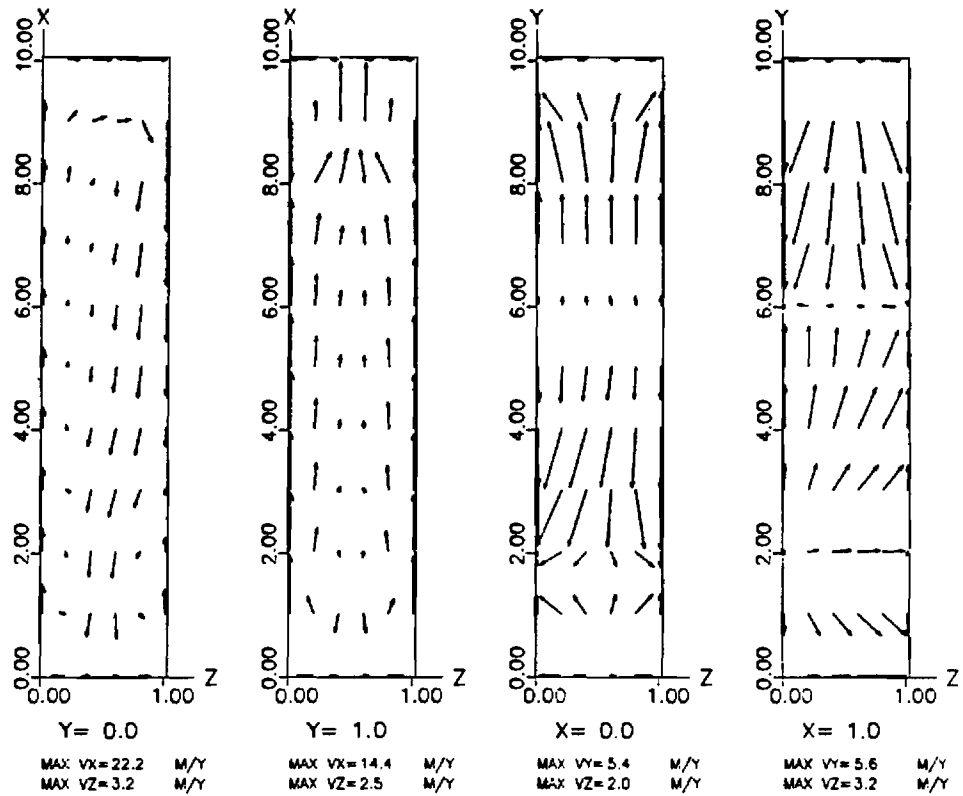


C.

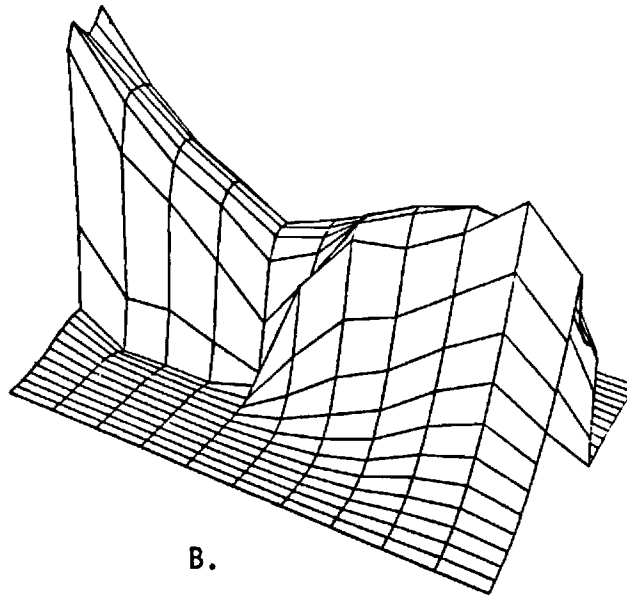


D.

Figure 6. (Continued)

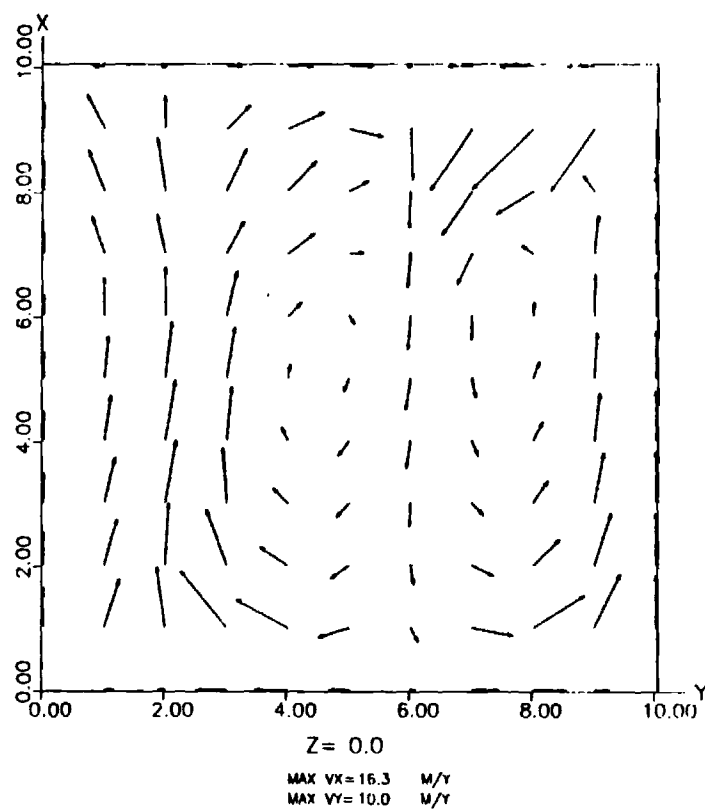


A.

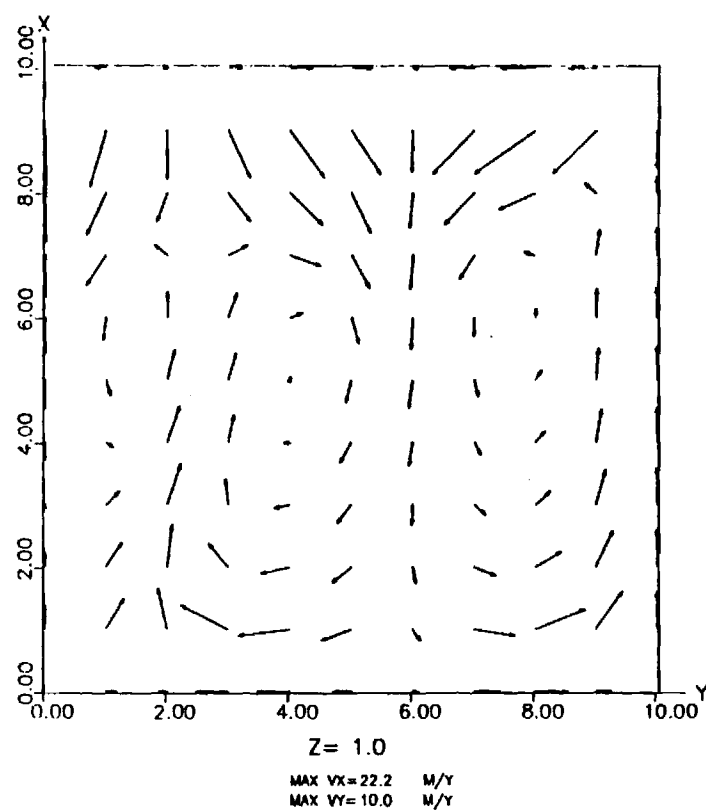


B.

Figure 7. a), c) and d) show the flow vectors at the faces of a porous box in contact with material of finite heat conductivity. b) shows a 3-D plot of the heat flow at the upper surface. $A=B=0.1$, $R=5R_c$ and $t=12,000$ years. Initial condition: fluid was caused to rise in lower left-hand corner at $y=0$.

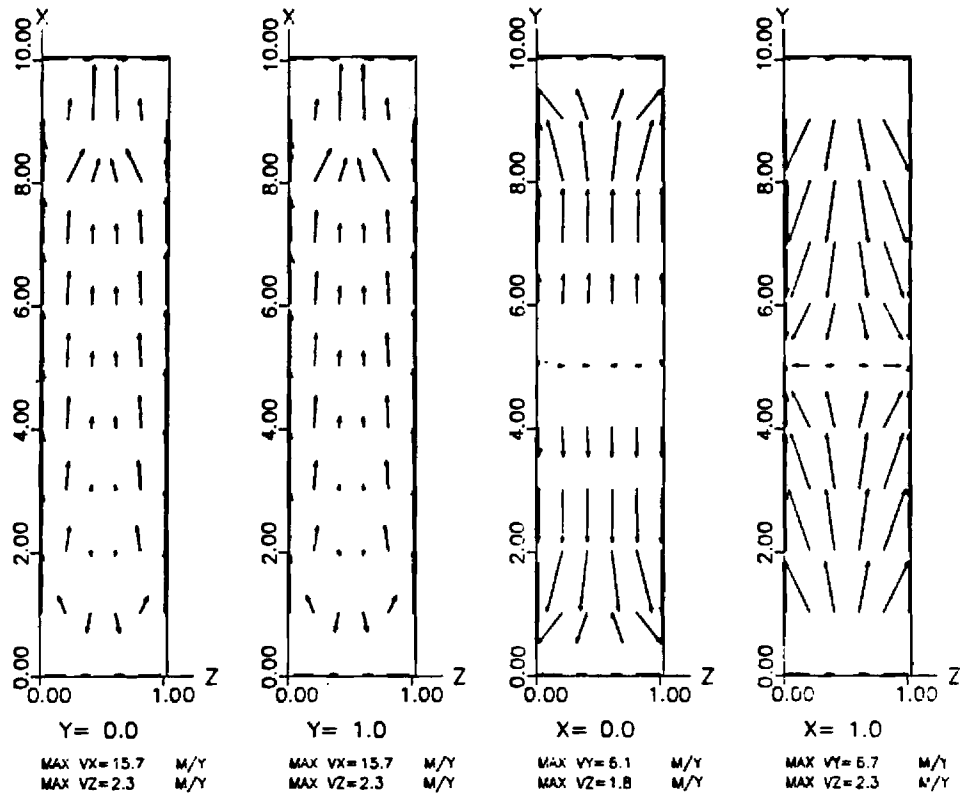


C.

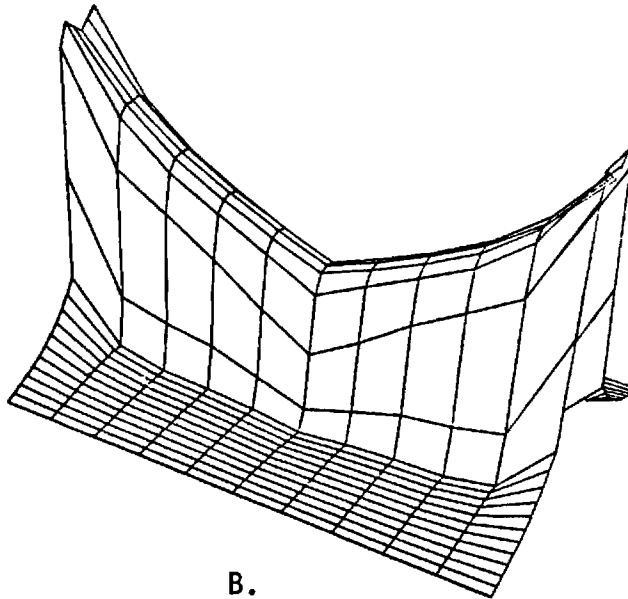


D.

Figure 7. (Continued)

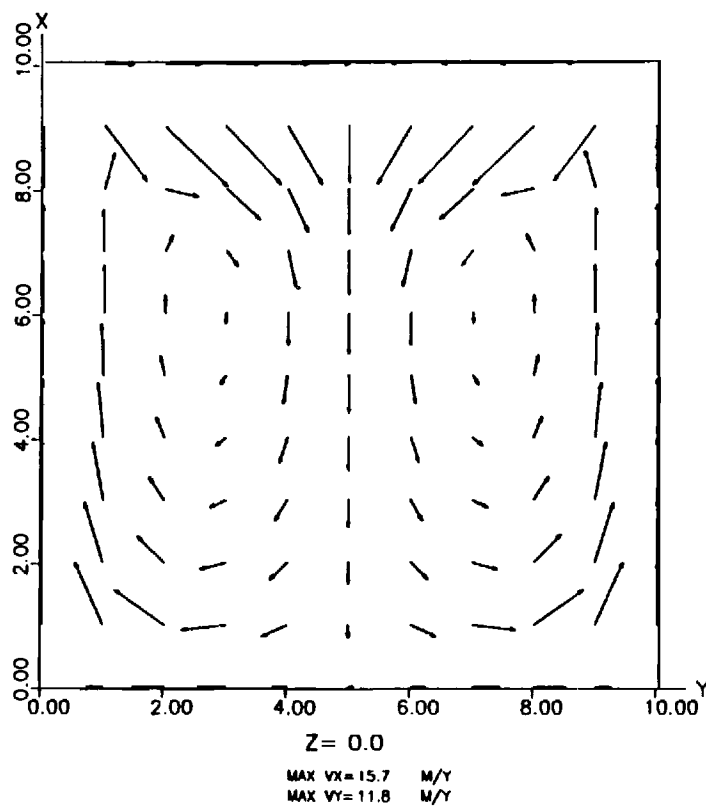


A.

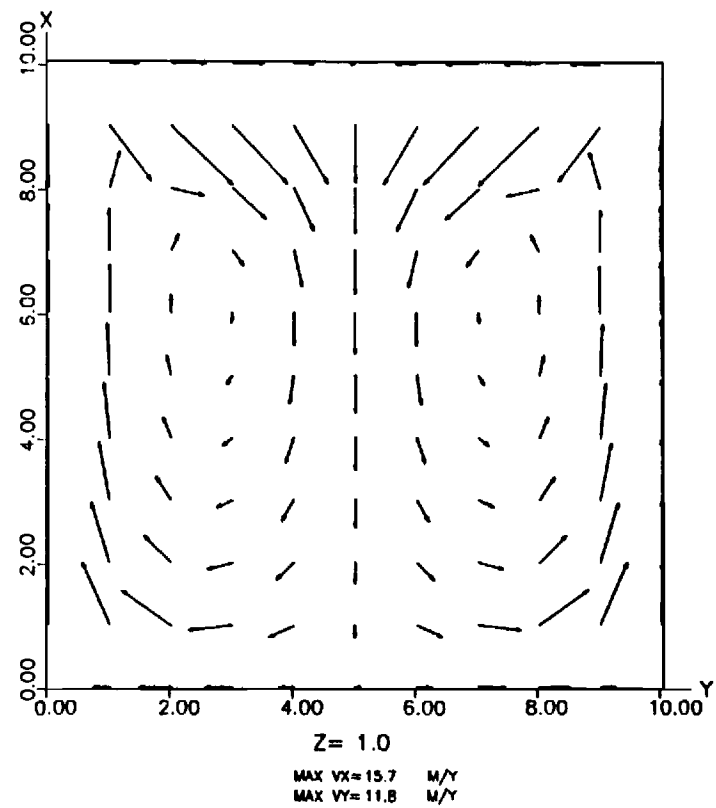


B.

Figure 8. a), c) and d) show the flow vectors at the faces of a porous box in contact with material of finite heat conductivity. b) shows a 3-D plot of the heat flow at the upper surface. $A=B=0.1$, $R=5R_c$ and $t=12,000$ years. Initial condition: fluid was caused to rise along the planes $y=0, 10$

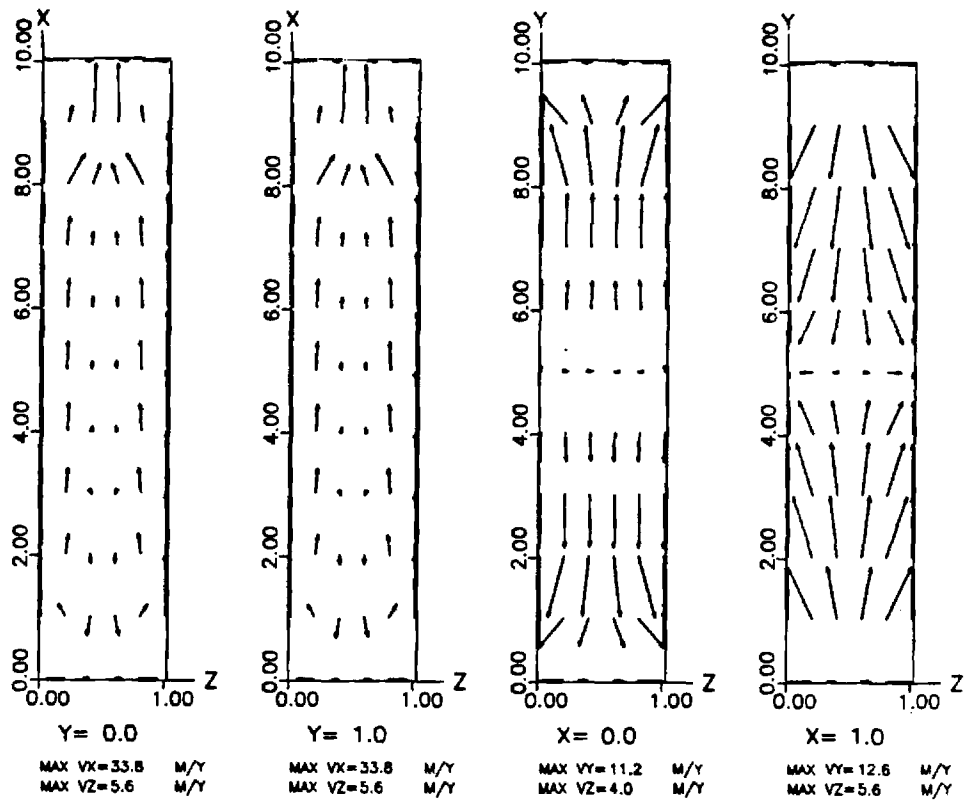


C.

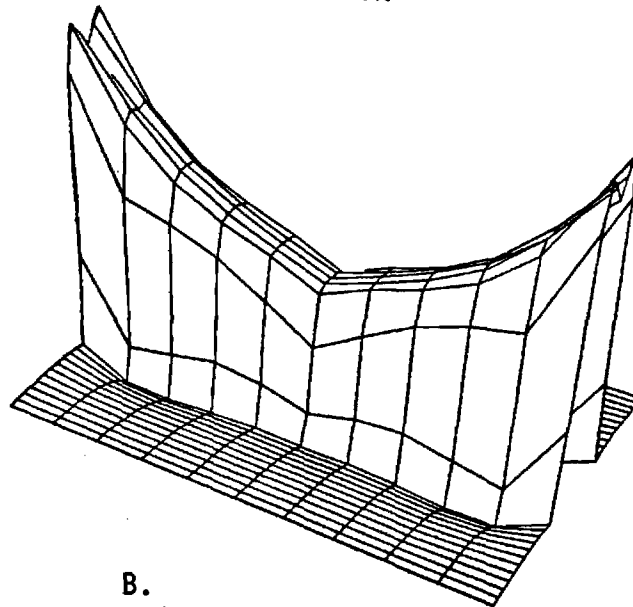


D.

Figure 8. (Continued)

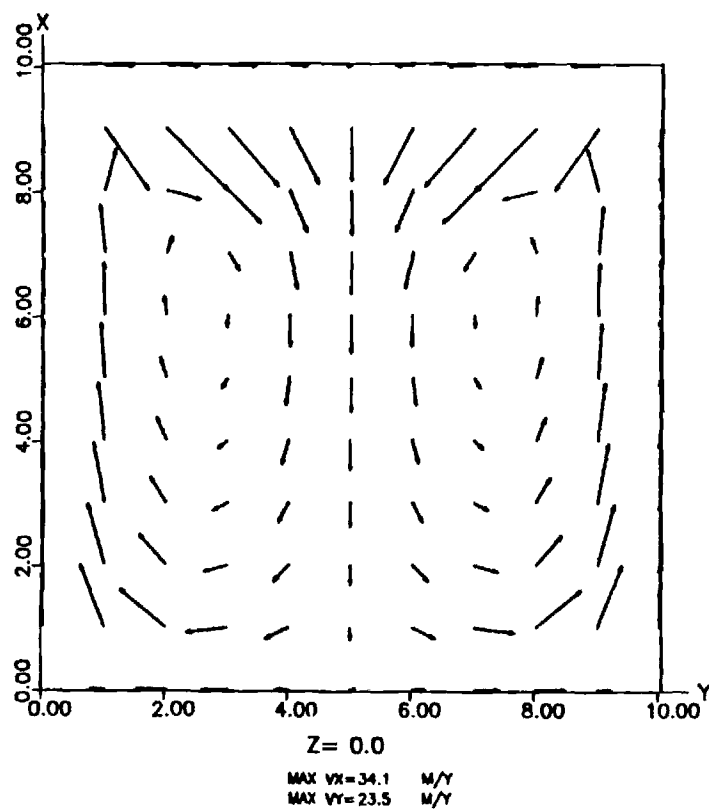


A.

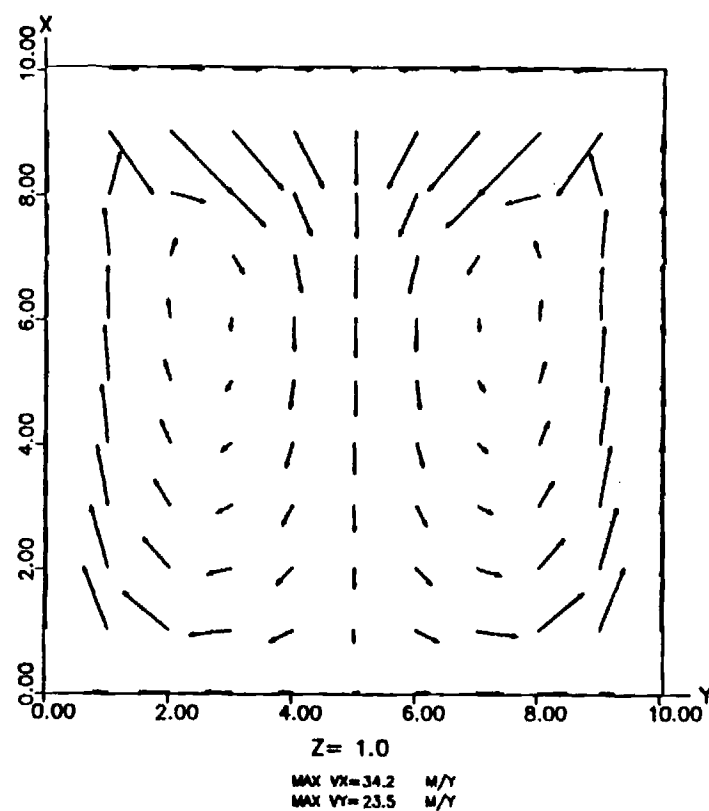


B.

Figure 9. a), c) and d) show the flow vectors at the faces of a porous box in contact with material of finite heat conductivity. b) shows a 3-D plot of the heat flow at the upper surface. $A=B=0.1$, $R=10R_c$ and $t=7,000$ years. Initial condition: fluid was induced to rise along plane $y=0,10$

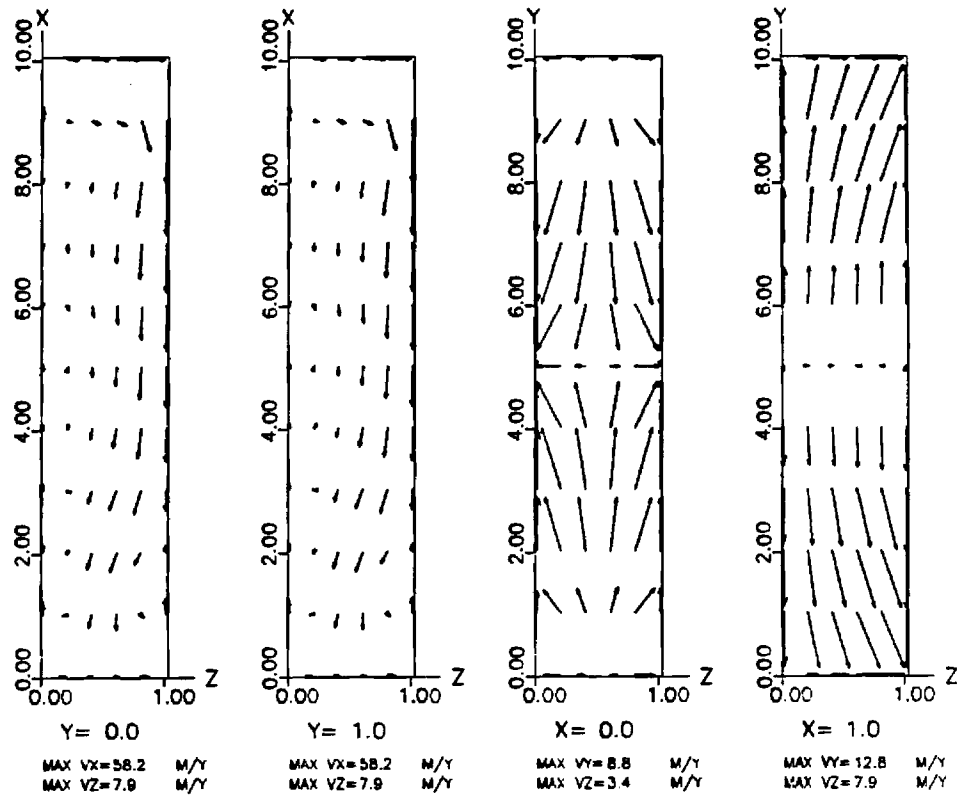


C.

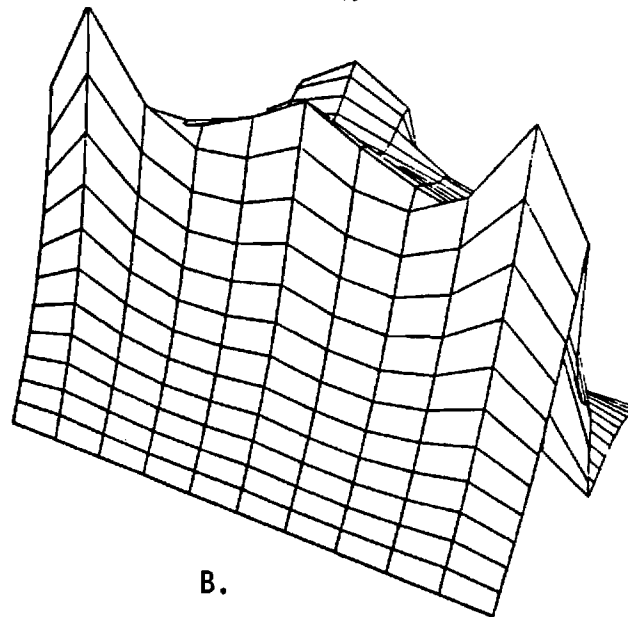


D.

Figure 9. (Continued)

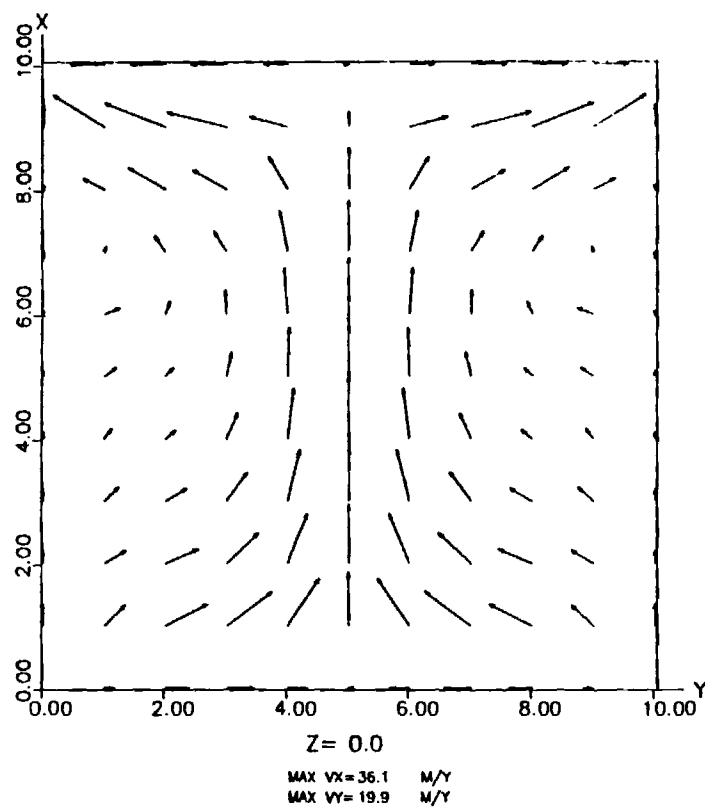


A.

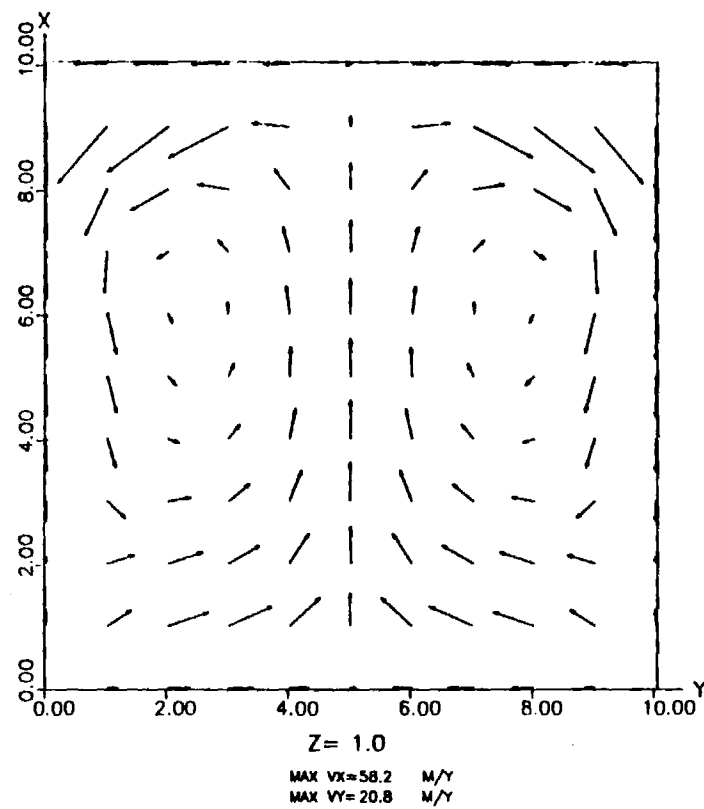


B.

Figure 10. a), c) and d) show the flow vector of the faces of a porous box in contact with material of finite heat conductivity. b) shows a 3-D plot of the heat flow at the upper surface. $A=B=0.1$, $R=10R_c$ and $t=13,500$ years. Initial condition: fluid was caused to rise along the left-hand, basal edge of porous zone.

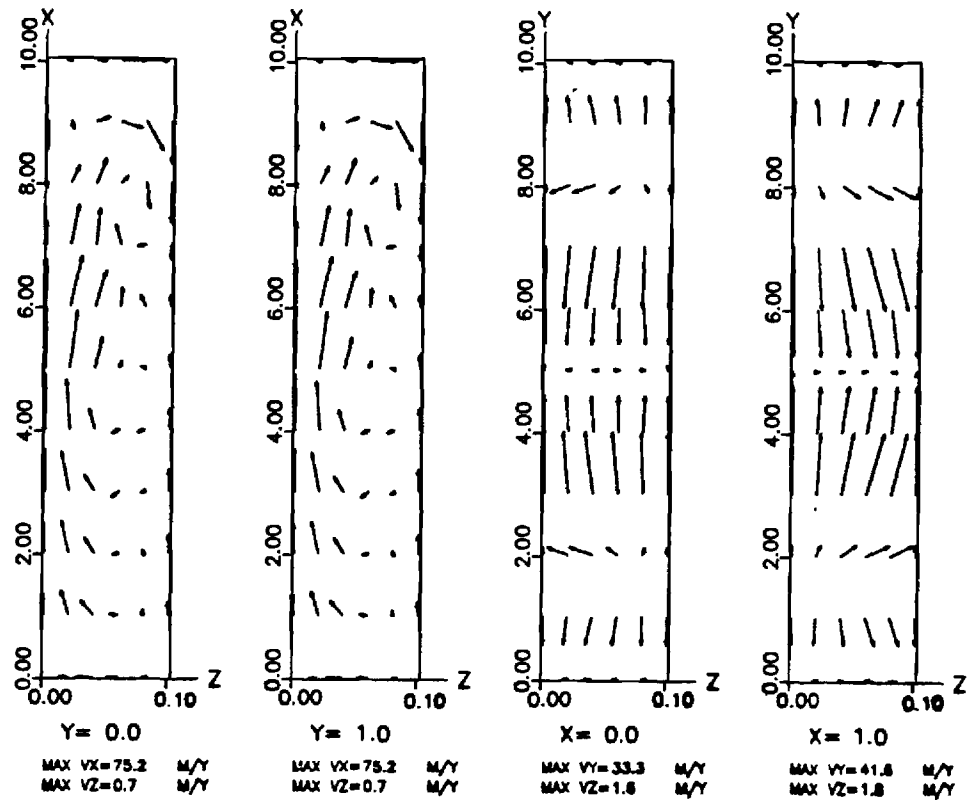


C.

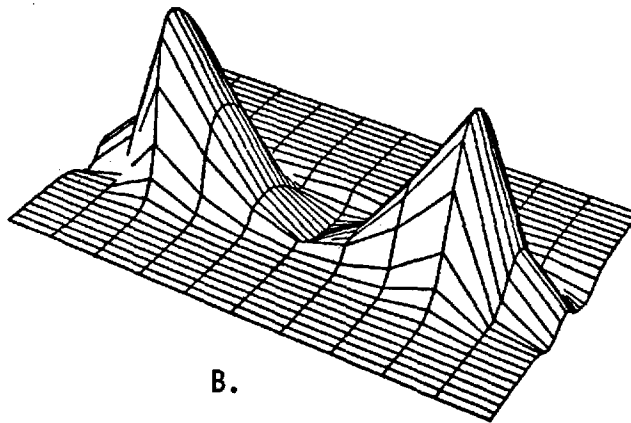


D.

Figure 10. (Continued)

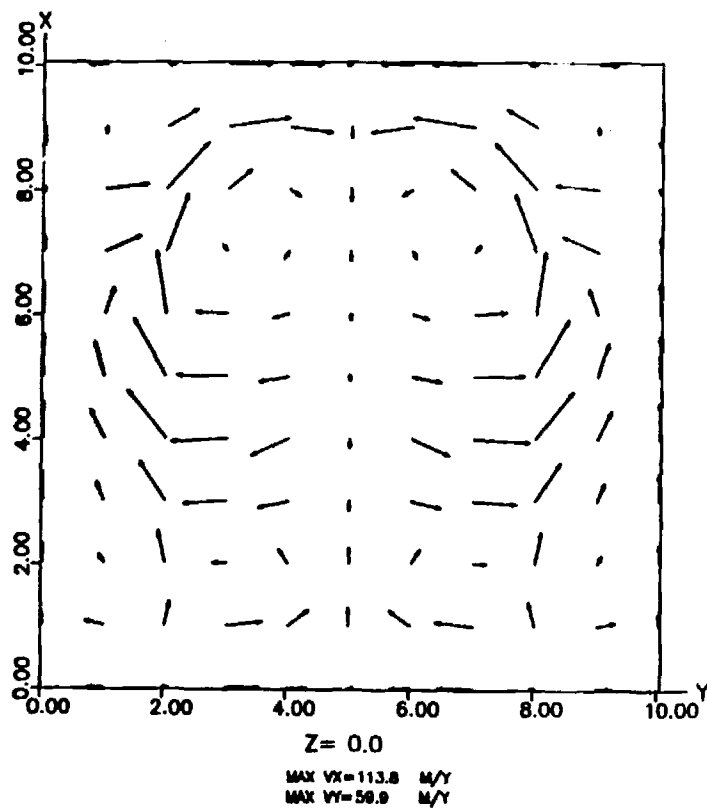


A.

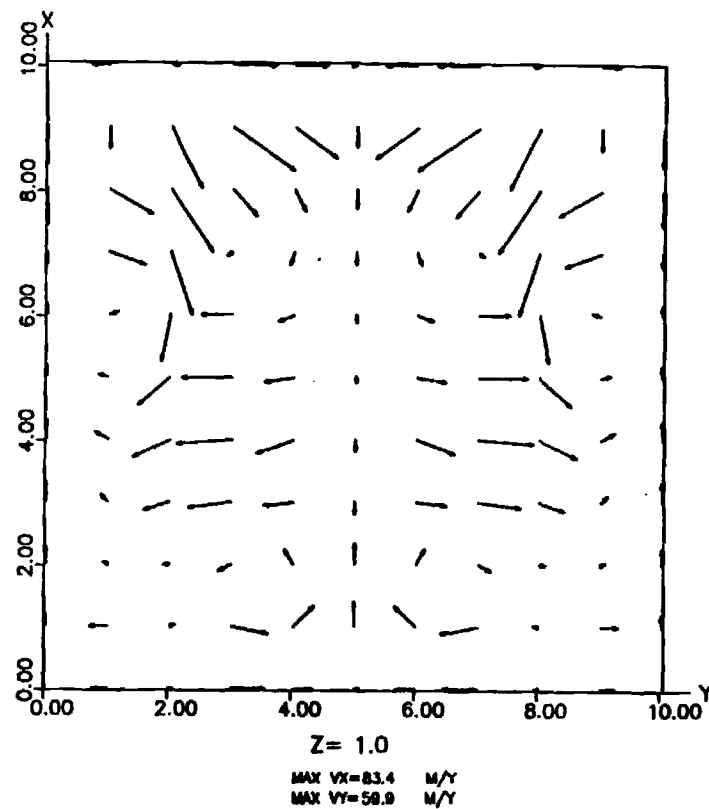


B.

Figure 11. a), c) and d) show the flow vectors at the faces of a porous box in contact with material of finite heat conductivity. b) shows a 3-D plot of the heat flow at the upper surface. $A=B=0.01$, $R=5R_c$ and $t=6,000$ years. Initial condition: fluid was caused to rise along the left-hand, basal edge of porous zone.

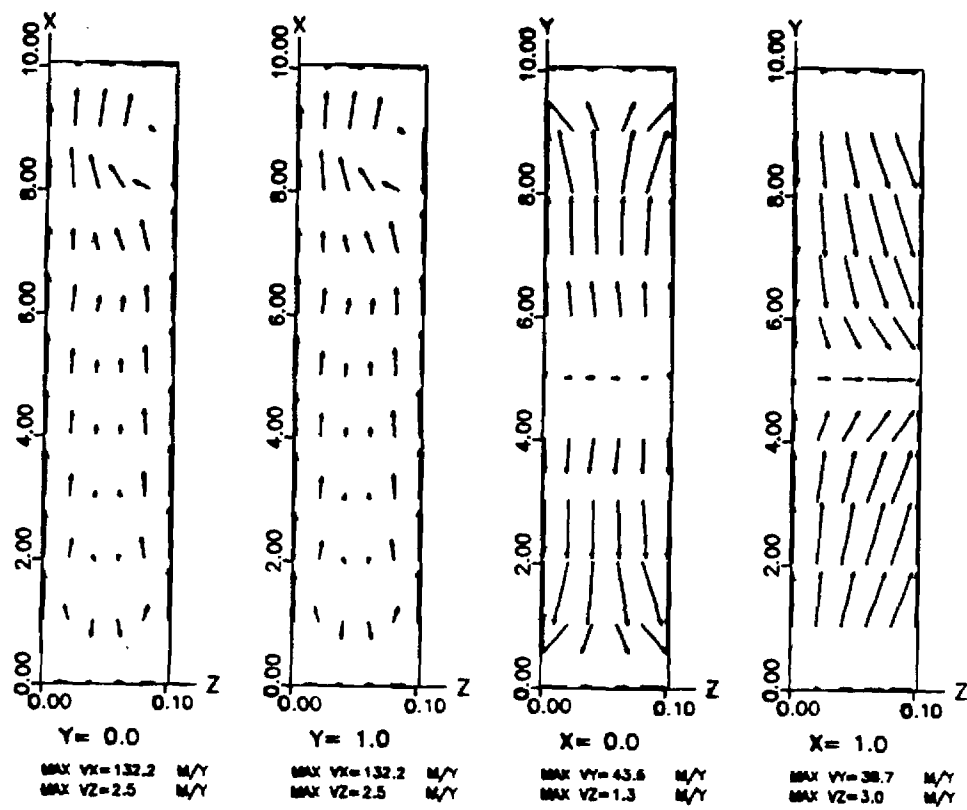


C.

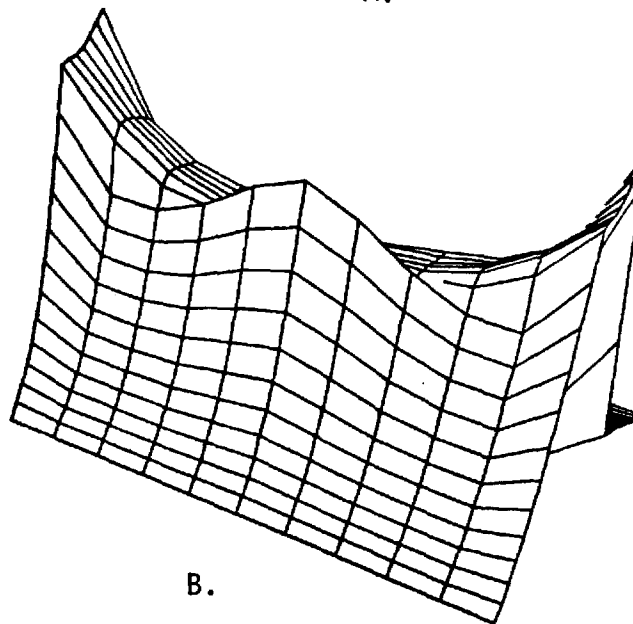


D.

Figure 11. (Continued)

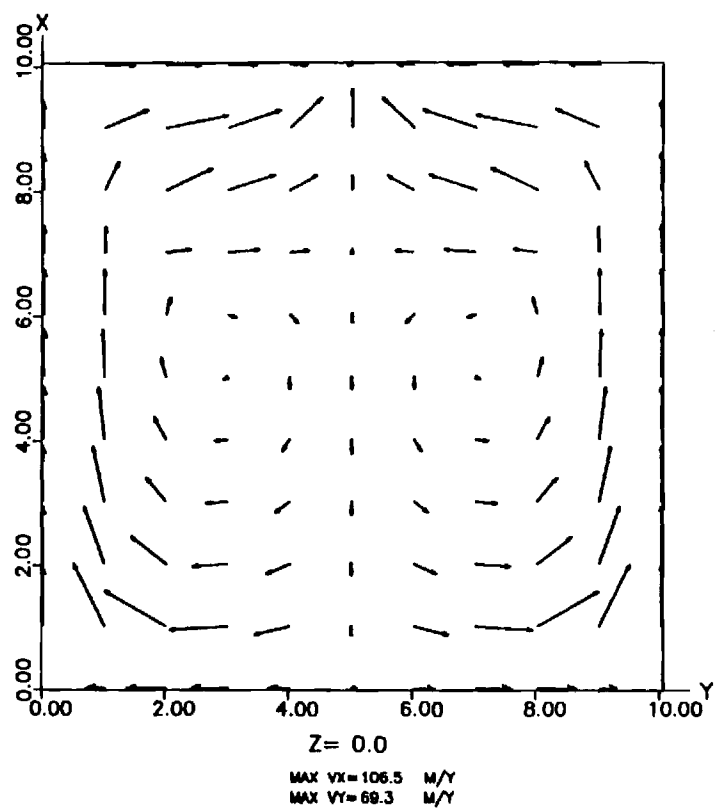


A.

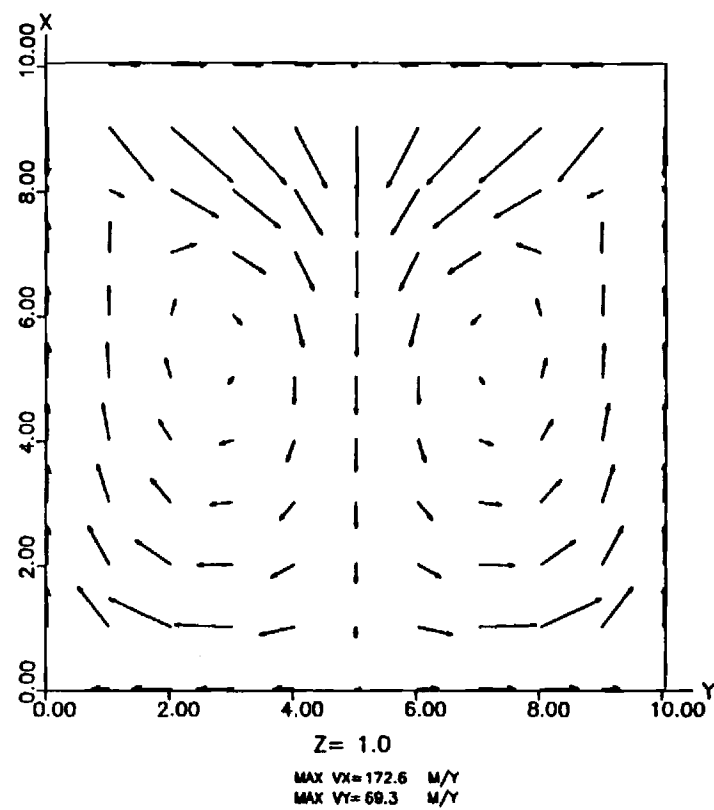


B.

Figure 12. a), c) and d) show the flow vectors at the faces of a porous box in contact with material of finite heat conductivity. b) shows a 3-D plot of the heat flow at the upper surface. $A=B=0.01$, $R=5R_c$ and $t=13,500$ years. Initial condition: fluid was caused to rise left-hand, basal edge of the porous zone.

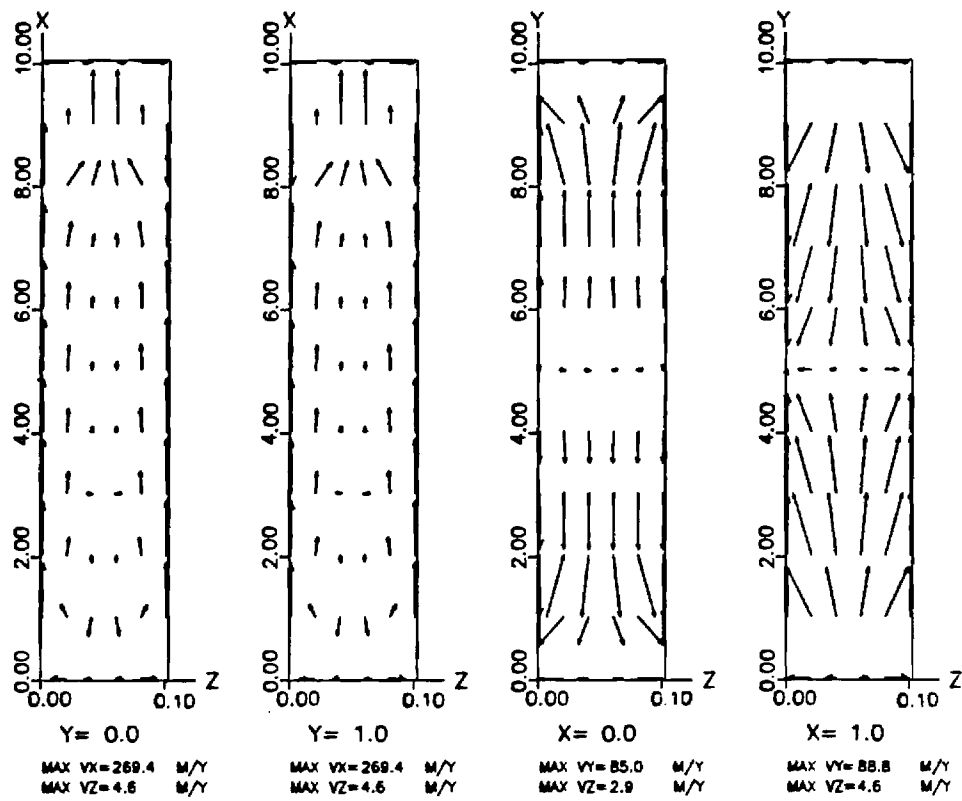


C.

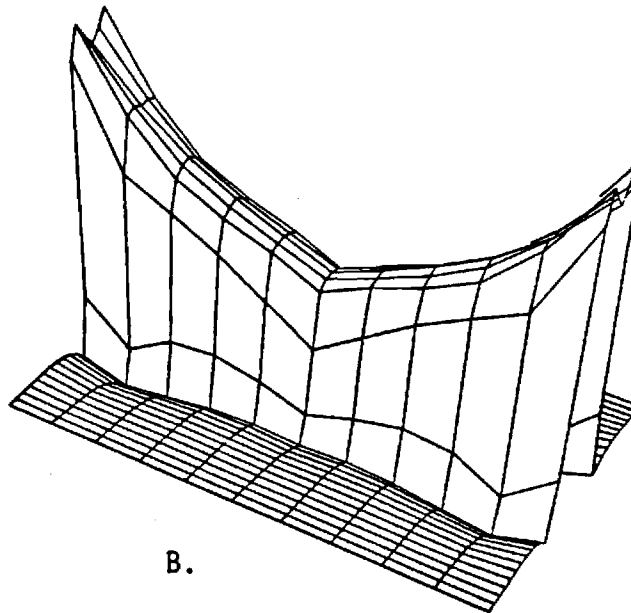


D.

Figure 12. (Continued)

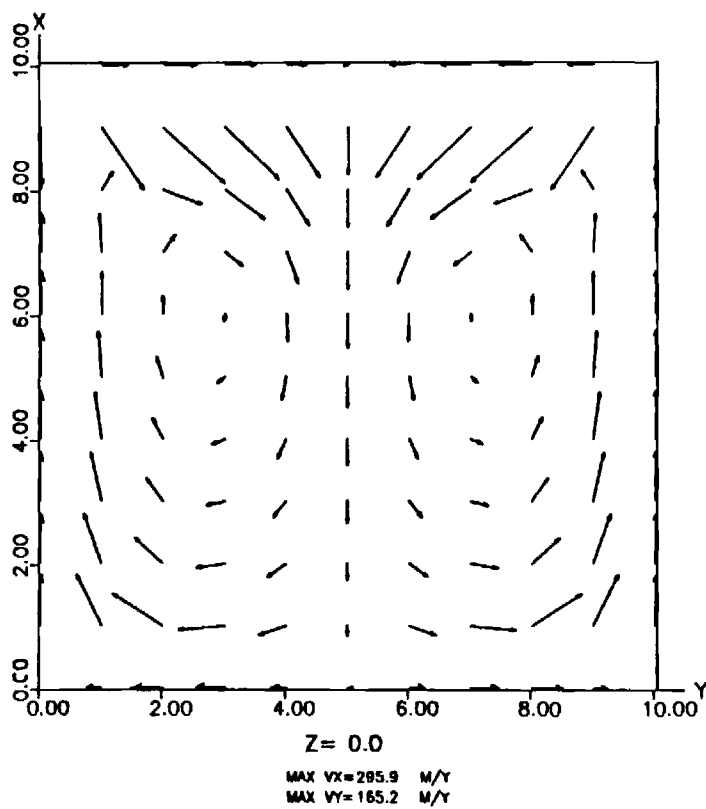


A.

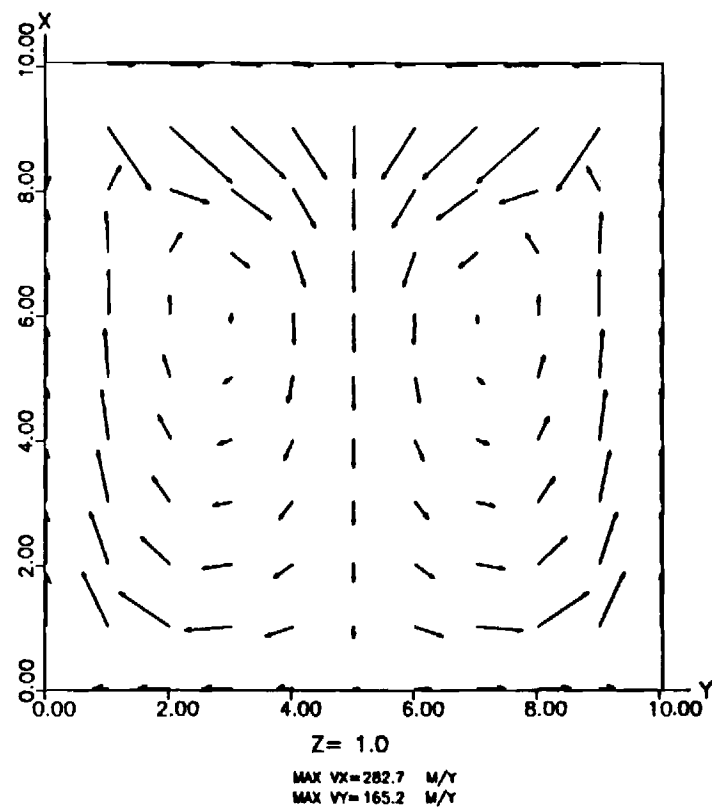


B.

Figure 13. a), c) and d) show the flow vectors at the faces of a porous box in contact with material of finite heat conductivity. b) shows a 3-D plot of the heat flow at the upper surface. $A=B=0.01$, $R=10R_c$ and $t=6,000$ years. Initial condition: fluid was caused to rise along the planes $y=0,10$



C.



D.

Figure 13. (Continued)

different times for $R = 5R_c$ for an initial perturbation selected to induce a longitudinal roll. The figures indicate a tendency to form transverse rolls despite the initial forcing. Again, because of the finite conductivity bounding material, the asymmetry arising from the input perturbation is still apparent. Figure 13 depicts the flow pattern for $R = 10R_c$ for an initial perturbation designed to induce transverse rolls. Such rolls were rapidly formed.

C. Discussion and Conclusions

C.1 Preferred Cell Pattern - Role of Initial Condition

The principal purpose for choosing a variety of initial perturbations was to try to resolve some of the seemingly conflicting results in the literature regarding the cell patterns in confined convecting fluids in porous media with fault-like geometry. Basically the conflict appears as follows: a) Beck (1972) for containers with insulated walls, showed that at $R = R_c$, the cell pattern took the form of transverse rolls. b) Lowell (1977a, c) and Lowell and Shyu (1978), however, showed that for perfectly conducting walls, the motion at $R = R_c$ took the form of longitudinal rolls. Furthermore, Shyu (1979) determined the critical Rayleigh number R_c for several fault models, assuming two-dimensional longitudinal rolls. c) Murphy (1979) pointed out an error in Lowell (1977a, c). Murphy contested that Lowell's results actually give rise two-dimensional transverse rolls, and therefore Murphy assumed transverse rolls in order to determine R_c for a fault zone with imperfectly conducting walls.

While I agree with Murphy's observation of error in Lowell (1977a, c), I believe Murphy's correction leads to a 3-dimensional pattern rather than transverse rolls (Lowell, 1979, unpublished calculations).

Moreover, Lowell and Shyu's (1978) results indicated that R_c for a three-dimensional pattern was only slightly greater than for two-dimensional longitudinal rolls, and they suggested that at finite amplitude the 3-D pattern might be preferred. Finally in cubic containers with insulated walls and for $R_c < R < 5R_c$, Straus and Schubert (1978) showed that either a two or three dimensional pattern could be generated by a suitably chosen initial condition.

In regard to the above conflict as to the preferred cell pattern in containers with fault-like geometry with perfectly or imperfectly conducting walls under finite-amplitude conditions, the model studies conducted here can be summarized:

1. In models with perfectly conducting walls, the flow is weakly three-dimensional. Thus the suggestion made in Lowell and Shyu (1978) is affirmed, the transverse velocity is significantly less than the longitudinal; and hence the pattern, in the main, has the appearance of 2-D transverse rolls. This pattern obtains even if the initial condition tends to force longitudinal rolls. The result does not appear to depend on R for $5R_c \leq R \leq 10R_c$.
2. In models with imperfectly conducting walls, the flow tends toward 2-D transverse rolls, regardless of the initial condition. Asymmetries in the initial condition are not quickly dissipated, due to the finite thermal conductivity of the wall material; however, transverse rolls are quickly established in models in which the initial condition is more conducive.

The results presented here do not resolve the question of the preferred cell pattern at initial instability $R = R_c$. At finite amplitude, however, the preferred pattern definitely is that of

transverse rolls. Thus the results of Straus and Schubert (1978) as to an initial condition associated non-uniqueness do not carry over to the present models. It is not entirely clear if the non-uniqueness is resolved by the application of different boundary conditions on the vertical walls or by the fault-like geometry of the container. More than likely it is the geometry which is the determining factor.

The results presented here also strongly suggest that Shyu's (1979) models cannot be carried into the finite amplitude regime. There is no indication that longitudinal cells persist at $R > 5R_c$, regardless of the boundary conditions or aspect ratio.

C.2 Application to Known Geothermal Systems

Available data on fault-controlled geothermal systems is very sketchy; so it is difficult to compare the model results with field data. Two thermal anomalies which appear to be fault controlled are the East Mesa Anomaly in the Imperial Valley, California (Swanberg, 1975) and the Izmir-Seferihizer Area in western Turkey (Esder and Simsek, 1975). In both of these areas, Figures 14 and 15, respectively, the heat flow, or thermal contours, as the case may be, show an alternating pattern of highs and lows which follow the linear trend of the fault zone. The spatial scales are of the order of a few kilometers for both areas and the thermal pattern may be associated with the ascending and descending portions of transverse convective rolls within the fault zone. Thus it may be possible to model the thermal anomalies with fault-zone convection models of the type presented here, e.g. see Figs. 8 and 13. At present, both the field data and the models are too unrefined to offer more than a qualitative comparison.

IV. CONVECTION IN A FAULT OR FRACTURE ZONE - ANISOTROPIC PERMEABILITY

In natural geothermal systems, the permeability distribution may be

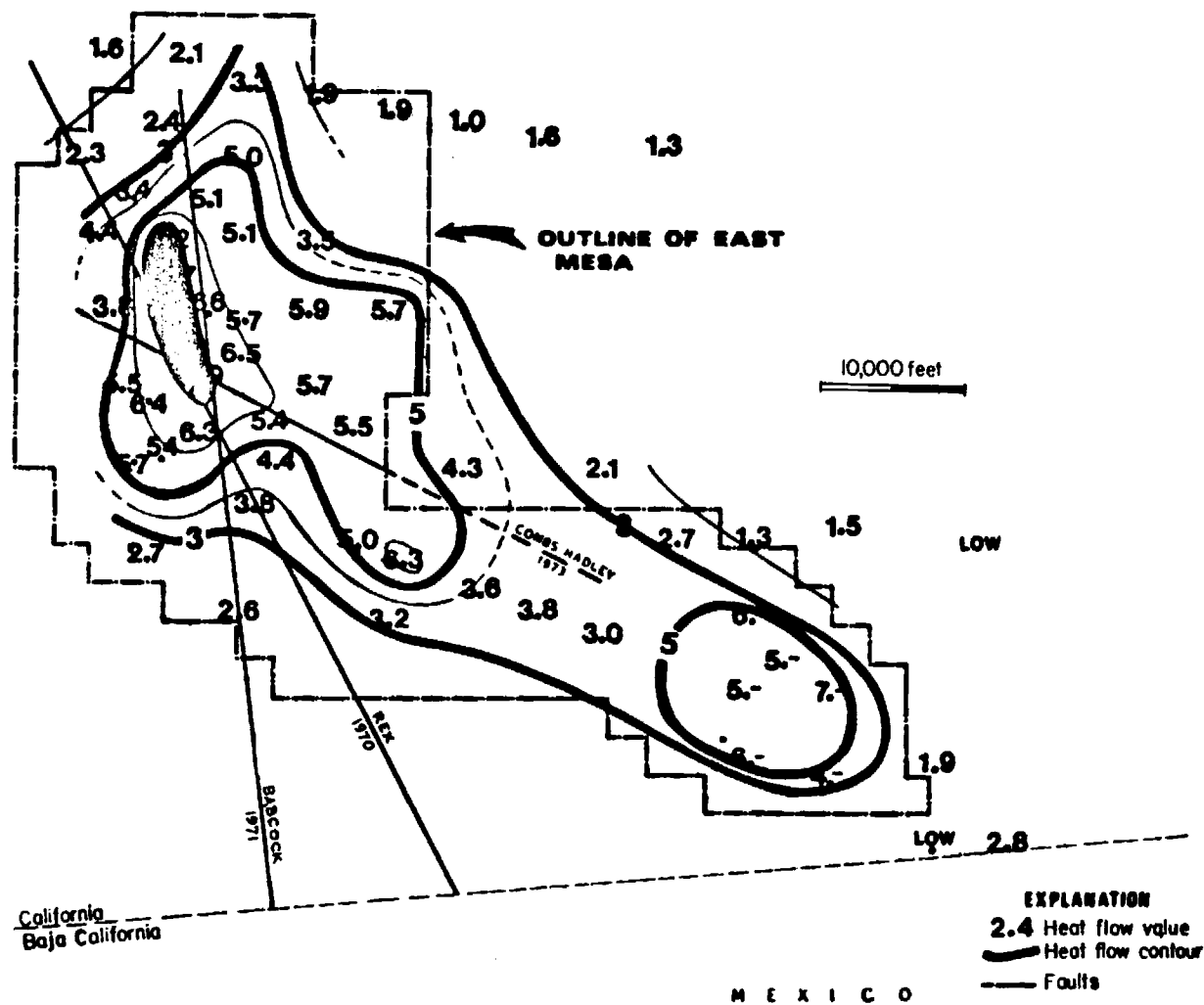


Figure 14. Distribution of the heat flow over the East Mesa heat flow anomaly and Border anomaly (Southeast Lobe). Data from Swanberg (1975).

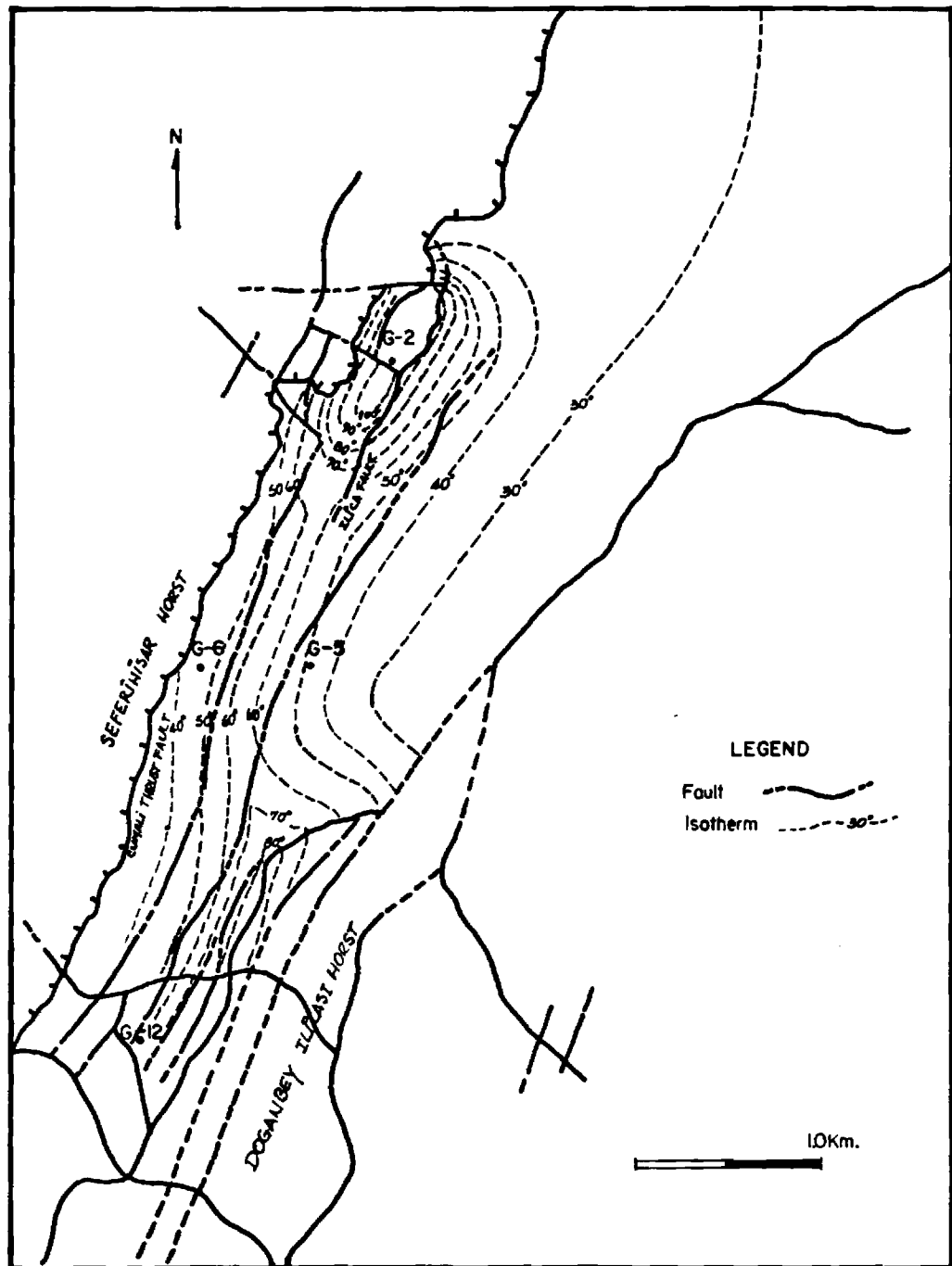


Figure 15. Isotherm contour map for 100 m. depth inside the Graben-I in the Izmir-Seferihisar area. Data from Esder and Simsek (1975).

quite complicated. Regional stresses may give rise to a preferred orientation of fractures and hence to anisotropies in the permeability. There is little data available, but one might intuitively expect that vertical permeability and permeability along the strike of the fault or fracture may be larger than the permeability transverse to the structure.

The critical Rayleigh number for the onset of convection has been determined for several idealized cases of anisotropic permeability and for fracture zones with either insulated or conducting vertical walls aligned along the strike. For insulated walls, the convection pattern at $R = R_c$ was shown to be transverse rolls, whereas an approximate solution assuming conducting walls indicates a 3-D pattern. (An analogy with the numerical models discussed in section III, however, would suggest that the pattern is only weakly 3-D and that at finite amplitude transverse rolls would ensue. Table 2 summarizes the principal results, assuming insulated walls, where a is the dimensionless aspect ratio L_y/L_x and γ is the ratio of the vertical to the horizontal permeability. Table 2 shows that if $\gamma < 1$, $R_c < R_{c,iso}$, whereas if $\gamma > 1$, $R_c > R_{c,iso} = 4\pi^2$, the critical Rayleigh number under isotopic conditions. Moreover, for a given fault aspect ratio, the cell aspect ratio decreases as γ increases. These results applied qualitatively to the the Double Hot Springs area of the Basin and Range, Figure 16, (Hose and Taylor, 1974) suggest that vertical permeability of the fault zone may be greater than the horizontal.

Details of these calculations have been reported earlier (Lowell, 1977b, 1979b, 1979c).

V. CONVECTION IN A VERTICAL FLUID-FILLED FRACTURE

The basic model for free convection in a narrow, fluid-filled open

TABLE 2. CRITICAL RAYLEIGH NUMBERS AND MODE FOR
SEVERAL VALUES OF ANISTROPY AND FAULT ZONE LENGTH,
ASSUMING INSULATED WALLS

$a \downarrow \gamma \rightarrow$	0.01	0.1	1	10
1	$R_C = 2.02\pi^2$ $m = 1$	$R_C = 2.2\pi^2$ $m = 1$	$R_C = 4\pi^2$ $m = 1$	$R_C = 17.5\pi^2$ $m = 2$
2	$R_C = 1.3\pi^2$ $m = 1$	$R_C = 1.75\pi^2$ $m = 1$	$R_C = 4\pi^2$ $m = 2$	$R_C = 17.5\pi^2$ $m = 4$
3	$R_C = 1.21\pi^2$ $m = 1$	$R_C = 1.77\pi^2$ $m = 2$	$R_C = 4\pi^2$ $m = 3$	$R_C = 17.4\pi^2$ $m = 5$
4	$R_C = 1.23\pi^2$ $m = 1$	$R_C = 1.75\pi^2$ $m = 2$	$R_C = 4\pi^2$ $m = 4$	$R_C = 17.3\pi^2$ $m = 7$

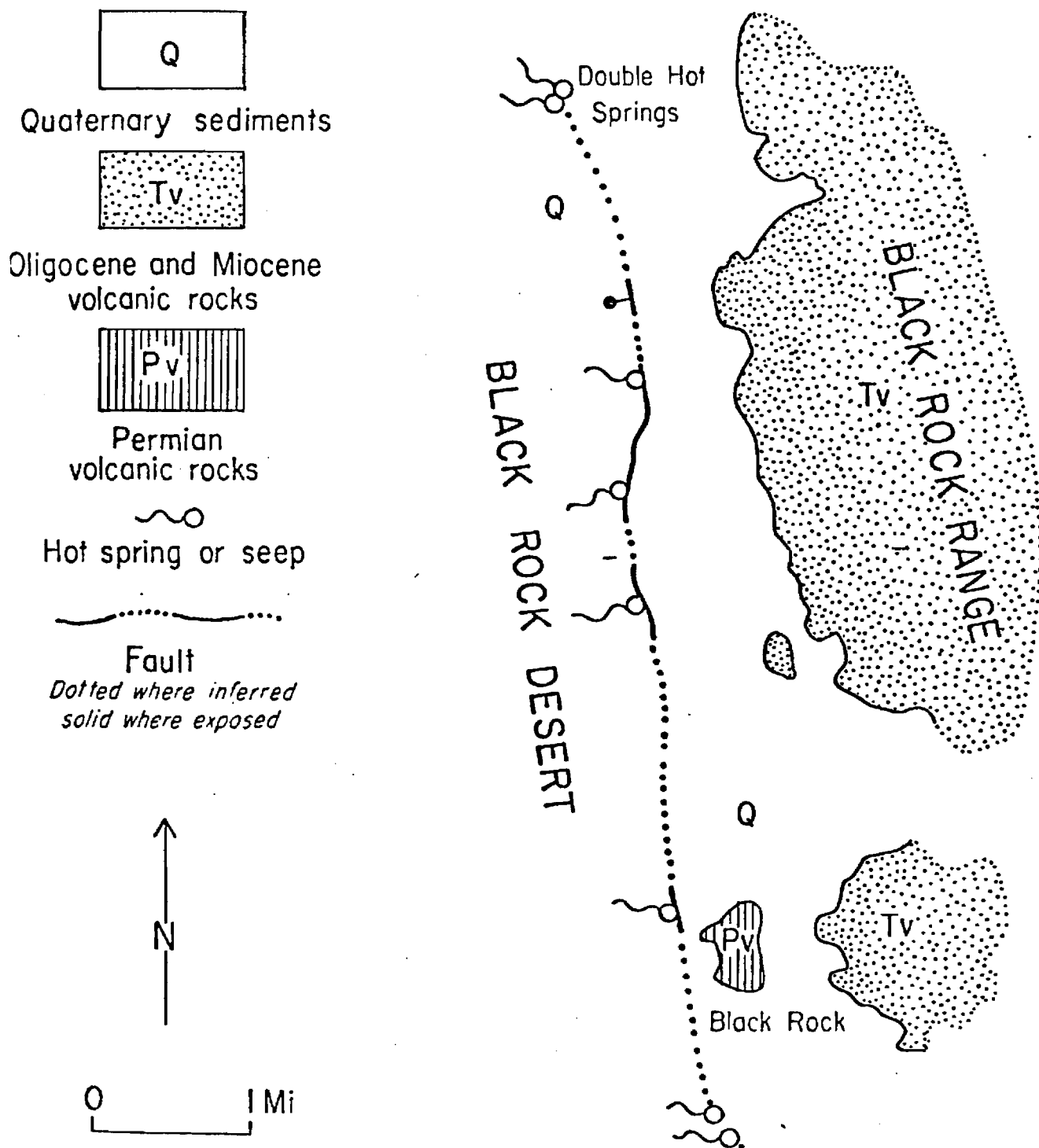


Figure 16. Hot spring along fault, Double Hot Springs - Black Rock area (from Hose and Taylor, 1974).

fracture, or fracture system, has been derived by Lowell (1975). Lowell's model stems from the earlier work on temperature of water flowing in fractures under an unspecified driving force (Bodvarsson, 1969). Bodvarsson (1978) has done further work on some aspects of convection in open fractures - in particular, the temporal development and thermoelastic effects. The emphasis in the present study has been on three topics: the temporal development of convection in a single fracture, the temporal development of convection in a system of fractures, including thermoelastic effects, and convection in a fracture, or system of fractures, in which the velocity and temperature are allowed to vary across the fracture aperture. The details of this work have been reported previously, and only a brief summary of the main results will be given here.

A. Temporal Evolution

The basic equations of Lowell (1975) were separated into spatial and temporal variables. By assuming that heat transfer from the rock to the fluid in the fracture varied as $t^{-1/2}$, it was possible to show that

$$\begin{aligned} q &\propto t^{-1/4} \\ \theta &\propto t^{-1/4} \end{aligned} \quad (19)$$

where q , θ are convective flow rate and fluid temperature, respectively. The similar time dependence of q and θ were shown to agree with the numerical results of Lowell (1975). Details of this work were given in Lowell (1979a).

B. Thermoelastic Effects

The above result for the temporal evolution of the flow rate and fluid temperature was made under the assumption of a constant fracture

width. Bodvarsson (1978) showed, however, that for a single fracture, imbedded in an infinite homogeneous half-space, that thermal contraction or expansion effects would lead to a fracture width which varied with time as

$$d \propto t^{1/2} \quad (20)$$

Including this effect in the model of Lowell (1979a) led to

$$\begin{aligned} \theta^2 d^3 &\propto t^{-1/2} \\ \theta &\propto t^{-1} \end{aligned} \quad (21)$$

and

$$\begin{aligned} q &\propto d^3 \\ q &\propto t^{1/2} \end{aligned} \quad (22)$$

These results indicate that as the system cools, thermal expansion of the fracture increases the permeability so much that the convective flow rate increases monotonically with time. On the other hand, the temperature is decreasing with time, so that the convective heat transport $q\theta$ decreases as $t^{-1/2}$, as in case of no thermal expansion.

Nevertheless, the concept of monotonically increasing permeability based on a single fracture is an oversimplification that is intuitively unsatisfactory. In natural systems, one would expect, rather, a system of closely spaced fractures. In this situation, thermal interference between the adjacent fractures will slow the rate of expansion, and will ultimately lead to a final, equilibrium fracture width. To illustrate this effect the conductive heating, or cooling, of a slab of thickness $2h$ which has isothermal boundaries at temperature T_0 (see Carslaw and Jaeger, 1959, p. 100 and p. 309). Based on these temperature distributions one finds that the displacement u of the boundaries, due to thermal expansion is:

$$u \propto t^{1/2} \quad (23)$$

for small values to time; i.e. $at/h^2 \ll 1$, and

$$u_f = 5\alpha^* T_0 h/q \quad (24)$$

where u_f is the final displacement, α^* being the thermal expansion coefficient. The $t^{1/2}$ dependence found for small values of time is reasonable since, in this case, there is no thermal interference, and it is as if the fracture is bounded by a semi-infinite medium. Equation (14) gives a useful estimate of the maximum amount of opening or closing of a set of parallel fractures imbedded in impermeable rock. For example, if $\alpha^* = 2 \times 10^{-5}/^\circ\text{C}$; $T_0 = 100^\circ\text{C}$, the displacement is:

$$u = 10^{-3} h \text{ meters}$$

Thus fractures of 1 mm width and separated by 2 m or more may close due to thermal expansion effects. Conversely, the fractures may double in width due to thermal contraction. Since the flow rate varies as d^3 a doubling of the fracture width would lead to an eightfold increase in the flow.

Another useful rule which can be obtained on the basis of these results, involves the time scale on which thermoelastic effects are important in geothermal systems. Thermoelastic effects should decrease once there is appreciable thermal interference. Thus, the time at which thermal interference effects dominate is given by:

$$\tau > h^2/a \quad (25)$$

Assuming $a = 10^{-6} \text{ m}^2/\text{sec}$, (25) shows that:

$$h = 1 \text{ m}; \tau = 10^6 \text{ sec.}$$

$$h = 10 \text{ m}; \tau = 10^8 \text{ sec.}$$

$$h = 100 \text{ m}; \tau = 10^{10} \text{ sec.}$$

Thus in natural, undisturbed geothermal systems, thermoelastic effects may be important on time scales of a few hundred years, or less, which

is short compared to the lifetime of a geothermal system. On the other hand, thermoelastic effects may be very important in natural systems under production as well as in man-made, hot, dry rock reservoirs.

Details of these calculations were given in Lowell (1979b).

C. Effect of Non-Uniform Velocity and Temperature Across the Fracture Aperture

All the studies of convection in open fractures which have been done previously have assumed a uniform velocity and temperature across the aperture of the fracture. In reality, however, assuming a smooth, flat-walled, fracture, a laminar flow will give rise to a parabolic velocity profile. There will also be, partially as a consequence of the velocity profile, a temperature variation across the aperture. These variations are expected to be small and may be unimportant as regards the overall heat transfer characteristics of the fracture; however, geochemical effects such as clogging of the fractures due to precipitation of certain chemical species (e.g. silica) and other water-rock interactions may depend critically upon details of temperature structure within the fracture.

An estimate of the magnitude of the temperature variations across the aperture was made under the assumption of a given velocity field with a parabolic profile across the fracture aperture, periodic along the strike of the fracture, and vanishing at the upper and lower boundaries. The initial geothermal gradient was assumed to be uniform; and the velocity field was assumed to be small enough that a first order, linear perturbation analysis could be used to find the temperature variations arising from the imposed velocity field. The calculations showed that magnitude of the temperature variation was

proportional to h^2/L^2 where h was the half width of the fracture and L the distance between adjacent fractures. For widely spaced fractures $h/L \approx 10^{-5}$, whereas for closely spaced fractures $h/L \approx 10^{-2}$. Thus the temperature effects will be negligible if the fracture spacing is large; however, it may be potentially important for closely spaced fracture systems. In this latter case, it may be useful to go beyond the linear analysis used here.

Details of this work were given in Lowell (1980).

VI. CONVECTION IN A HORIZONTAL, POROUS SLAB - RADIATIVE TOP BOUNDARY CONDITION

To date studies of the onset of convective instability in an infinite, porous slab of thickness h , bounded by horizontal planes have focused on thermal boundary conditions in which either the temperature or heat flux through the surface has been prescribed. In the natural setting, however, the porous zone is often overlain by a layer of impermeable cap rock. In this case, it is more reasonable to consider a mixed, i.e. radiative, boundary condition on the upper surface. That is, the cap rock may be assumed to act as a thin skin of poor conductor and zero heat capacity through heat transfer takes place. The thermal boundary condition would then be of the form

$$\lambda_m \partial T / \partial x + \zeta T = 0 \quad (26)$$

where ζ is the heat transfer coefficient.

Using the standard linearized perturbation technique, assuming exchange of stabilities, leads to a transcendental equation for the Rayleigh number R_y :

$$-2\bar{K} = D \cot D + Q \coth Q \quad (27)$$

where

$$\bar{K} = \zeta h / \lambda_m$$

$$D = [(R_y n)^{1/2} a - a^2]^{1/2}$$

$$Q = [(R_y n)^{1/2} a + a^2]^{1/2}$$

$$n = \bar{K} / \bar{K} + 1$$

$$a^2 = m^2 + n^2, \text{ the dimensionless semi-wavelength.}$$

Figure 17 gives solutions of equation (27) for some values of \bar{K} . The critical Rayleigh number \bar{R}_y is denoted. The results in Figure 17 show that as \bar{K} gets large \bar{R}_y approaches the critical value of $4\pi^2$ for a isothermal upper boundary. As \bar{K} decreases, the critical Rayleigh number increases slightly and the semi-wavelength decreases slightly. It is not until $\bar{K} \approx 1$ that the radiative boundary condition produces a significant change in \bar{R}_y .

To interpret these results for a natural geothermal system, let the heat transfer coefficient $\zeta \approx \lambda' / d$, where λ' is the thermal conductivity of the cap rock, and d is its thickness. Then $\bar{K} = (\lambda' / \lambda_m)(h / d)$. Assuming a thickness ratio of 10 and a conductivity ratio of 0.25 gives $\bar{K} = 2.5$. For these values \bar{R}_y is increased by about 20% and the cell aspect ratio is decreased by approximately the same amount. A thickness ratio of 10 is, perhaps, a little extreme; e.g. a cap rock of 300m overlying a porous layer of 3 km, but not totally out of line. Moreover, for such a thick layer of cap rock, its capacity is probably not negligible, as assumed here.

Details of this work were given in Lowell (1979a) and Fulford (1979).

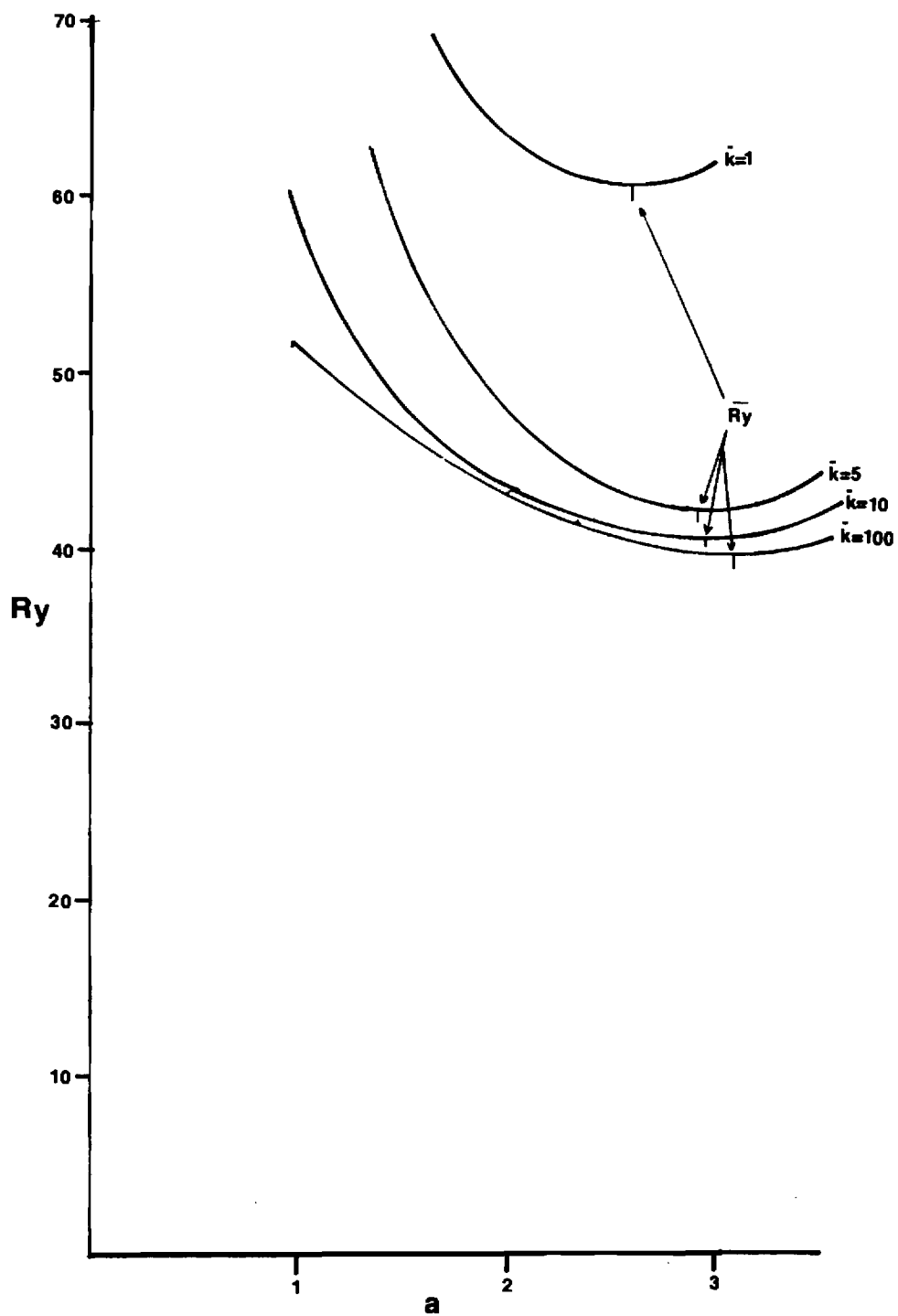


Figure 17. Rayleigh number versus semi-wavelength for isothermal bottom, rigid upper surface.

VII. BIBLIOGRAPHY

- Beck, J. L., Convection in a box of porous material saturated with fluid, *Phys. Fluids*, 15: 1377-1383, 1972.
- Bodvarsson, G., On the temperature of water flowing through fractures, *J. Geophys. Res.*, 74:1987-1992, 1969.
- Bodvarsson, G., Convection and thermoelastic effects in narrow vertical fracture spaces with emphasis on analytical techniques, Final Report, U.S.G.S., Grant No. 14-08-00001-G-398, 111 p., 1978.
- Carslaw, H. S. and J. C. Jaeger, Conduction of Heat in Solids, 2nd ed., the Clarendon Press, Oxford, 510 p., 1959.
- Esder, T., and S. Simsek, Geology of Izmir-Seferihizar geothermal area, Western Anatolia of Turkey; determination of reservoirs by means of gradient drilling, In: Proceedings of Second United Nations Symposium on the Development and Use of Geothermal Resources, San Francisco, 1: 349-361, 1975.
- Fulford, J. K., Thermal Convection in Porous Media with Application to Hydrothermal Circulation in the Oceanic Crust, M.S. Thesis, Georgia Institute of Technology, Atlanta, 54 p., 1979.
- Hernandez, H. Numerical Modeling of the Convection in a Fault Zone, M. S. Thesis, Georgia Institute of Technology, Atlanta, 112 p., 1980.
- Holst, P. H., and K. Aziz, Transient three-dimensional natural convection in confined porous media, *Int. J. Heat Mass Transfer*, 15: 73-90, 1972.
- Hose, R. K., and B. E. Raylor, Geothermal systems of Northern Nevada, U.S.G.S. Reports, open-file series, 74-271, 1974.
- Kassoy, D. R., and A. Zebib, Variable viscosity effects on the onset of convection in porous media, *Phys. Fluids*, 18: 1649-1651, 1975.
- Lapwood, E. R., Convection of a fluid in a porous medium, *Proc. Cambridge Phil. Soc.*, 44: 508-521, 1948.
- Lowell, R. P., Circulation in fractures, hot springs and convective heat transport on mid-ocean ridge crests, *Geophys. J. R. Astr. Soc.*, 40: 351-365, 1975.
- Lowell, R. P., Convection in narrow, vertical fracture spaces. Semi-Annual Technical Report No. 1, U.S.G.S., Grant No. 14-08-00001-G-365, 10 p., 1977a.
- Lowell, R. P., Convection in narrow, vertical fracture spaces, Semi-Annual Technical Report No. 2, U.S.G.S., Grant No. 14-08-00001-G-365, 16 p., 1977b.

- Lowell, R. P. Thermal convection in fault and fracture zones, EOS, 58: 541, 1977.
- Lowell, R. P., Convection in narrow vertical fracture spaces, Semi-Annual Technical Report No. 1, U.S.G.S., Grant No. 14-08-00001-G-540, 28 p., 1979a.
- Lowell, R. P., Convection in narrow vertical fracture spaces, Semi-Annual Technical Report No. 2, U.S.G.S., Grant No. 14-08-00001-G-540, 18 p. 1979b.
- Lowell, R. P., The onset of convection in a fault zone: effect of anisotropic permeability, in: Geothermal Resources Council Transactions, 3: 377-380, 1979c.
- Lowell, R. P., Convection in narrow vertical fracture spaces, Semi-Annual Technical Report No. 3, U.S.G.S., Grant No. 14-08-00001-G-540, 13 p., 1980.
- Lowell, R. P., and C. T. Shyu, On the onset of convection in a water saturated porous box: effects of conducting walls, Letters in Heat and Mass Trans., 5: 371-378, 1978.
- Murphy, H. D., Convective instabilities in vertical fractures and faults, J. Geophys. Res., 84: 6234-6245, 1979.
- Ribando, R. J., K. E. Torrance, and D. L. Turcotte, Numerical models for hydrothermal circulation in the oceanic crust, J. Geophys. Res., 81: 3007-3012, 1976.
- Shyu, C. T., Numerical Analysis of Critical Field Functions for Thernam Convection in Vertical or Quasivertical Darcy Flow Slabs, Ph.D. Thesis, Oregon State University, Corvallis, Oregon, 1979.
- Sleep, N. H. and T. J. Wolery, Egress of hot water from mid-ocean ridge hydrothermal systems: some thermal constraints, J. Geophys. Res., 83: 5913-5922, 1978.
- Straus, J. M., Large amplitude convection in porous media, J. Fluid Mech., 64: 51-63, 1974.
- Straus, J. M., and G. Schubert, Thermal convection of water in a porous medium: effects of temperature - and pressure-dependent thermodynamic and transport properties, J. Geophys. Res., 82: 325-333, 1977.
- Straus, J. M. and G. Schubert, Three-dimensional convection in a cubic box of fluid saturated porous material, Space Sciences Lab., Report No. SSL-78(7684)-3, 1978.

- Swanberg, C. A., The Mesa Geothermal anomaly, Imperial Valley, California: A comparison and evaluation of results obtained from surface geophysics and deep drilling, In: Proceedings of Second United Nations Symposium on the development and use of geothermal resources, San Francisco, 2: 1217-1229, 1975.
- White, D. E. and D. C. Williams, eds., Assessment of Geothermal Resources in the United States - 1975, U.S.G.S. Circular 726, 1975.
- Wooding, R. A., Influence of anisotropy and variable viscosity upon convection in a heated, saturated porous layer, Applied Math. Div. Tech. Rept. No. 55, DSIR, Wellington, N.Z., 23 p., 1976.
- Zebib, A., and D. R. Kassoy, Three-dimensional natural convection motion in a confined porous medium, Phys. Fluids, 21: 1-3, 1977.

VIII. STUDENTS SUPPORTED AND THESES

1. Mr. James K. Fulford performed the work on the onset of convection with a radiative-top boundary condition. This work formed a part of his M.S. thesis. He is currently a doctoral student in the Atmospheric Sciences program within the School of Geophysical Sciences at Georgia Tech.

2. Mr. James C. Herbert was supported briefly under this project. He changed to another field of specialization and recently finished his M.S. thesis. He is currently employed by Mobil Oil Corporation, Dallas, Texas.

3. Mr. Heroel Hernandez performed the numerical work on finite-amplitude convection in a fault zone, which has been the bulk of this final report. He recently completed his M.S. thesis and is currently employed by Chevron Oil Field Research Company, LaHabra, California.

M.S. Thesis: Mr. James K. Fulford, Thermal Convection in Porous Media with Application to Hydrothermal Circulation in the Oceanic Crust, Georgia Institute of Technology, 54 pp., 1979.

M.S. Thesis: Mr. Heroel Hernandez, Numerical Modeling of the Convection in a Fault Zone, Georgia Institute of Technology, 112 pp., 1980.

IX. PUBLICATIONS AND PAPERS

A. Publications

Lowell, R. P., C. H. Chen, and J. K. Fulford, 1978, On transient temperature inversions in geothermal boreholes, in: Geothermal Resources Council Transactions, 2, 407-409.*

Lowell, R. P. and T. C. Shyu, 1978, The onset of convection in a water-saturated porous box: effect of conducting walls, Lett. Heat and Mass Trans., 5, 371-378.*

Lowell, R. P., 1979, The onset of convection in a fault zone: effect of anisotropic permeability, in: Geothermal Resources Council Transactions, 3, 377-380.*

Lowell, R. P. and H. Hernandez, 1980, Numerical models of finite amplitude convection in a fault zone, (in preparation).

B. Papers

Lowell, R. P., 1978, Heat transfer processes related to fluid flow in fractured rock, Presented at Penrose Conference on Heat Transport Processes in the Earth, Vail, Colorado, November 12-16, 1978.

*Much of the research which resulted in these papers was performed under U.S.G.S. Grant No. 14-08-00001-G-365.

